



TAMPEREEN TEKNILLINEN YLIOPISTO
TAMPERE UNIVERSITY OF TECHNOLOGY

JUUSO TORISEVA
MATERIAL PERFORMANCE DEPENDENCE ON POLYOLEFIN
FILM TEMPERATURE IN PROCESSING

Master of Science Thesis

Examiners: Professor Jurkka Kuusi-
palo, Senior Research Fellow Jo-
hanna Lahti
Examiner and topic approved by the
Faculty Council of the Faculty of
Engineering Sciences
on 31th May 2017

ABSTRACT

JUUSO TORISEVA: Material Performance Dependence on Polyolefin Film Temperature in Processing

Tampere University of technology

Master of Science Thesis, 116 pages, 32 Appendix pages

August 2017

Master's Degree Programme in Materials Science

Major: Polymers and Biomaterials

Examiner: Professor Jurkka Kuusipalo, Senior Research Fellow Johanna Lahti

Keywords: polyolefin, film temperature, air gap, heat sealing, pinhole

This thesis is focused on the examination of extrusion coating product performance, which is aspired to improve with resin choice and essential process parameters such as melt temperature and air gap distance. The performance is defined via two main testing methods, which are hot air sealing and pinhole measurements. Furthermore, infrared (IR) thermometry is applied to monitor the polymer film temperature during processing and contribute the conclusions of the laboratory measurement results.

Theoretical part presents essential information about polymer material, extrusion coating process and parameters, product properties and fundamentals of IR thermometry. Firstly, the structure, properties and polymerization of polyethylene are discussed, followed by the principles of extrusion coating process. The knowledge of extrusion coating is reinforced with process parameters and their influence is considered via product properties. Finally, IR thermometry is examined including theoretical basis, equipment introduction and measurement method.

Experimental part includes trial runs to produce product samples and laboratory measurements that focus on the quality control. Experiments concentrate on three main variables; melt temperature, air gap and resin choice, which are adjusted through the measurements. Hot air sealing and pinhole analyses are performed after each trial run in order to monitor the product quality and discover optimal process conditions for every material. The ultimate goal is to examine combination of melt temperature, air gap distance and material, which produces the best possible hot air sealing and pinhole results with the lowest possible coating weight.

The measurements of experimental part offer a few confirmed outcomes, which enable conclusions concerning optimal melt temperature and air gap settings. Furthermore, comparison between different resin choices is possible. Higher melt temperature setting mainly improves hot air sealing and pinhole results. However, some resins do not endure excessive heating and degradation and the properties start to decline. The effect of air gap is similar to the melt temperature. Higher air gap setting decreases sealing temperature and reduces pinholes almost invariably despite increased cooling of the film. Moreover, increased neck-in must be noticed as the advantages of higher air gap are considered. The comparison of resin choice produce the most controversial results and the effect of blending is partially indefinite. First set of measurements support the blending in order to improve hot air sealing and pinhole results, but the advantage is disappeared in subsequent examination. Furthermore, increased material cost do not support the use of blends.

TIIVISTELMÄ

JUUSO TORISEVA: Material Performance Dependence on Polyolefin Film Temperature in Processing

Tampereen teknillinen yliopisto

Diplomityö, 116 sivua, 32 liitesivua

Elokuu 2017

Materiaalitekniikan diplomi-insinöörin tutkinto-ohjelma

Pääaine: Polymeerit ja biomateriaalit

Tarkastaja: Professori Jurkka Kuusipalo, Yliopistotutkija Johanna Lahti

Avainsanat: polyolefiini, kalvon lämpötila, ilmaväli, kuumasaumaus, huokosreikä

Tämä työ keskittyy ekstruusiopäällystetyn tuotteen ominaisuuksiin, joita pyritään parantamaan materiaalivalinnalla ja merkittävillä prosessiparametreilla kuten sulalämpötilalla ja ilmavälin korkeudella. Ominaisuudet määritellään kahden päätestimenetelmän avulla, jotka ovat kuumailmasaumaus- ja huokosreikämittaukset. Lisäksi sovelletaan infrapunasäteilyyn (IR) perustuvaa lämpötilamittausta sulan muovikalvon lämpötilan mittaamiseksi prosessoinnin aikana ja tukemaan laboratoriomittausten johtopäätöksiä.

Teoriaosuus esittää oleellista tietoa polymeerimateriaalista, ekstruusiopäällystysprosessista ja -parametreista, tuoteominaisuuksista sekä perusteet IR lämpötilamittauksesta. Aluksi käsitellään polyeteenin rakenne, ominaisuudet ja polymerointi, jonka jälkeen siirrytään ekstruusiopäällystykseen peruserusperiaatteisiin. Ekstruusiopäällystykseen syvennytään prosessiparametrien avulla ja niiden vaikutusta tutkitaan tuoteominaisuuksien kautta. Lopuksi IR lämpötilamittausta tarkastellaan teoriapohjan, laite-esittelyn ja mitausmenetelmän kannalta.

Kokeellinen osa sisältää koeajot joissa valmistetaan tuotenäytteitä, sekä laboratoriomittaukset jotka keskittyvät tuotteen laadunvalvontaan. Testit keskittyvät kolmeen päämuuttajaan; sulalämpötilaan, ilmavälin korkeuteen ja materiaalivalintaan, joita säädetään läpi mittausten. Kuumailmasaumaus ja huokosreikämittauksia suoritetaan jokaisen koeajon jälkeen, tuotteen laadun mittaamiseksi ja optimaalisten prosessiolosuhteiden löytämiseksi jokaiselle materiaalille. Perimmäinen tavoite on selvittää sulalämpötilan, ilmavälin korkeuden ja materiaalin yhdistelmä, joka tuottaa parhaat mahdolliset kuumailmasaumaus- ja huokosreikätulokset, pienimmällä mahdollisella päällystemäärällä.

Kokeellisen osan mittaukset tarjoavat muutaman vahvistetun lopputuloksen, jotka mahdollistavat optimaalisiin sulalämpötilaan ja ilmavälin korkeuteen liittyvät johtopäätökset. Lisäksi vertailu materiaalivalintojen välillä on mahdollista. Korkeampi sulalämpötila pääasiassa parantaa saumautuvuutta ja vähentää huokosreikiä. Kaikki materiaalit eivät kuitenkaan kestä liiallista lämpötilaa ja rakenteen hajoamista, jolloin ominaisuudet kääntyvät laskuun. Ilmavälin korkeudella on samankaltainen vaikutus kuin sulalämpötilalla. Korkeampi ilmaväli alentaa saumauslämpötilaa ja vähentää huokosreikiä lähes poikkeuksetta, huolimatta lisääntyneestä muovikalvon jäähtymisestä. Lisäksi lisääntynyt kalvon kurouma täytyy ottaa huomioon, kun korkeamman ilmavälin hyötyjä arvioidaan. Materiaalivalinnan vertailu tuottaa kiistanalaisimmat tulokset, ja sekoitusten vaikutus on osittain epävarmaa. Ensimmäiset mittaukset tukevat sekoituksia kuumailmasaumaus- ja huokosreikätulosten parantamiseksi, mutta etu pienenee myöhemmissä mittauksissa. Lisäksi lisääntyneet materiaalikustannukset eivät tue sekoitusten käyttöä.

PREFACE

This Master of Science Thesis was made at Tampere University of Technology's Paper Converting and Packaging Technology Research Unit.

I would like to thank the examiners of my thesis Professor Jurkka Kuusipalo and Senior Research Fellow Johanna Lahti. Special thanks to Project Manager Esa Suokas for all the knowledge that I have received during this work. I would also like to thank the staff of the pilot line and laboratory at Paper Converting and Packaging Technology Research Unit.

Finally, I want to show my gratitude to my family and friends for the support and encouragement during this work.

Tampere 23.8.2017

Juuso Toriseva

CONTENTS

1.	INTRODUCTION	1
2.	POLYETHYLENE (PE)	3
2.1	Classification and basic properties	4
2.2	Chain branching.....	5
2.3	Processability.....	7
2.4	Properties of PE.....	8
2.4.1	Crystallinity and density.....	8
2.4.2	Molecular weight and melt index (MI)	9
2.4.3	Molecular weight distribution (MWD)	10
2.5	Manufacturing methods of PE.....	10
2.5.1	Basic properties of autoclave and tubular PE-LD	11
2.5.2	Autoclave and tubular processes.....	13
3.	EXTRUSION COATING PROCESS.....	16
3.1	Extrusion coating equipment.....	16
3.2	Flame and corona treatment	20
3.3	Co-extrusion	20
4.	KEY PROCESS PARAMETERS AND PRODUCT PROPERTIES	23
4.1	Melt flow and temperature profile in extrusion.....	23
4.1.1	Melting mechanism.....	24
4.1.2	Temperature profile.....	25
4.1.3	Effects on product properties.....	26
4.2	Adhesion	26
4.2.1	Factors affecting adhesion.....	27
4.2.2	Orientation and oxidation.....	28
4.2.3	Time in the air gap	30
4.3	Heat sealability	31
4.3.1	Factors affecting heat sealability and seal strength.....	32
4.3.2	Influence of polymer properties.....	32
4.3.3	Influence of product manufacturing process	33
4.3.4	Influence of heat sealing process parameters	33
4.4	Pinholes.....	34
4.5	Coating weight, draw down and neck-in	34
5.	INFRARED (IR) THERMOMETRY	37
5.1	Theory of the IR-based temperature measurement.....	37
5.1.1	Planck's law.....	38
5.1.2	Stefan-Boltzmann's law	40
5.1.3	Grey bodies, grey body radiation and emissivity	41
5.2	Types of IR thermometers.....	42
5.2.1	Total radiation thermometers.....	42
5.2.2	Ratio thermometers	42

5.2.3	Spectral band thermometers	43
5.3	IR temperature measurement of plastics	44
5.4	Advantages of the IR thermometers	45
5.5	Sources of error	46
5.6	Thermal imagers	48
5.7	Correlation between theory and practical IR temperature measurements ...	50
6.	EXPERIMENTAL MATERIALS AND METHODS	53
6.1	Materials.....	53
6.2	Pilot line and process parameters	53
6.3	Process parameters	55
6.4	Temperature measurement set-up.....	57
6.5	Hot air sealing measuring method.....	60
6.6	Pinhole measuring method.....	62
7.	RESULTS AND DISCUSSION	64
7.1	Effect of melt temperature and material on product properties.....	64
7.1.1	Trial runs 20170125	64
7.1.2	Trial runs 20170131-B17	67
7.1.3	Trial runs 20170216-B18	71
7.1.4	Trial runs 20170223-B19	73
7.2	Effect of air gap distance and material on product properties	76
7.2.1	Trial runs 20170302	77
7.2.2	Trial runs 20170308	80
7.2.3	Trial runs 20170309-B20	83
7.2.4	Trial runs 20170404-B21	86
7.2.5	Trial runs 20170406-B22	89
7.2.6	Trial runs 20170411-B23	93
7.3	Comparison of melt temperatures and materials	96
7.4	Comparison of air gap distances and materials	103
7.5	IR temperature measurements of co-extrusion.....	107
8.	CONCLUSIONS.....	110

APPENDIX A: LABORATORY RESULTS OF TRIAL RUNS

APPENDIX B: HOT AIR SEALING RESULTS

APPENDIX C: HOT AIR SEALING GRAPHS

LIST OF SYMBOLS AND ABBREVIATIONS

EVA	ethylene-vinyl acetate
FTIR	Fourier transform infrared spectroscopy
IR	infrared
L/D-ratio	length per diameter ratio
MI/MFI	melt index/melt flow index
MWD	molecular weight distribution
PA	polyamide
PE	polyethylene
PE-HD	high-density polyethylene
PE-LD	low-density polyethylene
PE-LLD	linear-low-density polyethylene
PP	polypropylene
TIAG	time in the air gap
TUT	Tampere University of Technology
C_p	heat capacity
C_1	the first radiation constant
C_2	the second radiation constant
E	total emissive power for a blackbody
$E(\lambda)$	spectral emissive power for a blackbody
g_f	coating thickness
h	heat transfer coefficient
M	mass flow rate
Q	flow rate
T	temperature
T_{air}	ambient temperature
T_0	temperature of the film at the die exit
v_f	line speed
w	width of the film
z	distance from the die exit
Δp	pressure drop
ε	emissivity
λ	wavelength
λ_{max}	wavelength of the temperature maximum
ρ_f	density of the polymer
σ	Stefan-Boltzmann constant

1. INTRODUCTION

Extrusion coating is a process, where a substrate material is coated with a molten polymer film to form a uniform final product that combines advantages and properties of both materials. In extrusion coating, the substrate material is usually paper or paperboard but other materials such as aluminum foils are possible to coat as well. The coating material can be practically any kind of thermoplastic polymer that can be processed into molten film in extruder. Concerned materials define the process parameters and conditions and consequently ease of processing. The most common coating materials are polyolefins e.g. polyethylene (PE), polypropylene (PP) and their copolymers.

Applications of extrusion coating are numerous and especially in the paper and paperboard converting and packaging, possibilities are wide. Extrusion coated products offer several advantages that consist of the individual properties of substrate and polymer materials. In packaging, the paperboard form a rigid structure that is lightweight, low-priced and sustainable. The polymer material in turn, enables heat sealing of the product and provides liquid and gas barrier, which prevent leaking and protect the product from external factors that can cause deterioration.

Melt temperature of the polymer film is unquestionably one of the most important factors in manufacturing of high quality extrusion coated products. Melt temperature can be measured during the extrusion process by thermocouples attached to the extruder. The polymer film proceeds in the air gap before encountering the substrate and starts to cool immediately after the die lip. Air gap distance and time as well as the ambient airflow affect the cooling and consequently to the temperature value of the film.

Melt temperature has a great influence on many key properties of the final product such as adhesion, heat sealability and pinholes and therefore knowing the exact temperature value of the film is essential. The temperature measurement is rather awkward with traditional conductive methods due to high temperatures and set-up. Therefore non-conductive infrared thermometry, which utilizes electromagnetic radiation, is excellent and reliable option to meter the film temperature in real-time.

The theory part of this thesis focuses on understanding and explaining the different factors that relate to the extrusion coating process and affect the quality of final product. The theory part encompasses information about the main polymer material i.e. polyethylene, extrusion coating process and important process parameters, which individually and together define the most important product properties. Furthermore, infrared thermometry,

that is the foundation of the temperature measurements, is covered widely from the physical basis to the performance of measurements.

The experimental part focuses on the temperature measurements of the film, heat sealing measurements and pinhole measurements. The variables in the trial runs are the resin, melt temperature, air gap distance and line speed. The main goal of this thesis is to research the effect of the variables on the most important product properties. The temperature measurements are conducted in every trial run with the pyrometer. Furthermore, every sample point is later analyzed in the laboratory to quantify the sealing temperature, pinholes, adhesion and coating weight. These values are compared to the trial run variables in order to achieve the best possible combination of resin, process conditions and product properties. The ultimate goal of all the measurements and analysis is source reduction, which denotes decreasing of the film thickness and consequently reduction of material consumption and costs.

2. POLYETHYLENE (PE)

Polyolefins are a group of thermoplastic polymers that consist of carbon and hydrogen atoms [1, 2]. These hydrocarbons originate from petroleum-based gases [2]. The molecular structure is based on monomers that include a double bond in the 1-position. Therefore, polyolefins are sometimes referred as α -olefins. Polyolefins comprise some of the most widely used and significant polymer materials in the world such as polyethylene (PE), polypropylene (PP) and co-polymers of polyethylene that can contain various comonomers [1].

Ethylene gas is the major raw material for plastic production and it's used for producing PE [2]. PE is evidently the most important polymer material and its production and consumption is by far largest among the synthetic polymers. The favor of PE results from wide range of properties, ease of manufacturing and low costs [1]. PE and most other polyolefin resins are produced to pellets that are small, spherical translucent and usually white colored. Commonly, the resins contain some additives such as stabilizers or colorants [2].

Ethylene monomer (C_2H_4) is formed from hydrogen and two carbon atoms that are connected with the double bond [1, 2]. In the polymerization process, processing conditions cause the breakage of the double bond. This enables the combination of ethylene monomers and eventually forming of the long molecular chains. After the polymerization, the monomers have reacted with each other and as a result the higher molecular weight PE resin is formed [2, 3]. Not all of the monomers react with each other and they are separated and restored to the start of the process [3]. PE can be produced by several different reaction and processing methods. These polymerization mechanisms are high pressure and free radical polymerization and coordination polymerization that can be performed e.g. with Ziegler-Natta or metallocene catalysts [1, 3]. The polymerization methods and their influence on the polyethylene resin properties are presented in table 1 [1].

Table 1. *The effects of polymerization methods on PE resin [1].*

Polymerization method	Polyethylene properties
High pressure i.e. free radical	Broad molecular weight distribution, both short and long branches, low density and melting point
Coordination catalysts:	
Ziegler-Natta	Broad molecular weight distribution, few branches, linear polymers, high density and melting point, co-monomers control crystallinity
Metallocene	Narrow molecular weight distribution, controlled level of branching, good control of co-monomer distribution
Metallocene-Ziegler	High co-monomer incorporation

2.1 Classification and basic properties

The classification of polyethylenes is founded on their density. Three of the most common PE grades are low-density (PE-LD), linear low-density (PE-LLD) and high-density polyethylene (PE-HD). The crystallinity and consequently density of PE grade is mainly defined by the chain branching. The density of PE generally decreases when the mole fraction of side groups is increased. Furthermore, many other major properties of PE such as melting temperature and mechanical behavior are dependent on the polymerization and manufacturing process, since they define the molecular weight of the material [1, 4]. The most common PE grades and their properties are presented in table 2 [1, 2, 5].

Table 2. *The basic properties of PE-LD, PE-HD and PE-LLD [1, 2, 5].*

Polymer	Density range (g/cm ³)	Crystallinity range (%)	Melt index range (g/10 min)	Melting temperature range (°C)	Degree of branching (CH ₃ /100 C)
PE-LD	0.91-0.94	45-55	3-15	105-115	2-7
PE-HD	0.94-0.97	70-90	5-15	130-137	0,1-2
PE-LLD	0.91-0.94	45-55	3-15	122-128	2-7

PE-LD is clearly the most common PE grade in extrusion coating applications. It provides great melt strength and drawdown properties with minimal neck-in. PE-LLD offers improved stiffness, toughness and tear and puncture resistance compared to PE-LD. PE-LLD that is produced with metallocene catalysts has even better resistance against tears and punctures. Furthermore, PE-LLD has better heat sealing and hot tack properties. PE-LLD can be blended with PE-LD to improve processability, but the ratio must be appropriate to achieve the benefits of linearity. [6, 7]. PE-HD offers better barrier properties, grease resistance, temperature resistance and higher stiffness compared to PE-LD and PE-LLD. However, higher density causes the increase of heat sealing temperature and weakening of the processability. Furthermore, PE-HD has tendency to increase neck-in and therefore it is normally blended with PE-LD [4, 6].

2.2 Chain branching

Polymer chains that are formed in the polymerization process can be of variable lengths and consequently of variable molecular weights [2]. Furthermore, side chains or chain branching of the polymer material result from the polymerization. Shorter side chains are due to a backbiting phenomenon and longer side chains originate in hydrogen abstraction and consequential branching during the polymerization [1, 8]. Long chain branching indicates to the amount of long side chains that are attached to the polymer backbone. These branches are crucial for the processability of the polymer film. Melt strength and stability are increased, when the long chain branching increases. Furthermore, neck-in usually decreases. However, drawdown and impact resistance usually decrease and tendency for edge tear increases [4, 6].

The main backbone of PE and especially PE-LD can have multiple side chains or branches. The chain branches are the areas in the polymer structure, where the oxidation occurs, which makes them highly important considering the extrusion coating process [2]. The structure of PE-HD does not include significant branching and the amount of side chains is minor. PE-LLD combines the properties of PE-LD and PE-HD and the main structure of the material is rather straight although it contains short side chains [1, 8]. The branching and structure of different PE grades is illustrated in figure 1 [1].

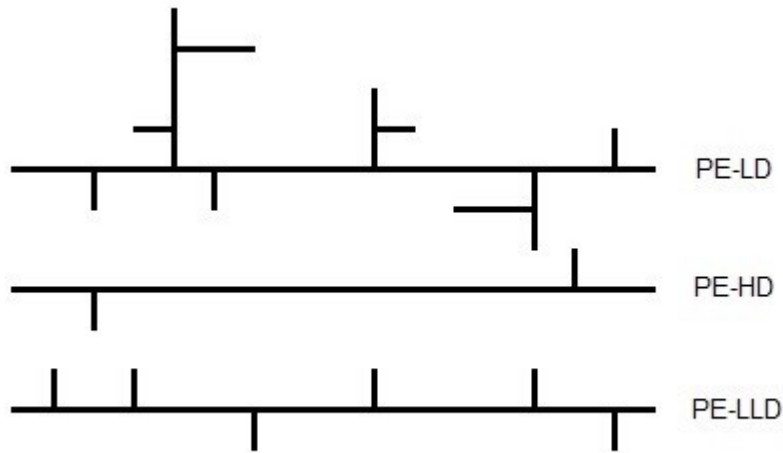


Figure 1. The chain structure of different PE grades [1].

The degree of branching can be increased via copolymerization, whereupon small amount of co-monomer is added during the polymerization [1]. Ethylene is copolymerized with other monomers in order to change the structure and provide specific additional properties. The common co-monomers that are used with PE-LLD and PE-HD are butene and hexene. They affect e.g. the degree of chain branching, which alters the molecular weight and density and consequently the properties of the material [2]. Co-monomer type refers to the number of carbon atoms in the side chain that are attached to the polymer backbone. For example, butene co-monomers create a side chain with two carbon atoms, whereas hexene co-monomers form longer side chain containing four carbon atoms. Few co-monomers and their influence on strength of the PE are shown in figure 2 [6].

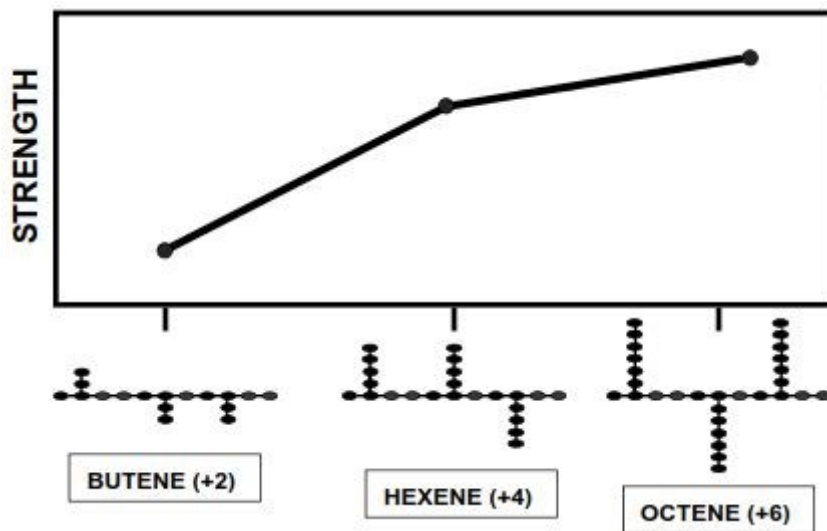


Figure 2. Example of co-monomers and their effect on the strength of PE [6].

2.3 Processability

PE materials and especially PE-LD are commonly used polymer materials in extrusion coating. It can withstand rather inappropriate conditions and still work sufficiently through the process and answer the original goal. Although PE is flexible material considering most of the processing conditions, it is still sensitive to the very high temperatures that are used in extrusion coating process. Some PE grades endure the processing conditions and work better than others, which is consequence of their better melt stability [4].

The melt stability of polymer can be analyzed via structural changes of the material, which occur during the extrusion process. One way to examine the structural changes is to measure the melt index of the extruded film [4]. As the extrusion temperature is increased with constant output rate, the melt index starts to decrease. This is consequence of the structural changes, more accurately crosslinking of the material. Crosslinking signifies bonding between the polymer chains, which increases viscosity and reduces the material flow. If the extrusion temperature is increased high enough, melt index starts to increase again. This is due to degradation and breakdown of the molecular structure. The polymer chains broke into shorter chain lengths, which decreases the viscosity and enhances the material flow [4, 9, 10]. Shear rate has also an effect to the structural changes during extrusion process. Lower shear regions enhances the crosslinking of the material and consequently melt index, if the temperature is not excessive high. Higher shear regions in turn, increase the degradation of the material and decrease melt index [9, 10]. Furthermore, the structural changes can also result from excessive residence time that is increased, as low output rates are used. The relationship between the melt temperature and melt index variation is illustrated in figure 3 [4].

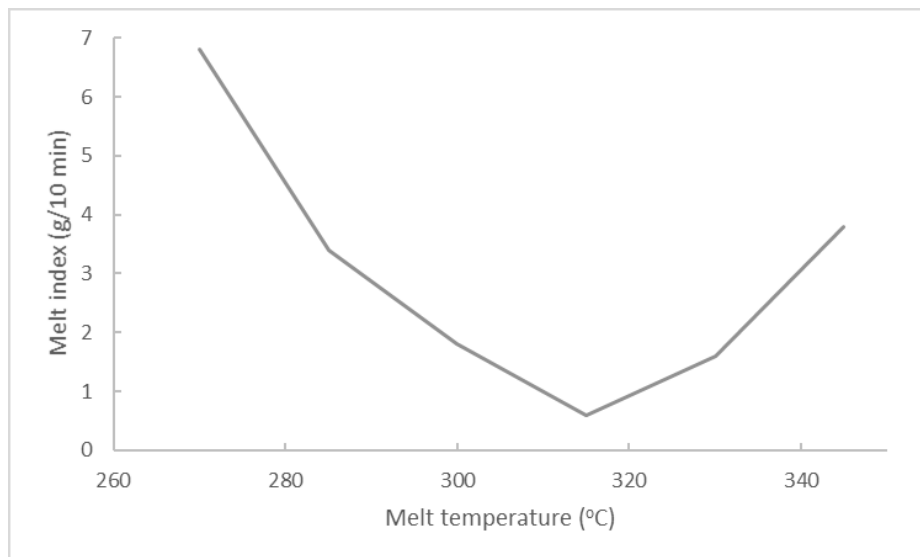


Figure 3. The relationship between the melt temperature and melt index [4].

The density of polymer varies during extrusion coating process similarly to melt index. The density of solid PE resins are usually over 0.90 g/cm^3 . As the material melts, the density decreases and PE grades have density around 0.80 g/cm^3 in the molten state [4]. However, the density does not return to its original solid phase level after the solidification, but remain slightly lower level. This is due to very rapid cooling of the molten film on the chill roll surface. The film cannot reach the original crystallinity during the very short solidification time and consequently the density remains lower than the original density [4, 9, 10]. This phenomenon intensifies when the density is increased. Consequently, PE-HD coatings have larger difference between the original density and film density than PE-LD. The decrease of density can cause problems concerning the quality of the product, since e.g. barrier properties and stiffness are worse than expected [4].

2.4 Properties of PE

PE has a few critical material properties that affect significantly the characteristics and quality of the PE film and consequently the extrusion coating product. These properties include average molecular weight and consequently melt index, molecular weight distribution and density that is proportional to crystallinity [2, 9]. Furthermore, the chain branching that is discussed above have a significant influence. The polymerization mechanism and manufacturing process conditions that are used to produce polyethylene material determine these essential material properties [2, 6].

2.4.1 Crystallinity and density

Polyethylene is semi-crystalline material that contains both amorphous and crystalline regions. In the amorphous areas, the polymer chains are located randomly i.e. random coil state. In the crystalline areas, the chains are arranged and packed partly parallel with each other. This increases the density of the material and therefore, the degree of crystallinity is proportional to the density [2, 6]. Furthermore, materials that have lower degree of branching are more crystalline and consequently the density is higher. PE-HD consists of polymer chains that have minor amount of side branches. Therefore, the chains can pack tightly next to each other, which increases the crystallinity value up to 90%. Alternatively, PE-LLD contains slightly more side branches and PE-LD can be branched widely. Therefore, they have smaller crystallinity and density values. Generally, the crystallinity of PE-LD and PE-LLD is around 50%. Crystallinity and consequently density affect many material properties that are significant and define the suitability for the extrusion coating applications [2]. Furthermore, it is notable that the original resin density is usually higher than the coating density, as explained above in section 2.3 [9, 10].

2.4.2 Molecular weight and melt index (MI)

Polyethylene, especially PE-LD, is polydisperse material that contains a mélange of different chain lengths and as a result, molecular weights vary significantly. Molecular weight affects via the viscosity greatly to the processability of the material. Melt viscosity of material is generally quantified by melt index. Melt index is inversely proportional to molecular weight and normally high molecular weight causes low melt index. Melt index is a crucial property relative to processing because it represents the flow of molten polymer. The flow resistance increases as the melt index decreases, since higher molecular weight constrain the flow more [2, 6]. Normally, increasing temperature enhances the material flow. However, the pressure can also affect the flow and therefore combination of different factors is crucial, when measuring and analyzing the material flow [6]. Higher melt index materials can be used in extrusion coating to achieve lower coating weights because of their good processability and drawdown, although higher melt index causes the neck-in value to increase [2]. Melt index and consequently molecular weight of polyethylene does not stay constant during the extrusion coating process. As explained above in section 2.3, the increase of melt temperature decreases the melt index at first but the value starts to grow again, when the very high temperatures are used. [9, 10]. The influence of melt index and density on crucial properties considering extrusion coating are collected in table 3 [2].

Table 3. *The effect of melt index and density on various properties [2].*

Characteristic	As melt index increases	As density increases
Melt viscosity	Decreases	Increases
Heat resistance	Stays the same	Increases
Chemical resistance	Stays the same	Increases
Permeability	Stays the same	Decreases
Extrusion speed	Increases	Increases
Drawdown	Increases	Increases
Elongation at break	Decreases	Decreases
Tensile strength at break	Decreases	Increases
Stress crack resistance	Decreases	Decreases
Flexibility	Stays the same	Decreases
Clarity	Increases	Increases
Gloss	Increases	Stays the same

2.4.3 Molecular weight distribution (MWD)

Another important property concerning the polyethylene properties is the relative distribution of different chain lengths and molecular weights in the material. This property is quantified by molecular weight distribution [2, 6]. Molecular weight distribution can be notably different between two materials, although the average molecular weight is the same [6]. The distribution is narrow, when the chain lengths are close to the average value and broad, when the variety of chain lengths is wide and numerous [2]. Molecular weight distribution has significant effect on the material properties. It is the most important factor that defines neck-in value in extrusion coating. Broad molecular weight distribution causes neck-in value to decrease [9, 10] Furthermore, broad molecular weight distribution improves the processability, melt strength and impact strength. However, the properties such as tensile and tear strength, stress cracking resistance, drawdown and optical properties are decreased at the same time [2, 6]. The difference between narrow and broad molecular weight distribution is illustrated in figure 4 [6].

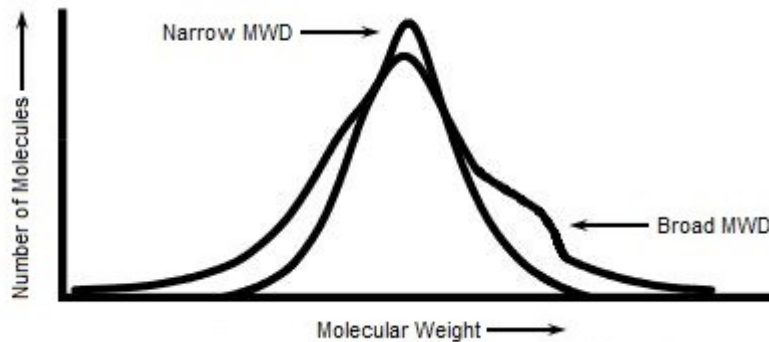


Figure 4. Comparison between the narrow and broad molecular weight distribution [6].

2.5 Manufacturing methods of PE

Traditionally, PE-LD has been manufactured with high temperature and pressure reaction systems. The two main systems that are used to produce PE-LD resin are autoclave and tubular processes. Both processes use pure ethylene gas as the feedstock of the reaction and oxygen or organic peroxide catalyst are mostly used to initiate the polymerization [4, 11]. The processing conditions are in key role for successful polymerization. The reaction temperature is roughly 150-300°C and the pressure is up to 2000 bar in autoclave reactor and up to 3500 bar in tubular reactor. After the polymerization reaction, the molten PE resin is granulated into final form, small spherical granulates. Not all the feedstock reacts in the process and depending on the process, only 20-35% of ethylene gas reacts into PE in the cycle [3, 4, 11]. This is due to the heat balance in the reactor [3]. Unreacted ethylene gas is separated and recycled back to the process. The basic structure of an autoclave reactor is a cylinder equipped with a stirrer that enables the mixing of the material and

more efficient heat transfer [3, 4, 11]. The tubular reactor is long and coiled tube that has relatively small diameter. The reactor does not include stirrers and the mixing is accomplished with turbulent flow [4, 11].

PE is also produced with several other polymerization and manufacturing methods in addition to autoclave and tubular systems. Low-pressure polymerization systems are developed to produce PE grades with specific and improved properties such as PE-LLD and PE-HD. The reactor pressures of the low-pressure systems are significantly lower compared to the autoclave and tubular processes [3, 4]. Depending on the method, the pressure is only up to 35 bar. Furthermore, the temperature is usually reduced [3]. Since the ethylene is compressed with lower pressure and temperature, these methods consume less energy [4]. Low-pressure systems utilize complex metal-based catalysts such as Ziegler-Natta, Phillips and metallocene catalysts [3, 4]. The manufacturing methods include particle form, solution and gas phase reactors, which all have their special conditions and purposes. In PE-LLD production, co-monomers such as butene and hexene are commonly incorporated to increase the branching and reduce the density [3, 4, 6]. The most common manufacturing methods and their suitability for producing different PE grades are presented in table 4 [6].

Table 4. *Manufacturing methods of common PE grades [6].*

	PE-LD	PE-LLD	PE-HD
Autoclave	x		
Tubular	x		
Particle form		x	x
Solution		x	x
Gas phase		x	x

2.5.1 Basic properties of autoclave and tubular PE-LD

Formerly, the autoclave reaction system was much more common way to produce PE-LD, but the favor of the tubular reaction system is constantly increasing [4, 12]. Currently, the production of tubular PE-LD grades are already higher e.g. in North America and the manufacture and market share are expected to increase further [12]. Furthermore, the tubular process has higher capacity and lower investment costs, which favors their use even more [13]. Generally, autoclave PE-LD grades have better film stability and as a result

lower neck-in compared to tubular PE-LD [12, 14]. In addition, processability of autoclave PE-LD grades is excellent. Processability and lower neck-in is due to high degree of chain branching and broad molecular weight distribution [13]. Alternatively, the tubular reactor provides narrower molecular weight distribution [13, 14]. Tubular PE-LD grades have better drawdown and achievement of lower coating weights is possible [12, 14]. However, compromising is often necessary and in practice, the properties are combined by blending autoclave and tubular grades together [14].

The properties of both autoclave and tubular PE-LD are greatly affected by the degree of chain branching and molecular weight distribution [13, 14]. The chain branching and molecular weight distribution are defined by the manufacturing conditions of the reactor, where the polymerization reaction occurs. In autoclave reactor, the constant mixing of new feedstock and partly reacted PE causes back mixing and as a result chain branching. Furthermore, the residence time is irregular between the PE chains, which causes the formation of different chain lengths. In tubular reactor, the feedstock moves constantly forward inside the long tube and therefore the residence time is roughly the same for each PE chain. This induces more even polymerization and consequently molecular weight between PE chains than in autoclave reactor. The effect of manufacturing method shows clearly, as the molecular weight distributions of autoclave and tubular PE-LD are compared. This comparison is illustrated in figure 5 [13].

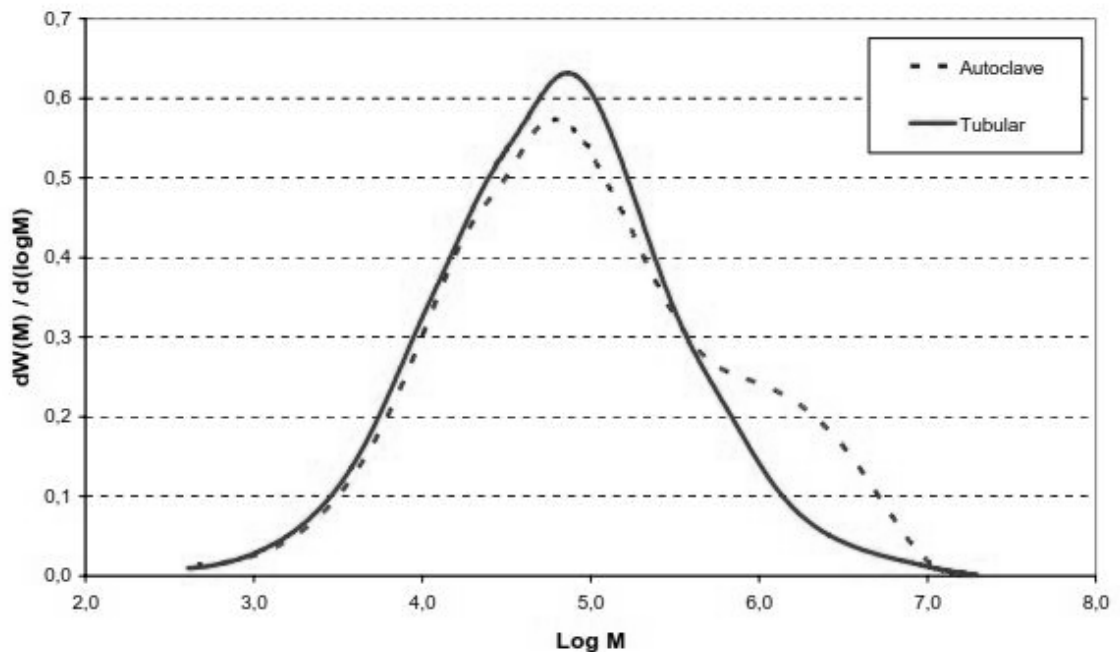


Figure 5. Molecular weight distribution of autoclave and tubular PE-LD [13].

2.5.2 Autoclave and tubular processes

Autoclave reaction system that uses high temperature and pressure is the most common method to produce branched PE-LD. The manufacturing process consists of several different stages, which convert ethylene gas into solid PE resin [3, 4, 11]. The process starts with the pressure increase of the ethylene, which is done in two stages. The pressure is raised in primary and secondary compressors and the end pressure is up to 2000 bar before ethylene is transferred into the reactor. The catalyst that initiates the polymerization reaction is inserted to the reactor with separate pump. Autoclave polymerization of PE is mainly done with organic peroxide catalysts, which initiate the free radical polymerization reaction. The temperature of the reactor is maintained at 150-300°C depending on the instance and the material is stirred constantly [3, 11]. The temperature cannot be excessive, since the decomposition temperature of PE is around 360°C in the reactor conditions. The ethylene stays in the reactor under a minute and the polymerization occurs simultaneously. The double bond of ethylene monomer is broken by the initiator and reaction conditions, which allows the combination of monomers by chain growth polymerization mechanism. In free radical polymerization, the ethylene does not polymerize into straight chains but forms plenty of different length side chains [3]. The free radical polymerization of PE-LD is shown and explained in figure 6 [3, 15].

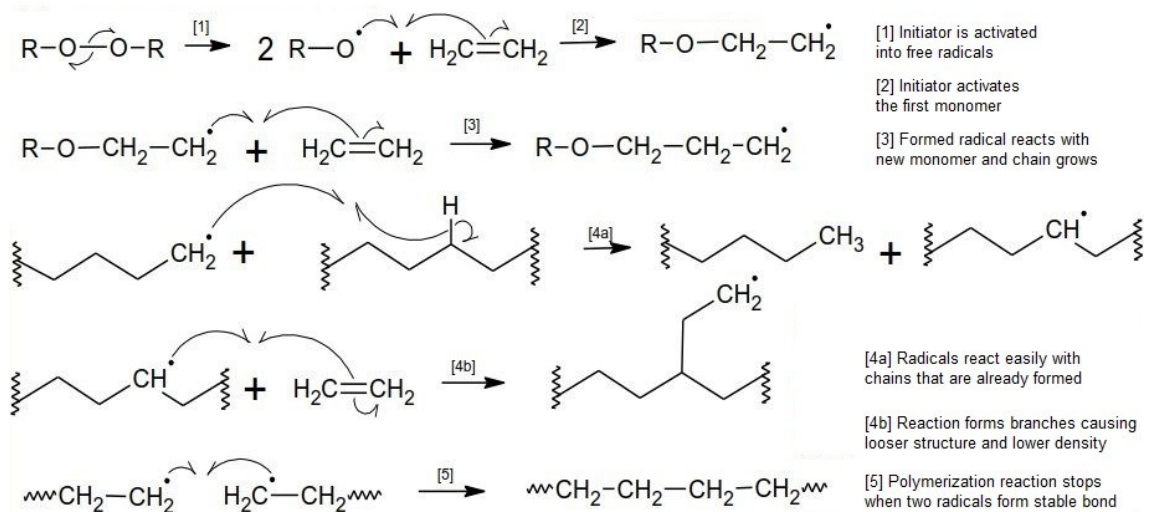


Figure 6. Free radical polymerization mechanism of PE-LD [3, 15].

The properties of reacted PE are not constant and the properties can be influenced by reactor temperature and pressure. Furthermore, degree of branching, length of branches and molecular weight can be modified by adding light hydrocarbons in the feedstock. After the reactor, the pressure is reduced in high-pressure and low-pressure separators. Conversion of the ethylene is nowhere near complete and in the separators, unreacted ethylene gas is diverged from the molten PE and recycled back to the process. Finally the molten PE is transferred into the extruder, where possible additives are added and the

material is extruded to granulates [3, 11]. The simplified process flow chart of an autoclave process is presented in figure 7 [3].

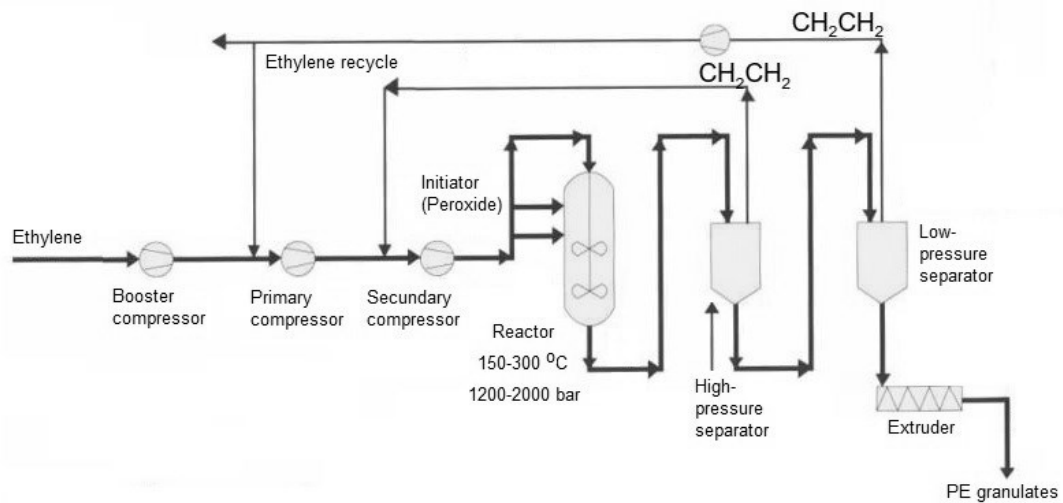


Figure 7. Autoclave manufacturing process of PE-LD [3].

The basic structure of the tubular reaction system is rather similar to the autoclave process. The pressure of ethylene feed is first increased to the reaction pressure level in primary and secondary compressors. Possible co-monomers are also inserted at the compression stage. Thereafter, the ethylene flow and oxygen or peroxide catalyst that initiates the reaction are transposed into the reactor [11, 16]. The structure and conditions of the reactor are the major difference compared to autoclave process. Tubular reactor is long and narrow coiled tube, where the residence time is some minutes and the mixing is generated by turbulent flow. Furthermore, the reaction pressure is significantly higher compared to autoclave process reaching over 3000 bar [4, 11]. The final stages of tubular process are high- and low pressure separators, where the pressure is dropped and unreacted ethylene gas is removed and recycled, and extrusion to granulates [11, 16]. The properties of the product are adjusted similarly to autoclave process by modifying the reaction temperature and pressure in addition to co-monomer insertion. As the temperature is increased in the reactor, density of the final product is decreased whereas melt index is increased. The pressure increase has the opposite effect and density is risen whereas melt index is reduced [11]. The simplified process flow chart of tubular process is illustrated in figure 8 [16]. Furthermore, the main differences between the autoclave and tubular processes are considered in table 5 [11, 13].

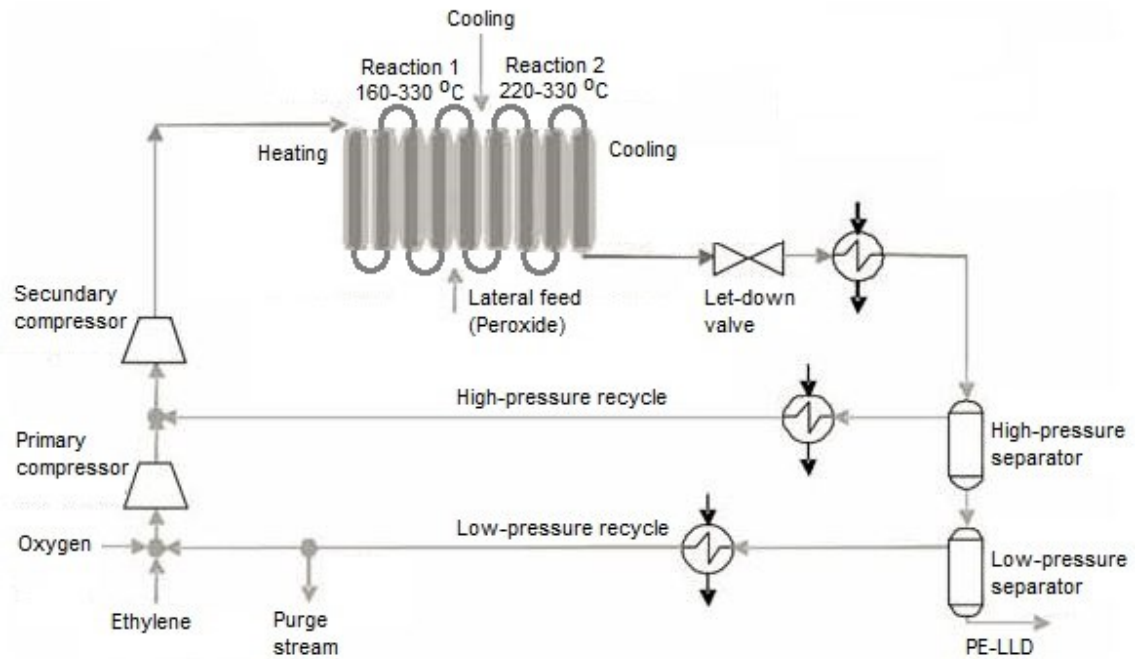


Figure 8. Tubular manufacturing process of PE-LD [16].

Table 5. Comparison of autoclave and tubular manufacturing method [11, 13].

	Autoclave	Tubular
Conversion	Around 20%	Up to 35%, (lower costs)
Pressure	1200-2000 bar	2400-3200 bar
Initiators	Peroxides only	Oxygen also possible
Heat removal	Removed by reactant only	Partly removed by coolant
Capacity	Lower (up to 150 kt/a)	Higher (up to 400 kt/a)
Product properties	Broad density range, broader molecular weight distribution, lower neck-in, higher copolymer content possible	Broad density range, narrower molecular weight distribution, better drawdown, higher clarity, cleaner products

3. EXTRUSION COATING PROCESS

Extrusion coating process contains extrusion of a molten polymer film onto a moving substrate. The product is usually paper or paperboard coated with thin layer of plastic, which can be used for example packaging applications. The main parts of extrusion coating equipment are hopper, extruder, adapter, die, laminator and auxiliary equipment. The main parts of extruder are considered next [17]. Extrusion coating equipment are shown in figure 9, which illustrates the pilot line of Tampere University of Technology (TUT) [18].

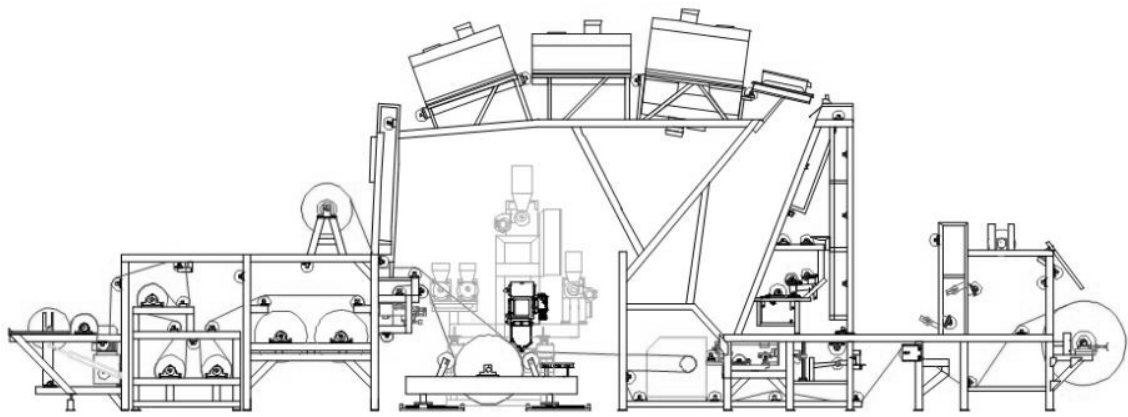


Figure 9. The extrusion coating line in TUT [18].

3.1 Extrusion coating equipment

A hopper controls constant and adequate feed to the extruder. Changes in the filling level of hopper can cause pressure variations at the feed throat and consequently instability to the extrusion process. A carriage base is the mount for extruders with their components such as motor, transmission, barrel and die supports and cooling system [17].

An extruder is the main device in extrusion coating process and it has several important functions [19, 20]. The extruder melts the solid polymer material and transfers it to the die lips at precise temperature and flow rate [19, 21]. Rotation of the screw conveys the polymer material forwards and simultaneously plasticizes it into homogenous melt [17, 19]. Sufficient mixing of the melted material is crucial to avoid any defects in the final product such as pinholes and voids [21]. Moreover, the extruder generates the required pressure to the process and meters the melt properties in the die [19, 20]. Single screw extruder is the most common extruder type and it covers over 90% of all extruders [19, 21]. The extruder can be divided into three sections based on the geometrical or functional

sections. The geometrical sections include feed, compression and metering and the functional sections contain solid conveying, melting and melt conveying. The structure and main components of single screw extruder is presented in figure 10 [19, 20].

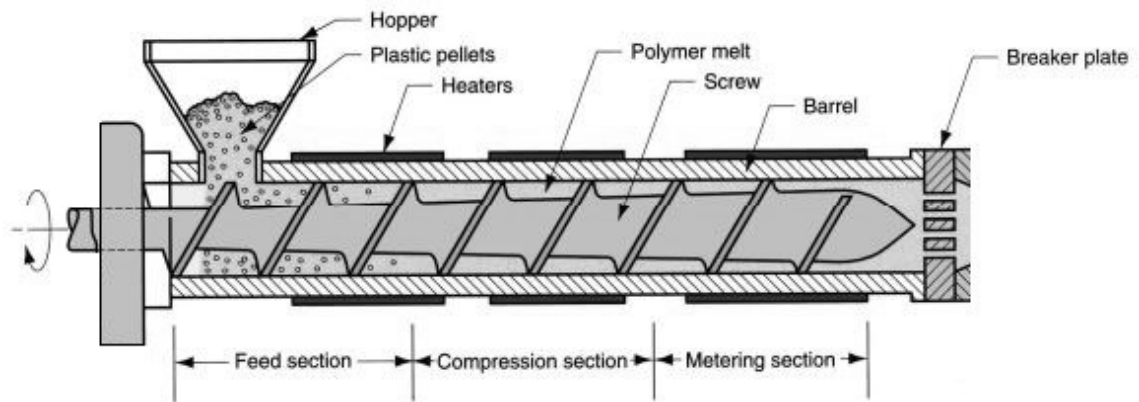


Figure 10. Components and geometrical sections of single screw extruder [19].

The feed section rations the polymer material into extruder and conveys it forward. Conveying of the material is dependent on the polymer friction between the barrel and screw [19, 20]. At the feed section, the friction between the barrel and polymer should be higher than between the screw and polymer to achieve effective conveying and optimum output. Therefore, the surface of barrel is often grooved whereas the screw is smooth [17, 19]. Cooling of the barrel is usually necessary to avoid bridging that is caused by premature melting of the plastic granulates [17].

Melting of the material occurs mainly in the compressing section. The diameter of screw usually increases in the compression section, which decreases the depth of screw channel [19, 20]. The barrel is surrounded by the heaters, which melt the material during start-up and control the barrel temperature at processing stage [17]. However, the heaters have low efficiency due to low thermal conductivity of polymers, which decreases their influence [19, 20]. Melting is mainly consequence of the friction between the material and screw and barrel [17]. The screw rotation and causes internal frictional heating of the polymer, which accelerate the melting [19, 20]. High output rates cause considerably high amounts of friction and consequently excessive heat. Therefore, water-cooling of the barrel is sometimes necessarily. Heating and cooling systems, thermocouples and temperature controllers enable a precise temperature control that is essential for some polymers due to narrow operating temperature area [17]. The process parameters related to extruder such as the temperature profile are discussed more closely in section 4.1.

The last section of the screw is the metering section. The polymer melt should be homogenous at the end of the screw and therefore metering section usually includes some kind of mixing device. The mixing can be distributive or dispersive and the mixing device is chosen according to the material properties and application requirements [19, 20]. At the

end of the barrel, the polymer melt flows through a screen pack and a beaker plate. The screen pack filters impurities from the melt and increases back pressure. The beaker plate supports the screens and produce a stable laminar flow. After the beaker plate the polymer melt proceed into the adapter, which includes melt temperature and pressure sensors. Sometimes back pressure valve can be used after the adapter to reach optimal melt temperatures without excessive back-pressure levels. The back pressure eliminates fluctuations of the output by generating pressure, that is distinctly higher than pressure variations of the melt in the extruder. Transmission of the mechanical energy from screw to polymer is also consequence of the appropriate back pressure [17].

The die shapes the melted polymer material into desired form cross sectional form, which means wide but thin film in extrusion coating applications [17, 19]. The die generates a uniform film thickness profile by control of the die gap. The die also maintains desired melt temperature and determines the coating width [17]. The two main types of extrusion coating dies are T-die and coat hanger die [17, 19, 21]. These die types are illustrated in figure 11 [19].

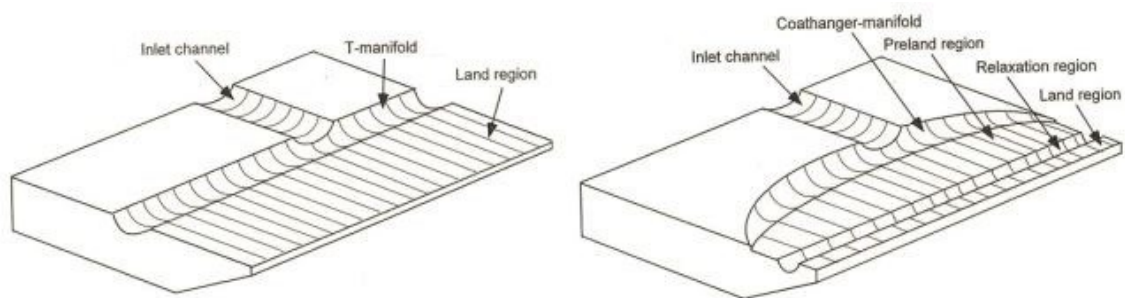


Figure 11. *Extrusion coating dies, T-die on the left and coat hanger die on the right [19].*

One of the essential functions of a die is to produce melt flow with uniform velocity and flow rate across the whole width of the die [17, 19, 21]. The uniform flow rate can be achieved by controlling the flow paths inside the die [5]. Generally, the die consist of three sections, which have different requirements and functions. The first section is the manifold that distributes the melt evenly to the preland [17, 19]. The resistance of flow can be controlled with the volume of manifold [17]. After the manifold, the melt flows to the die land or preland [17, 19]. The function of preland is to cause sufficient pressure drop so that the melt flow at lips is uniform across the whole width of die [17]. The final section of the die is the primary land or lips. The die gap is set across the width of die and the lips determine the thickness of film. [17, 19] The final width of film can be adjusted by an internal or external deckling system [17]. There are few essential differences between T-die and coat hanger die. The advantage of coat hanger die is that the melt flow of polymer is increasing from the center to each side causing the same resistance to flow across the whole width of die [17, 19]. Moreover, the cross section area of the manifold decreases from the center to sides, which causes as short residence time as possible [17].

Laminator system consist of pressure, chill and stripper rolls. The chill roll is metallic, double-walled and water-cooled [17, 21]. The surface finish of chill roll is important because it defines release characteristics, optical properties and the coefficient of friction [17]. The function of chill roll is to remove as much heat as possible from the polymer film, when it is solidifying and the water-cooling ensures the effective heat transfer. In addition, the diameter of roll should be large enough to enable the sufficient contact time, which decreases at high line speeds [21]. The pressure roll or nip roll is rubber coated and water-cooled [17, 21]. It creates sufficient pressure at the nip. The rubber coating must have great resistance to heat ageing and work hardening properties [21]. The pressure roll has great influence on adhesion, coating integrity and appearance [17]. The structure of laminator system is shown in figure 12 [17, 19].

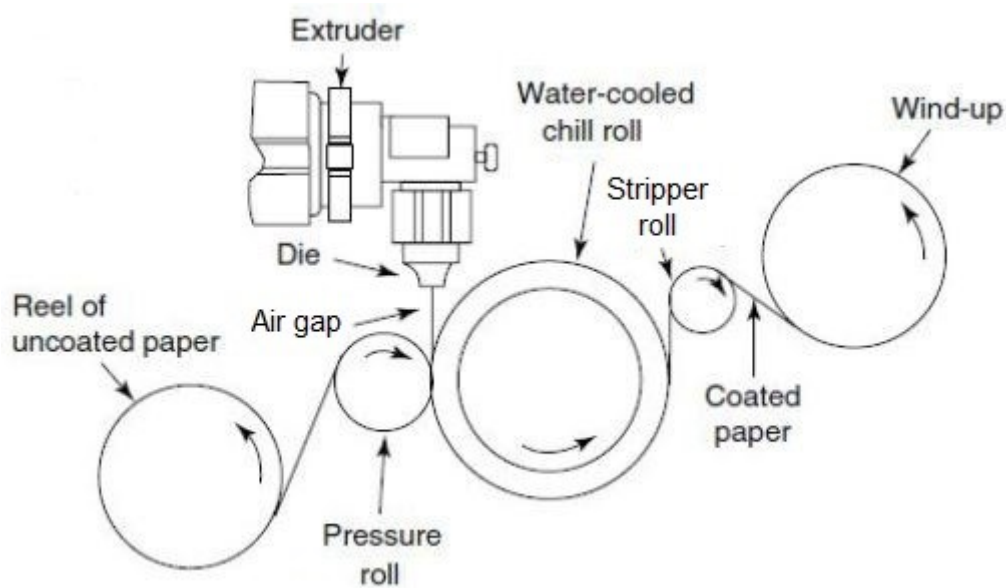


Figure 12. Laminator system of extrusion coating [17, 19].

The main function of laminator system is to form adhesion between the polymer film and the paper or paperboard. It also solidifies the molten material. Usually the design of laminating system allows vertical and horizontal moving so that the air gap between die and nip can be varied. In some cases, it can be achieved also by moving the extruder carriage [17]. The height of air gap or curtain height determines the oxidation time of the polymer melt in atmosphere [17, 21]. The air gap affects greatly to many key properties of the final product [21]. Air gap and consequently residence time must be optimized for each application and material [17]. High residence time increases oxidation and consequently improves the adhesion but also increases cooling of the molten film, which simultaneously weakens the adhesion. High residence time also leads to large neck-in when operating at high line speeds [17, 21]. Neck-in in turn causes forming of thicker edges and wastes material [17]. However too small air gap and residence time causes deterioration of adhesion since the oxidation of the polymer film is not sufficient [21]. Due to previous

reasons, optimizing the system is crucial [17]. The air gap, oxidation and their influence on adhesion and other key properties are discussed more closely in section 4.2.

3.2 Flame and corona treatment

Flame and corona treatment methods are means to improve adhesion between the polymer film and substrate [17]. The flame treatment is mainly used for coatings of heavy paper and paperboard [2]. The flame treatment system consists of a ribbon burner that is equipped with one or more oxidizing flames and the width of the flames can be adjusted [17]. The substrate is exposed to direct flame when it passes by the burner. This modifies and oxidizes the surface of substrate slightly [2, 17]. Free electrons and thermally activated polar groups such as -O-, -OH, and -NO are formed in the combustion reaction. This matter reacts with the surface and form functional groups that promote adhesion [17]. The advantages of flame treatment devices are simple design and operation as well as low costs. Flame treatment can also prevent the formation of pinholes [2].

The corona treatment can be used both pre- and post-treatments of the extrusion coating process. The system includes the high-frequency generator, high-voltage transformer and treater station equipment. The treater station contains dielectric roll cover, grounded roll and electrode [17]. The electrode is usually made of ceramic or quartz [2]. The corona treatment is based on the difference in the dielectric breakdown voltage of air gap and paperboard. When the high-voltage and -frequency power is applied across the system, the air gap ionizes and forms gaseous conductor [2, 17]. The surface of substrate is bombarded with electrons, which breaks molecule bonds and the oxidants in the corona such as ozone and oxygen form oxidized groups with free radicals of the surface [17]. Introduction of polar groups to the surface increases surface tension and energy and consequently improves adhesion [2, 17]. The corona treatment produces ozone so a ventilation system is usually needed at the treater station [2].

3.3 Co-extrusion

Co-extrusion enables to combine multiple polymer layers into one film [17, 22]. Many processes use co-extrusion to optimize performance of the product. This is achieved by combining polymers with different properties into products with combined features that are not feasible using single polymer [23]. Compatibility of different polymers has great importance in co-extrusion and certain materials does not match with each other and form adhered structure. The compatibility of some polymer materials is shown in table 6 [22].

Table 6. *Compatibility between polymers for co-extrusion [22].*

Material	PE-LD	PE-HD	PP	PA	Ionomer	EVA
PE-LD	3	3	2	1	3	3
PE-HD	3	3	2	1	3	3
PP	2	2	3	1	2	3
PA	1	1	1	3	3	1
Ionomer	3	3	2	3	3	3
EVA	3	3	3	1	3	3

1: Layers easy to separate.
2: Layers can be separated with moderate effort.
3: Layers difficult to separate.

There are two basic types of co-extrusion system, which are a single manifold or a feed-block die and a multimanifold die. In addition, combination of the previous and dual slot die are occasionally used [17, 22, 23]. Generally, co-extrusion systems use the single manifold die with combining adapter and two or more extruders and feedblocks in the line. The thickness of each layer is regulated by the screw speed of each extruder and the total thickness profile of film is adjusted by the die gap control as in normal extrusion [17]. The different melt flows are combined together before entering the die via special adapter [22]. The advantage of single manifold die is the integration of melt flows before the die. This enables simpler and less expensive structure for the die [23]. The single manifold die system has also some problems concerning the viscosity [17]. The melt flows of polymers must be laminar to avoid the mixing [22, 23]. This is achieved, when the viscosities of materials are similar and secondary effects are not present [23]. Difference in viscosity values can cause irregular melt flow, uneven product surface and layer thicknesses and encapsulation of a layer [17, 23].

The multimanifold die has own manifold for conveying each polymer material and the combining of melts takes place inside the die before the lips. The multimanifold die system is more complicated than single manifold die system and the use of several extruders is possible [17, 22, 23]. The combining adapter can also join more melt flows and hence layers together than the system has extruders [17, 22]. The main advantage of multimanifold system is that the different polymer melts can be in distinctly different temperature. This is result of brief contact time of melts before cooling and therefore viscosity and flowing differences does not affect the product much [17]. Multimanifold system also enables more precise control of the layer thickness [22]. The short contact time of melts can also be a disadvantage to the product, because diffusion of different polymers and consequently proper adhesion can require longer time. The other clear disadvantage of multimanifold system is the costs of the equipment and especially the die due to complicated structure [17, 22]. The main differences of single manifold or feedblock and multimanifold die systems is presented in table 7 [22].

Table 7. *Comparison of feedblock and multimanifold dies [22].*

Characteristic	Feedblock	Multimanifold
Structure	melt streams meet before the die	melt streams in separate manifolds, meeting before the lips
Cost	lower	higher
Operation	simpler	more complex
Complexity	simpler	more complex
Number of layers	not restricted	generally 3 or 4 layers
Layer uniformity	individual layer thickness $\pm 10\%$	$\pm 5\%$ is possible
Viscosity range	ratio between materials up to 3/1	usually larger than 3/1
Heat sensitivity	larger	smaller
Bonding	potentially better, longer contact time for layers	worse

The co-extrusion process in general has numerous advantages that can improve the product quality or ease the processing and some of them are considered next [17]. One of the main reasons for co-extrusion process is the costs. Quantities of expensive polymer can be decreased by thinning the layer thickness and using supporting layers of cheaper polymer [17, 22]. Cost reduction can also be achieved by using additives only in the surface layer. Moreover, the capacity of process may be increased by co-extrusion. Another reason for co-extrusion is improving the properties of product. Adhesion can be improved by choosing an adhesive polymer to the bottom layer against a substrate [17]. Amount of pinholes can be decreased and consequently improve the barrier properties by processing multilayer structures [17, 22]. Pinholes can be reduced even with a single extruder and material by dividing the melt into two-layer structure [22]. Heat sealability can be improved by choosing a suitable polymer to surface layer. Processing can be eased by using supporting polymers to run polymers that are hard to machine [17]. Other advantages of co-extrusion include reduction of delamination and air entrapment [22].

4. KEY PROCESS PARAMETERS AND PRODUCT PROPERTIES

There are multiple process parameters and product properties, which affect the quality of extrusion coating products. The end use of the product define the desired properties, which are tailored by adjusting the process conditions and parameters. The most significant factors and properties considering PE coating of the paperboard are discussed next. These include melt temperature of the polymer, adhesion, heat sealability, pinholes, coating weight, drawdown and neck-in [17, 21].

4.1 Melt flow and temperature profile in extrusion

Extruder converts polymer materials from solid to molten state by using the frictional heating as well as the external heat source. The process parameters and technical limits are determined by the properties of material, energy requirement and output. The output of extruder is dependent on the properties of polymer, screw geometry and back pressure [17]. The flow of material inside the extruder consists of couple of different components. Drag flow is caused by the relative motion between the material and screw and barrel. Pressure flow in turn is caused by the back pressure, which is affected by the type of die. There can also be some leakage flow between the flight of screw and barrel but it is usually considered negligible [19, 20]. The screw and die of the extruder have characteristic curves. They can be illustrated by plotting the pressure drop as a function of flow rate. The optimal operating point of the extruder is the intersection of the characteristic curves. The operating point will change along with the modifications to the die or screw settings. The operating point and its shift along with the characteristic curves is shown in figure 13 [19].

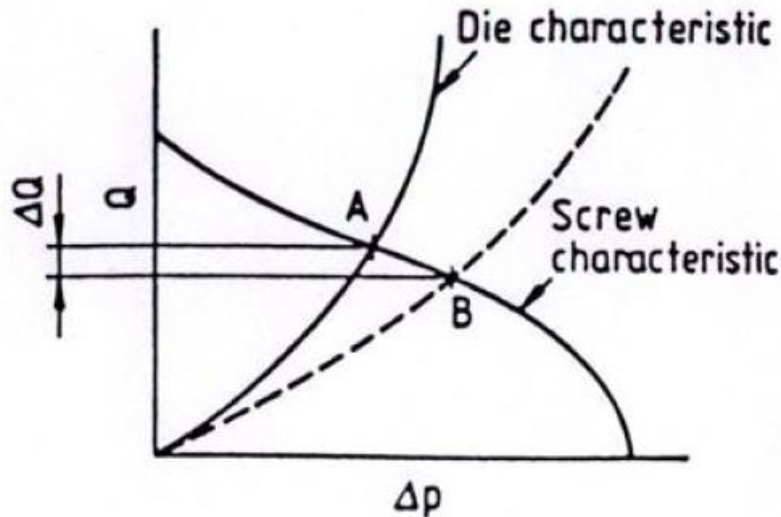


Figure 13. Shift of operating point in consequence of characteristic curves [19].

The melt conveying capacity of the screw is very important factor in any extrusion process. Generally, the three zone screws are used, which include feed, compression and metering sections. Length per diameter (L/D) ratio is affected by the screw design and usually the goal is to get the highest possible output [17, 19]. L/D ratio is usually at least 25 to ensure the homogeneity of the melt [21]. The mixing of material is increased by decreasing the channel depth of the metering section but its significance diminishes at the high temperatures of extrusion coating process. The homogeneity of melt and further the melt temperature are significant factors in extrusion process. The melt temperature affects greatly to the rheological behavior of the material. The extrusion process is considered ideal if the polymer melt does not have rheological gradients in machine and cross directions after the die [17].

4.1.1 Melting mechanism

Generally, the melting of the polymer begins with a dissipative melting mechanism. The solid bed melts along the screw channels and melt pool increases. When the solid bed becomes too small, it cannot hold together and breaks into pieces. This is called solid bed break-up. Thereafter, the melting occurs via conduction melting mechanism, which is inefficient due to the low thermal conductivity of polymers. This can result in non-homogenous melt including small solid polymer particles. Therefore, the solid bed break-up can cause fluctuation to the pressure and flow rate and therefore it should be avoided. The problem with solid bed break-up can be solved by using a barrier screw. The barrier screw has own channels for melted and solid materials and therefore solid bed break-up cannot occur. In that case, the operating window is narrower than with the conveying type screw design [19, 20]. Solid bed break-up and the barrier screw are illustrated in figure 14 [19].

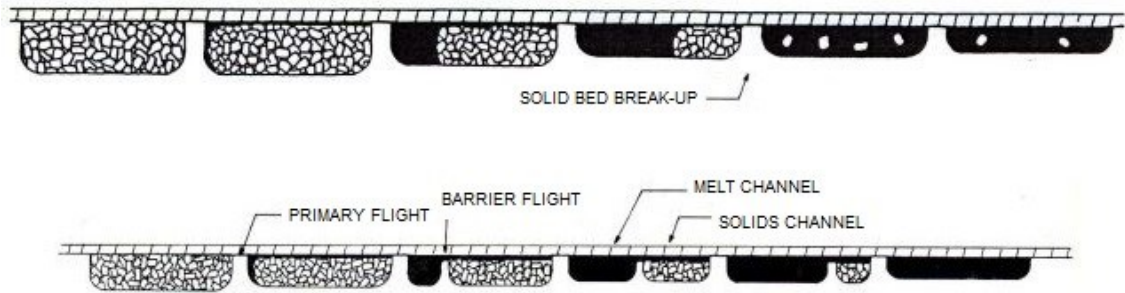


Figure 14. *Solid bed break-up in conventional screw and barrier screw with two channels [19].*

4.1.2 Temperature profile

There are several different ways to determine the optimum temperature profile such as raw material supplier recommendations, trial and error methods and statistical tools. Moreover, when working with familiar materials and products it is possible to use previous information and experience from the process and conditions. Material supplier can usually provide important information such as recommended temperature profile and L/D ratio, optimum screw design and suitable die design and drawdown ratio. Some parameters can be used as such and some require adjustment to the current process. Especially the temperature profiles of barrel zones and die may need varying until the product meets the quality standards. It is essential to record the process conditions along with the product samples during optimization. This information can be utilized later for example with statistical methods to find the optimum temperature profile. The temperature profile that works best with current extruder and material is always a function of many different factors. It depends on the resin type and viscosity, screw design and throughput [24].

The most common temperature profiles are increasing, decreasing, flat and humped profiles. Increasing and humped temperature profiles are generally used in extrusion coating of polyolefin products. The feed section has the lowest temperature, which increases in the compression section and finally moderates or slightly decreases before the metering section [17, 24]. Lower feed zone temperature restrains untimely melting and minimizes melt plug formation i.e. bridging. Too hot feed section temperature can also reduce the friction between the barrel and polymer and therefore affect the throughput. The feed section transfers the material to the compression section, where the temperature profile increases to the desired melt temperature value and moderates [19, 20, 24].

The compression section melts the material and the frictional heating between the material and the machine collaborate with the barrel heating. In many applications, the barrel heating is mainly used for maintaining of the temperature because majority of the heat derives from the frictional heating. However, in extrusion coating the importance of barrel heating increases because the melt temperature is extremely high [19, 20, 24]. Conductive barrel heaters produce accurate and appropriate temperature during the process. Usually

the extruder is divided into several heating zones, which enable to create temperature gradient along the whole length of barrel. The heating is mainly performed with electrical resistance band heaters and temperature sensors are located at every heating zone to monitor the temperature value. However, the sensors monitor only the barrel wall temperature, which does not absolutely correspond the actual melt temperature. The cooling of the barrel or screw with heat conducting medium is also possible and often recommendable with thermally sensitive materials [19, 20].

In the metering section all the polymer material should be melted. If some solid particles are still present, it may cause the overheating as the screw processes solid material in the shallow channel. Moreover, solid material in the metering section cause solid bed breakup and consequently fluctuation [24]. In many cases, the homogeneity of temperature is accomplished by decreasing the temperature profile of barrel slightly at the metering section. This causes the moderation of melt temperature and prevents overheating near the barrel wall [17]. Temperature profile of the adaptor, connecting pipe and die should be set to only maintain the gained melt temperature [17, 24].

4.1.3 Effects on product properties

The optimum temperature conditions required to produce good quality extrusion coating products depend on several factors and different manufacturing units, material batches and suppliers cause variation to quality. The important product properties such as uniform coating weight and adhesion are greatly influenced by the temperature profile and melt temperature. Some properties such as gloss and clarity are improved by the increase of temperature. Adhesion is also promoted by the higher temperatures since the oxidation is intensified. However, too high temperatures lead to various problems. The melted material can be too running for coating, the cooling and winding up might become difficult. Moreover, the excessive oxidation may deteriorate the heat sealing properties. The degradation of material also accelerates, when the temperature is increased, which can lead to unwanted modifications in the appearance and properties of the product. Moreover, the uniformity of temperature across the melted material is as important as the right temperature value. Fluctuations can cause uneven coating thicknesses and widths, variations in gloss, clarity and wrinkles and pinholes. Typical temperature value for PE-LD extrusion coating is between 300 and 320°C but anything between 265 and 330°C is possible [21].

4.2 Adhesion

The properties and performance of the extrusion coating products depend on numerous material properties and process parameters. One of the most important property that defines the performance and quality of the product is adhesion between the polymer film and the substrate material [25]. Adhesion between the polymer and substrate isn't self-evident and achieving sufficient adhesion can be sometimes challenging especially when

the line speed is high and source reduction and thinner coating is desired [17]. If the adhesion is poor, the coating can be peeled off from the substrate and the product becomes useless for its original purpose [21].

The adhesion mechanism of polymer materials can be mechanical, chemical or both depending on the substrate that is coated [21, 26]. Paper and paperboard are porous substrates and the adhesion with the polymer is usually considered as mechanical bonding, although chemical bonding have also minor role in promoting the adhesion [25]. Polymer coatings can form mechanical adhesion bonds with porous substrates as the melted material flows into the pores and the two surfaces lock physically together. If the substrate is non-porous and smooth, the coating does not have sufficient spots to get locked and therefore materials can't mechanically bond. In that case the adhesion must be induced with chemical bonding [21]. Mechanical adhesion is improved if the viscosity of the molten film is low and therefore it must not cool excessively in the air gap before contacting the substrate. Chemical bonding in turn, demands enough thermal energy and functional groups on the surface of the film to react with the surface of the substrate [25]. There are multiple factors that are affecting the adhesion value and some of them are presented in figure 15 [17, 21].

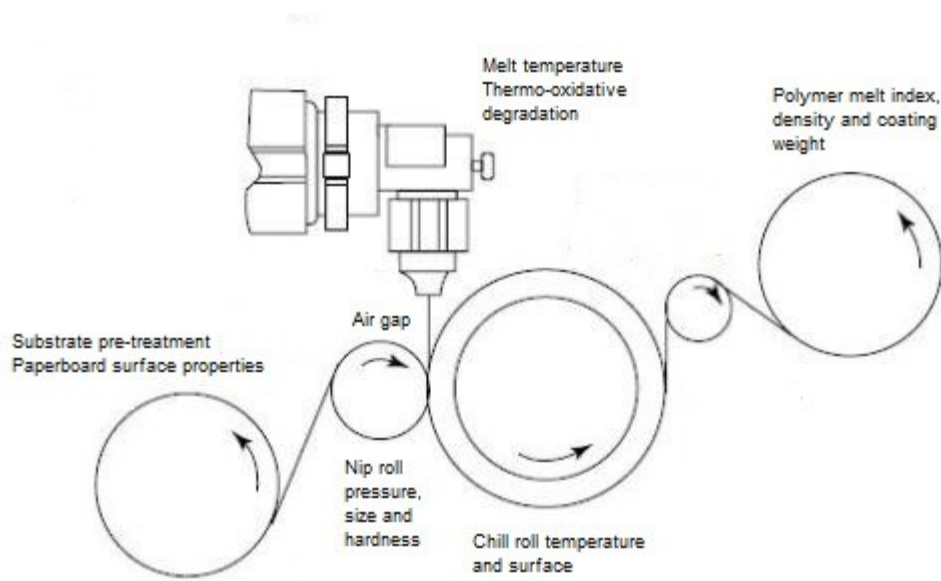


Figure 15. *The main factors that define adhesion properties [17, 21].*

4.2.1 Factors affecting adhesion

The chemical composition and topography of the paper or paperboard determine a large part of the adhesion properties [17, 21, 27]. Strong and sufficient adhesive bonding requires several different factors, which include lack of weak boundary layers, extensive interfacial molecular contacts and sufficient surface energy [17, 27]. Moreover, the polymer material has several important properties that are affecting the adhesion. Generally

lower viscosity or higher melt index values result in better adhesion because the contact with the substrate is extended and penetration is eased. An increase of the coating weight also improves adhesion properties because a larger mass flow contains more energy and improves the surface oxidation and fluidity [17, 21, 27]. However, the adhesion is very rarely improved with the heavier coating weight because the source reduction is essential for the reduction of costs. If the adhesion between the polymer and substrate is not sufficient despite the precise process and material control, additional surface treatments such as flame and corona can be applied to the substrate to improve adhesion [17].

In extrusion coating, the temperature profile of polymer material has substantial effect to the adhesion. Higher processing temperature enhance the mechanical adhesion properties such as interlocking. Additionally, the chemical adhesion is improved since the higher temperature increased the oxidation of film surface in the air gap, which enhances chemical bonding between the film and the substrate [17, 21, 27]. However, excessive high temperatures can result in over-oxidation and low molecular weight layer, which decrease the adhesion. Along with the air gap, thermo-oxidative degradation in the barrel has also significant effect on adhesion. Polymer material can degrade in the barrel as a result of thermo-mechanical stress and oxidize by ambient oxygen. The rate of reaction is mainly due to processing temperature but the material, screw, back-pressure and output have an influence too [17].

Some of the properties of successful coating including adhesion are determined during the solidification process, which occurs between the die gap and chill roll. The simplified principle of chill roll is that the excess heat of molten polymer is conducted into the cooling water inside the chill roll [17, 26, 27]. Too low chill roll temperature can weaken the adhesion because the polymer melt cools too rapidly [21, 26, 27]. The nip roll affects the adhesion through several important parameters such as roll size, hardness and pressure. Increase of the nip pressure generally improves adhesion but if the pressure is excessively high, pinholes can be formed into the coating [17, 21, 28]. Moreover, the increase of pressure excessively does not give extra benefit [21, 28]. An increase of the nip width generally improves the adhesion along with the pressure. Additionally, hardness of the roll must be sufficient to ensure proper adhesion properties [17, 28].

4.2.2 Orientation and oxidation

In the air gap, where the polymer film proceeds from the die to the nip, material undergoes changes that are affecting to the product properties especially to adhesion. The changes can be both chemical and physical such as chemical reactions, oxidation, cooling, orientation and stress relaxation. These chemical and physical changes are usually functions of time and therefore adjusting the air gap is crucial to the product properties [25, 29].

The molecular chains orientate in the machine direction, as the polymer film is drawn in the air gap. This orientation alters the mechanical properties of the material. When the

film contacts the chill roll, it quenches and solidifies very quickly. Consequently, the molecular chains are frozen at orientated state preventing relaxation back to the random coiled state. This causes forming of residual stress on the bonds between the film and the substrate, which decreases adhesion properties. Some residual stress is formed into the material in the extruder, particularly in the high shear rate zones but most of the stress is formed at the draw down phase, where the film achieves its final thickness. The amount of stress is associated with the amount of stretch and the rate of strain [29].

The chemical bonding between the substrate and the coating is achieved with oxidation of the polymer film surface. Proper oxidation of the polymer and consequently adhesion requires high melt temperature and an appropriate drawdown distance or air gap [21]. In spite of the cooling, adhesion usually enhances with increasing air gap distance. The main reason regarding polyethylene film adhesion is oxidation of the material [25]. Polyethylene is non-polar polymer and it requires oxidation to bond sufficiently to polar substrate such as paper and paperboard. Oxidation of the material causes formation of polar functional groups that enhance adhesion and the amount of functional groups depends on the oxidation time [25, 29].

Some factors such as higher air gap, higher melt temperature, greater coating weight and lower line speed increase the amount of polymer oxidation and therefore improve the chemical adhesion [17, 21]. However, excessively high melt temperature causes over-oxidation and too high air gap causes cooling of the film, which in turn reduces the oxidation. The decrease of the line speed is in most cases poor tradeoff, because it reduces the productivity of the process. Moreover, greater coating weight increases the polymer consumption and consequently the costs [17]. The most important parameters and their effect on adhesion are collected in table 8 [17, 21].

Table 8. *The influence of process and polymer properties on adhesion [17, 21].*

Increasing property	Adhesion
Melt temperature	Increases
Air gap distance	Increases
Nip pressure	Increases
Melt index	Increases
Coating weight	Increases

4.2.3 Time in the air gap

In the air gap, the polymer film oxidizes due to the atmospheric oxygen [21]. Time in the air gap (TIAG) is the timespan, in which the polymer film proceeds from the die gap into the nip [17]. TIAG can be defined simply by dividing the height of air gap with the line speed. However, the received value is not exact because it does not take into account the change of drawdown as the thickness changes [25]. Generally, TIAG is very short period, only up to couple hundred milliseconds, but it affects the adhesion significantly, since the cooling and surface oxidation of the film takes place meanwhile [17]. The recommended time in the air gap for polyethylene materials is around 80 to 120 ms [21]. Adequate TIAG is crucial because too long time causes excessive cooling of the melt that weakens the adhesion, although the oxidation increases [17, 21].

Increasing line speed causes the coating weight and TIAG to decrease. Adhesion generally decreases with the decreasing TIAG. However, if the coating weight is reduced with the constant TIAG, adhesion decreases nevertheless. The coating weight has usually more significant effect to the adhesion than TIAG or the coating temperature, which makes the source reduction difficult. This effect is shown in the figure 16, where the influence of different parameters to adhesion is analyzed. As mentioned earlier, the increasing TIAG increases the adhesion in spite of the increasing cooling of the film. Moreover, the substantial impact of the melt temperature and the coating weight is important, when the good adhesion properties are tried to achieve [25].

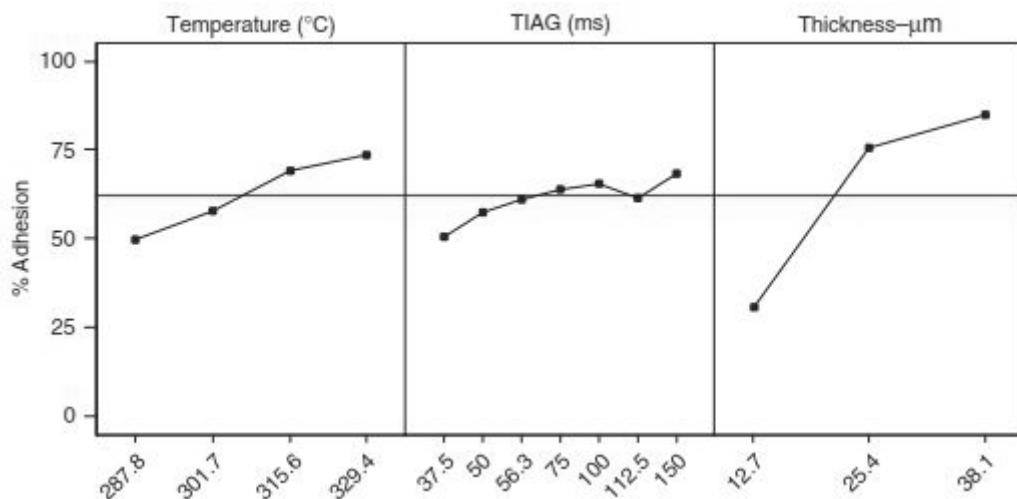


Figure 16. The effect of temperature, TIAG and film thickness on adhesion [25].

As seen in the previous figure, increasing TIAG and melt temperature enhance the oxidation and consequently the adhesion significantly. This is caused by chemical reactions, where polar functional groups are formed the acid functionality is increased. The oxidation of the polymer film is proportional to the acid functionality, which can be measured. Therefore oxidation level can be determined e.g. with FTIR (Fourier transform infrared

spectroscopy), which measures carbonyl index of the material. Carbonyl index provides crucial information from the oxidation amount of the film. This information can be exploited, when the reasons behind a certain adhesion value are determined. The relation between the carbonyl index and TIAG and temperature is presented in figure 17 [29].

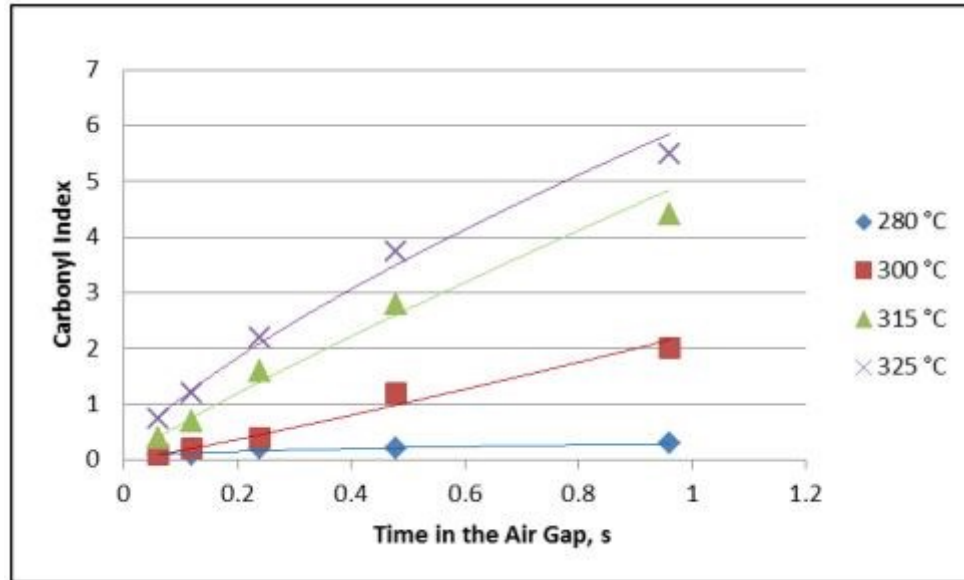


Figure 17. The influence of melt temperature and TIAG on carbonyl index and consequently adhesion [29].

4.3 Heat sealability

Heat sealability is one of the most important properties of the extrusion coated products since the heat sealing is widely used method in the packaging product manufacturing. The main requirements for heat seals are sufficient mechanical strength and leak tightness of gases and liquids [17, 30]. Crucial heat sealing properties include the minimum sealing temperature, seal strength and sealing range. Product properties define the minimum sealing temperature, which is the point where significant seal strength is formed. The heat sealing range continues to the point where the polymer structure starts to deform. Wide heat sealing range is advantageous property since it decreases the effect of machine variation. Moreover, high temperatures cause decline of polymer viscosity, which leads to excessive deformation and weakens the seal. Linear polymers such as PE-LLD have usually lower melt strength than branched polymers such as PE-LD and therefore they are more vulnerable to deformation [17]. Moreover, long-chain branching induces that PE-LD has generally lower sealing temperature and wider sealing range [31].

The polymer coating can be sealed with heat and pressure either to the substrate or to another coated surface. The surface of the coating is heated since bonding of the polymer coating occurs in a partially molten state. Sufficient bond requires enough pressure, which is created by pressing the surfaces together for a certain time and force. It causes the polymer chains to form bridges with each other [17, 32, 33]. On a small scale, the surface

of polymer film is rough and consequently the initial contact area is small [17]. Heating causes melting of the polymer and the pressure enhances molecular contact. Polymer chains diffuse over the interface and form molecular entanglements [17, 32, 33]. When the heat and pressure are removed, the polymer cools and the seal is formed [17]. Melting breaks up the original structure of the polymer and orientation of the film. Therefore, the mechanical properties of the coating are changed during the process [31]. Excessive pressure does not strengthen the bond because the sealing temperature and time are the main parameters for forming a strong and tight seal [17, 33].

4.3.1 Factors affecting heat sealability and seal strength

In packaging applications, the main task of heat seal is usually sufficient strength without a leakage. Usually, the minimum requirement is that the seal should endure as well as the package itself. Strong seal is accomplished when the interface is not visible and the materials have not degraded or thinned. However, in some applications the seal should be also easy to open [17]. There are several factors, which are affecting the heat sealability and seal strength of the extrusion coated product including the structure and thickness of polymer, the manufacturing process and the heat sealing process parameters [17, 21].

4.3.2 Influence of polymer properties

Different polymer grades have different properties and consequently heat sealability can be variable. The most important polymer properties affecting to the heat sealing include density, crystallinity, melt index, molecular weight and structure [17, 21]. The density of polymer depends on its crystallinity and consequently chain branching. The chain branching also affects the mechanical strength of material [17]. The general rule for heat sealing is that higher density of polymer causes increase of the minimum sealing temperature, but decreases the sealing range [17, 21, 34]. Higher density can also slightly increase the seal strength [21]. Low viscosity and high melt index are consequence of low polymer molecular weight and results to easy sealability [17]. Melt index along with the film thickness are the main factors that define the heat seal strength [21]. Generally, higher melt index induces weaker seal strength, but lowers the minimum seal temperature [17, 21, 34]. Moreover, higher molecular weight can increase the sealing range [34]. The influence of melt index and film thickness on the strength of heat seal is illustrated in figure 18 [21].

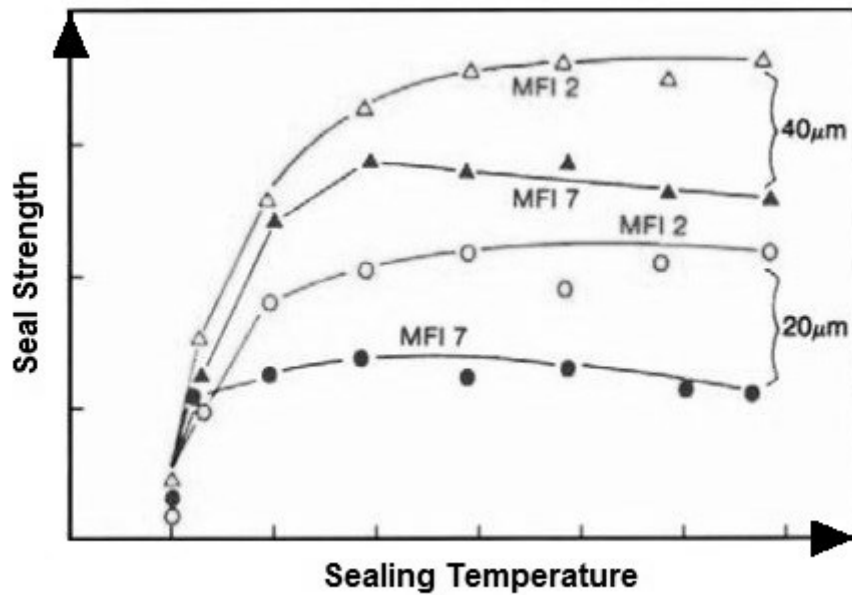


Figure 18. The effect of melt index and film thickness on the seal strength [21].

4.3.3 Influence of product manufacturing process

The heat sealability of the polymer is affected by manufacturing process via properties such as film thickness, homogeneity and uniformity. Moreover, the storage time can have an influence to the heat sealing properties. Humidity and oxygen can oxidize or degrade the film excessively and worsen the heat sealing performance [17]. The film thickness is important factor concerning the seal strength. Increase of the film thickness often enhances the seal strength [21, 34]. However, the strength can also weaken due to poor heat conductivity of polymers. A thick layer of film reduces the heat transfer, which can lead to lower strength. Moreover, thick layers generally increase the minimum sealing temperature and decrease the sealing range. The homogeneity and uniformity of polymer layer is also crucial for a proper seal because uneven thickness causes uneven sealing pressure, which can result in leakage and reduced seal strength [17]. Other factors related to the conditions manufacturing process include the extrusion temperature and shear as well as the air gap distance [21, 34]. The heat sealing properties are deteriorated by excessive oxidation of the polymer [21]. Higher temperature and shear values can cause decrease of the seal strength and sealing range [34]. Moreover, controlling the air gap distance is crucial and sometimes compromises between proper adhesion and sufficient heat seal strength is required [21].

4.3.4 Influence of heat sealing process parameters

The key parameters of heat sealing process are the sealing temperature, pressure and time. The sealing temperature can be considered as the most important parameter. In many

cases, the optimum temperature must be searched by trial and error method. The sealing temperature must be high enough to produce appropriate melting without excessive heating. Restrictive factors of the sealing temperature include material properties such as the chemical structure. The sealing pressure is important parameter for a sufficient seal but an increase of pressure does not always increase the seal strength. Too high pressure can decrease the film thickness in the contact area and consequently weaken the seal strength. The sealing time is the interval, when the seal is under pressure. The sealing temperature and pressure are defining factors for the sealing time and the precise adjustment is usually more important with increasing film thicknesses [17].

4.4 Pinholes

Pinholes are defects e.g. small tears or tiny holes in the polymer coating surface, which are generated during the extrusion coating process [17, 21, 35]. A pinhole is formed in the melt, when the deforming force surpasses the elastic limit of the material. Pinholes can be formed at several different phases in the extrusion coating process such as before the coating, at the contact point of the polymer and substrate, in the nip, during the stripping and during the handling [17]. There are also numerous possible reasons for forming of the pinholes such as gas bubbles and contaminants in the melt, loose fibers and roughness of the substrate and incomplete local bonding between the melt and substrate [17, 35]. An inadequate mixing and consequently non-homogenous melt, uneven coating profile and too low coating weight also cause the formation of pinholes [21, 35]. Because the pinholes are discontinuity points in the coating, they can constrain the further use of a product [17]. For example, materials that are used as oxygen or moisture barriers are unsuitable when containing the pinholes [17, 21]. Therefore, avoidance of pinholes is crucial in almost every application of the extrusion coating products [17]. However, in some cases limited number of pinholes is acceptable or even desirable [35].

4.5 Coating weight, draw down and neck-in

The thickness of polymer coating is expressed as the term of coating weight, which is usually defined as coating material weight in grams per square meter (g/m^2). In extrusion coating, coating weights can be very low and under $10 \text{ g}/\text{m}^2$ values are reachable. Coating weight is determined mainly by two factors, which are the line speed and the output of extruder. Coating weight is associated with two other important properties of the polymer film, which are neck-in and drawdown [21].

Usually the aim of extrusion coating is to apply highest possible line speed without breaking the film. Material specific draw down determines how low the coating weight or thickness can be and it is measured by accelerating the line speed to the point where the molten film breaks [15, 21]. Therefore, draw down mainly determines the maximum line speed. Draw down is very important parameter in extrusion coating of PE grades enabling

lower coating weights without any defects such as tears and holes [21]. Generally, the branched structure of PE-LD affects the draw down most and high melt strength causes better draw down properties. However, the tension stiffening of PE-LD results sudden and brittle melt breakage and therefore the best draw down and lowest coating weights are reached with PE-LLD and PE-HD [17].

The molten polymer film has to resist high forces without breaking because it is stretched at high deformation rate and the draw down ratios can be over hundred [17]. The coating width is always narrower than the die width. Neck-in indicates the reduction in film width that occurs at the air gap as the film cools down [17, 21, 36]. The neck-in increases with the higher air gap, which is required for longer oxidation times of PE-LD compared to linear polyethylenes. High extensional viscosity and consequently melt strength is beneficial to oppose the strengths that are pulling the melt towards center of the flow. However, due to tension stiffening behavior of PE-LD in stretching, it is less vulnerable to neck-in with high line-speeds than the linear polyethylenes. Generally, the increase of chain branching and extension of molecular weight distribution decrease the neck-in of polymer material [17]. Since the neck-in causes thicker layer at the edges of the coating, it should be as small as possible so that the trimming and material waste are reduced. The formation of neck-in during extrusion coating process is shown in figure 19 [21, 36].

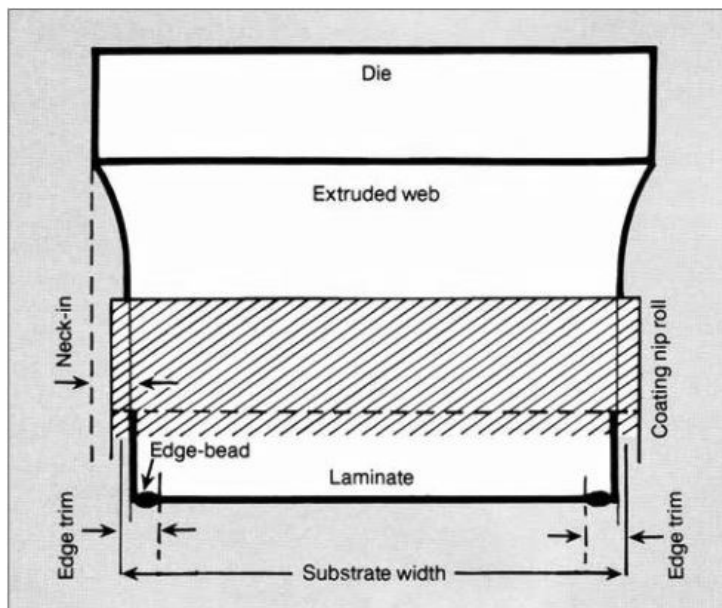


Figure 19. Neck-in in extrusion coating process [21].

The neck-in and draw down are affected by many different parameters such as melt temperature and air gap distance. The influence of these parameters can be contradictory and the draw down value can improve simultaneously as the neck-in value gets worse. Therefore, adjusting the draw down and neck-in is always compromising [21]. Some parameters and their effect on the neck-in and draw down are collected in table 9 [17, 21].

Table 9. *Process and polymer properties and their influence on neck-in and draw down [17, 21]*

Increasing property	Neck-in	Draw down
Melt temperature	Increases	Increases
Air gap distance	Increases	Increases
Line speed	Decreases	Increases
Melt index	Increases	Increases

5. INFRARED (IR) THERMOMETRY

Heat transfer takes place with three elementary mechanisms, which are conduction, convection and radiation [37]. Thermal radiation signifies the transfer of heat energy via electromagnetic radiation. The electromagnetic radiation emission can be utilized to measure temperature value of an object. IR thermometry uses this mechanism in temperature measurement [37, 38]. IR thermometer measurement system consist of few main elements which are radiating source, medium (atmosphere), optical system to gather radiation, transducers to convert radiation into temperature signal, amplification and interface circuitry to display and control the measurement [37, 39].

IR radiation can proceed through a medium or a vacuum, hence the temperature measurement sensor does not have to be in contact with the target. That enables placement of the equipment at suitable distance from the target. IR thermometry is the most common and widely used non-contact temperature measurement technique. Applications are comprehensive from moving objects to very hot temperatures [37, 38]. The temperature range of IR thermometers is from 50 K all the way to 6000 K [37]. IR radiation based measurement is especially useful at the hot temperatures because usage of contact-based devices is usually impossible there [37, 38]. There are several main types of infrared thermometers, which can be classified to spectral band thermometers, total radiation thermometers, ratio thermometers, fiber-optic thermometers and thermal imagers. Every type of thermometers has some uncertainty factors, which are widely associated with the measurement environment and its effect. Therefore, understanding of the basic principles of IR radiation is essential for successful measurement [37, 38, 39].

5.1 Theory of the IR-based temperature measurement

All materials that are above absolute zero temperature emit infrared radiation with respect to its temperature and that radiation is called characteristic radiation. It is caused by the internal movement of molecules, and the intensity of movement is dependent on the temperature of material [38, 39]. Movement of the molecules stand for charge displacement and consequently electromagnetic radiation, in this case photon particles, are emitted. Photon particles act according to known physical principles and move at the speed of light [39]. Since thermal radiation is a form of electromagnetic radiation, it does not need a medium to proceed and it can travel through a vacuum. The velocity of radiation decreases and it can scatter when going through a medium [37].

Thermal radiation is mainly situated at the infrared region of the electromagnetic spectrum above the visible light. Thermal radiation is often classified at the wavelength band from 0.1 μm to 100 μm as the whole infrared band is from 0.78 μm to 1000 μm . Infrared

radiation is an invisible part of the electromagnetic radiation. Thermal radiation in turn is partly at the visible light area and therefore very hot objects can be seen glowing visible light. Thermal radiation energy increases as the temperature rises and object become brighter [37, 39]. It is notable that the invisible part of spectrum contains up to 100 000 times more energy than the visible part and consequently is the basis of IR thermometers. The infrared range and its position in the electromagnetic spectrum is illustrated in figure 20 [39].

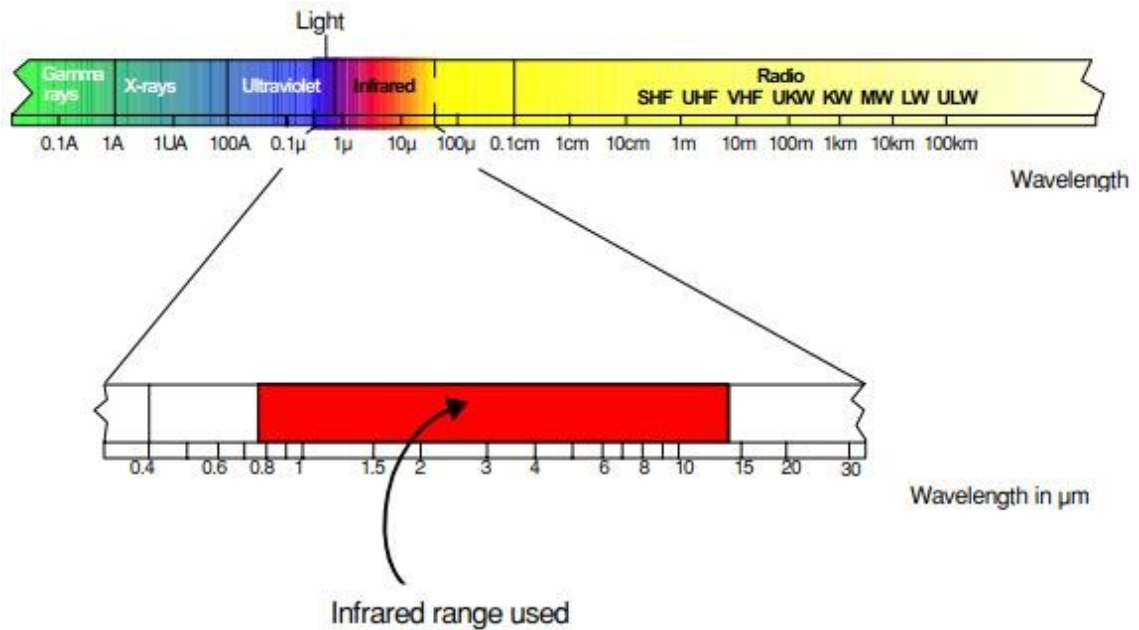


Figure 20. IR range of the electromagnetic spectrum [39].

5.1.1 Planck's law

Thermal radiation represents the electromagnetic radiation energy that is emitted from a body above absolute zero temperature. Radiation emits in all directions and when it hits another body, it can be absorbed, transmitted or reflected. Emitted thermal radiation is not distributed evenly over every wavelength. Moreover, absorbed, transmitted or reflected radiation are not necessarily distributed equally to all wavelengths. Since thermal radiation is dependent on the body, practical applications need a baseline where to compare the all results. This ideal surface is called a blackbody and it has three defining properties. Blackbody absorbs all incident radiation, no surface can emit more energy and blackbody radiation is independent of direction [37]. The spectral emissive power of a blackbody can be determined by Planck's law. It expresses the emission of thermal radiation per surface area (power density) at a particular wavelength [37, 40]. IR thermometers respond only to a narrow band of electromagnetic spectrum so it is crucial for measurements to assimilate Planck's law [40]. Planck's law is presented in equation (1)

$$E(\lambda) = \frac{C_1}{\lambda^5 e^{\frac{C_2}{\lambda T}} - 1}, \quad (1)$$

where $E(\lambda)$ is spectral emissive power for a blackbody (W/m^3), C_1 is the first radiation constant ($3.7417749 \cdot 10^{-16} \text{ Wm}^2$), λ is wavelength (m), C_2 is the second radiation constant (0.01438769 mK) and T is absolute temperature (K) [37, 41].

This equation can be plotted for a range of different wavelengths and temperatures to present that radiating energy is a function of wavelength at specific temperatures [37]. Figure 21 shows that the spectral emissive power of a blackbody has a maximum value. The wavelength that corresponds the location of maximum is dependent of the absolute temperature [37, 40].

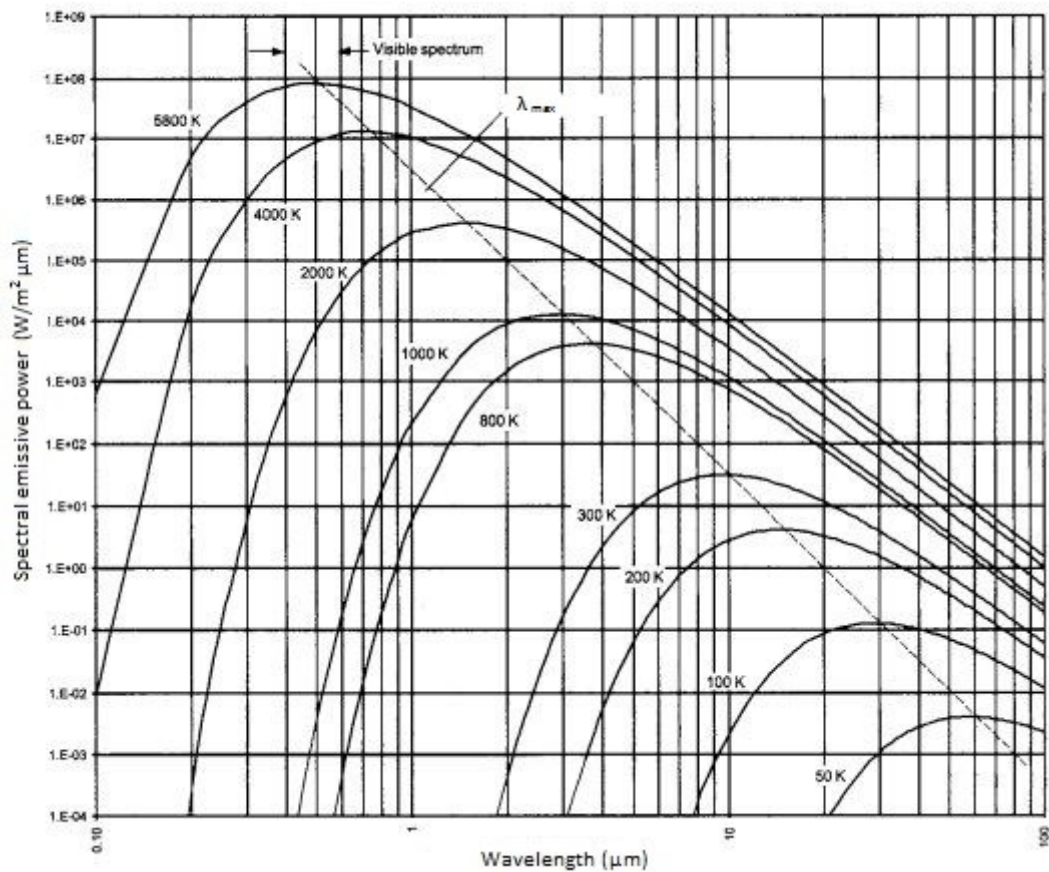


Figure 21. Spectral emissive power of a blackbody [37].

The dependency between the wavelength and the temperature maximum can be determined by Wien's displacement law. This law can be proven by differentiating Planck's law with respect to wavelength. The result of differentiating is then set equal to zero [37]. Wien's displacement law is presented in equation (2)

$$\lambda_{max} = \frac{0.028978 \text{ mK}}{T}, \quad (2)$$

where λ_{max} is wavelength of the temperature maximum and T is absolute temperature [37, 41].

Another property of blackbody radiation that can be seen in figure is that the curves plotted at different temperatures do not cross each other. Consequently, if the radiation intensity is measured at specific wavelength, the temperature can be uniquely determined. That feature is used in IR measurement devices. When the temperature increases, the rate of emission increases and the emphasis moves towards lower wavelengths. Therefore, only high temperature objects can be seen glowing although every object above absolute zero emit some radiation [40].

5.1.2 Stefan-Boltzmann's law

IR thermometers sense the radiation that emits from the surface of object and the energy is dependent on the surface and its properties [40]. The total emissive power of a blackbody is received by integrating Planck's law over all wavelengths. The result of the integration is known as Stefan-Boltzmann law, which presents a connection between total emissive power and temperature [37]. It describes the total rate of emission per unit surface area [40]. By means of this equation, it is possible to calculate the total emissive power that means radiation emitted in all directions over all wavelengths, just by knowing the temperature [37]. Stefan-Boltzmann's law is presented in equation (3)

$$E = \sigma T^4, \quad (3)$$

where E is total emissive power for a blackbody, σ is Stefan-Boltzmann constant ($5.67051 \cdot 10^{-8} \text{ W/m}^2\text{K}^4$) and T is absolute temperature [37, 40, 41].

Based on the Stefan-Boltzmann law, IR thermometer should be set up for the widest possible wavelength range to receive most radiant energy. However, that is not always advantageous or practical. For example, the intensity of radiation increases much more along the temperature at lower wavelengths. Consequently, IR thermometer works more accurately at those lower wavelengths. However, with low temperatures, too low wavelengths are useless because the radiation maximum moves to higher wavelengths and there is not enough radiation energy for sufficient measurement [39].

Deficiency of Stefan-Boltzmann and Planck's law is that they are valid only for an ideal blackbody. Materials used in practice are not ideal blackbodies and their surfaces need to be described by emissivity factor, which is comparative to ideal blackbody [37, 40]. This causes problems and errors to practical IR thermometer measurements [37]. The main reason for different wavelength range IR thermometers is the emissivity pattern of grey bodies [40].

5.1.3 Grey bodies, grey body radiation and emissivity

In practice, almost every object emit less radiation as described by Planck's law [40]. The amount of radiation that emits from a real surface depends besides the temperature also the surface properties. The property that restrain radiation quantity of a body is called emissivity (ϵ). Emissivity is determined as the ratio between electromagnetic flux of a surface and electromagnetic flux of an ideal blackbody at a specific temperature [37, 39, 40]. The value of emissivity is always between 0 and 1 because an ideal blackbody has the highest possible electromagnetic radiation flux and all other materials emit less radiation [27, 39].

Incident radiation on an object can be absorbed, transmitted and reflected. Conservation of energy determines that the total flux is constant. Consequently, the sum of absorptivity, transmissivity and reflectivity is constant and equals one with an ideal blackbody object. Values of absorptivity, transmissivity and reflectivity can vary between 0 and 1 but the sum must remain constant [39, 40, 41].

The emissivity value can vary with the temperature, wavelength, surface, shape and angle of view. It's important to notice that the measured temperature is dependent on the environment along with the surface and its emissivity [38, 30]. The emissivity can also change as a function of time [38]. Grey body emissivity differs from a blackbody by its spectral distribution along with the magnitude. The absorptivity of a grey body is not uniform and it can be dependent on wavelength. Moreover, real surface can show non-diffuse behavior when properties vary depending on direction [37]. If the emissivity of a grey body is known, the emissive power of a grey body can be calculated at a specific temperature by modifying the Stefan-Boltzmann law [37, 40]. This is presented in equation (4).

$$E = \epsilon\sigma T^4, \quad (4)$$

In practice, temperature measurement using IR thermometry can be rather challenging, since real surface can emit, absorb, transmit and reflect radiation. Especially, when the emissivity of the material is unknown or a function of temperature and wavelength. Furthermore, situations where the target object is near other objects in different temperature or powerful source of radiation measuring the correct temperature value can be difficult [37, 38]. However, if the environment temperature is relatively low compared to the object, the effect of absorbed radiation to total radiation and hence to temperature value is negligible. Moreover, emissivity is affected by reflectivity, which is a function of an angle of view. Reflectivity increases, when the angle of view increases from normality. When closing to 90° angle, the reflectivity increases rapidly and simultaneously emissivity decreases [40].

5.2 Types of IR thermometers

IR thermometers are classified in several groups, which are based on the properties and operation method. The classification of these groups is usually following, spectral band thermometers, total radiation thermometers, ratio thermometers, multiwaveband thermometers, special purpose thermometers and thermal imagers. The first three are the most common ones along with the thermal imagers that are discussed in section 5.6 [37, 38].

5.2.1 Total radiation thermometers

Total radiation thermometers measure radiation that is emitted from a target over wide wavelength area. The wavelength band is normally several micrometers and lies between 1 μm and 100 μm [37, 38]. Measurement principle is based directly on Stefan-Boltzmann law. The main components of total radiation thermometers are collector and detector [37].

Aperture size defines the amount of radiation that reaches detector. Sensitivity and spot size linked together because if the spot size decreases due to aperture size, the sensitivity decreases because of diminishing radiation amount. The distance of target does not directly have an influence to sensitivity but adding the distance will increase the spot size and therefore affect sensitivity. Total radiation thermometers use optical system including lenses or mirrors to focus the radiation onto detector and consequently eliminate the issue of lower sensitivity with decreased spot size. However, due to the optical system, all radiation doesn't end up to the detector. Lenses have certain transmittance values and they eliminate some radiation below and above specific wavelength range [37]. Detectors are usually thermopiles in order to improve sensitivity. Function of the detector determines that the device is quite slow and response time is 1 to 3 seconds. Wide wavelength area also results in exposure to different radiation and circumstance based interferences. Also small uncertainty in emissivity value causes significant error to results [38].

Overall, the total radiation thermometers have wide temperature range several possible applications. Wide wavelength area contains a lot of energy and therefore it is used more in qualitative applications. Moreover, it can be used at the low temperature measurements because the emitted radiant energy is in that case low. Special designed devices can also provide very exact results although spectral band thermometers have usually better precision [37].

5.2.2 Ratio thermometers

Ratio thermometers are also known as dual-wavelength and two-color thermometers. They measure emitted radiation of a target at two different and specific wavelengths that are usually close to each other [37, 38, 39]. The structure of equipment is such as two spectral band pyrometers are combined together [38]. The wavelengths are set as close to

each other as possible in order to minimize the effect of reflectance and emissivity. Consequently, the target is as similar as possible to both wavelengths [39]. The temperature value is determined from the ratio of radiations emitted at different wavelengths. If the emissivity value can be assumed equivalent, then the measurement does not depend on the surface emissivity. Therefore, surfaces with uncertain emissivity can be measured [37]. However, the ratio thermometers are very sensitive to changes in emissivity values during the measurement, which can vary the wavelengths that are suitable for the measurement. Therefore, large measurement errors are possible [38]. Moreover, the ratio thermometers are not as sensitive as spectral band thermometers [37, 38].

5.2.3 Spectral band thermometers

Spectral band thermometers are the most common IR temperature measurement devices and major part of measurements are done using this technique [37]. They measure thermal radiation energy at specific and rather narrow wavelength band, which is typically between $0.5\ \mu\text{m}$ and $25\ \mu\text{m}$ [37, 38]. Spectral band thermometers are sometimes called single-waveband, narrow-waveband or monochromatic thermometers. The selection of waveband is depended on a few key factors. These include temperature area, environment and the properties of surface. Function principle of spectral band thermometer is following. Radiation is collected from the surface of target [37]. Desired wavelengths are filtered and selected. Radiation is measured by the detector and information is processed [37, 38]. Schematic showing of the spectral band thermometer components is in figure 22 [37].

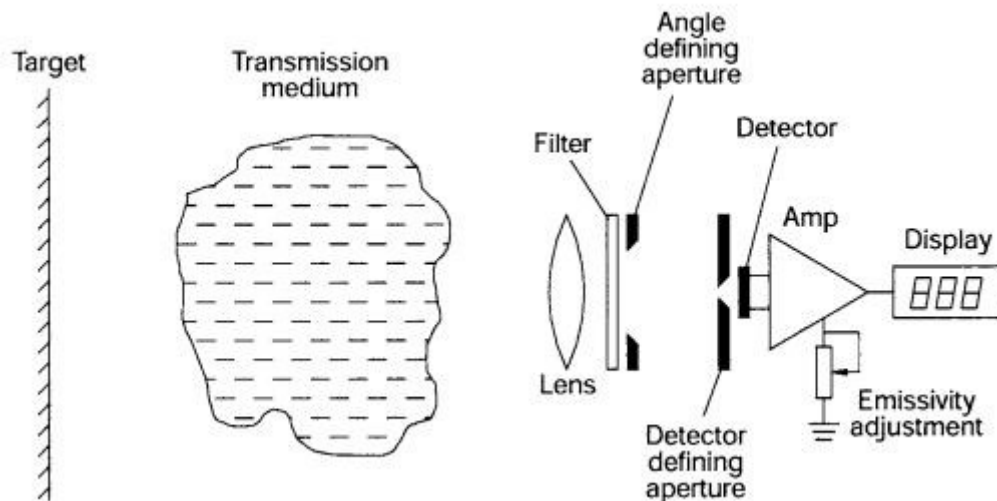


Figure 22. Components of the spectral band thermometer [37].

The detectors used in spectral band thermometers are diverse and based on the applications but the most commonly used materials are silicon and germanium. These detectors are in hered to short wavelength thermometers and they measure wavelength area between

0.5 μm and 2 μm [37, 38]. The use of these detectors is based on their great speed, sensitivity and stability. Silicon detector spectral band thermometer has small, only few millisecond response time. The speed makes it suitable device to measure temperature of moving objects [38]. The advantage of short wavelength area is high sensitivity because the radiant energy changes at fast rate with the temperature [37]. Moreover, error in results caused by uncertainty of emissivity is smaller than other types of thermometers show [37, 38]. Optical windows are used to restrain the wavelengths that are received by the detector of thermometer. For example, plastic materials are transparent over broad areas of spectral band. However, they have high opacity and low reflectivity at the specific wavelength areas that are dependent on the material. At those areas, IR temperature measurements can be made reliably [37]. The subsequent inspection of the choice and use, sources of error and advantages and disadvantages of IR thermometers is focused on the spectral band equipment, because they are the most common and widely used type of IR thermometers and the measurements of practical part are done using such equipment. [37, 39].

5.3 IR temperature measurement of plastics

Usually non-metallic materials such as plastics have surface that does not reflect much so the emissivity values are between 0.8-0.95. Emissivity can be determined with several different methods. Good estimations are found in the tables for most frequently used materials. In many cases, emissivity tables also provide right wavelength ranges for materials, which helps to select the measuring equipment. However, the only way to ensure exact result is to calibrate the equipment according to manufactures instructions. Thus, the right emissivity value and corresponding wavelength can be determined and set [39].

There are some guidelines and general principles for each material when executing the temperature measurement with IR thermometer. With plastics, it is very important to realize that certain materials have emissivity peaks at specific wavelengths and temperature measurement at these wavelengths is crucial [37]. The emissivity peaks are located at the wavelength areas where the transmittance is at its lowest. Transmittance of a plastic material varies along the wavelength and it is proportional to thickness of the object. Thin plastic materials have higher transmittance than thick ones. Optimal and reliable IR temperature measurement must be done at the wavelength area, where transmittance is as close to zero as possible. Some plastic materials including polyethylene have low transmittance around 3.43 μm wavelength. If the thickness of plastic film is over 0.4 mm or it is strongly colored, optimal wavelength area is between 8-14 μm [39]. In addition, the knowledge of surroundings is essential because air as well as other gases have absorption minima at specific wavelength areas [37]. The transmittance of polyethylene film is illustrated in figure 23 as a function of wavelength [39].

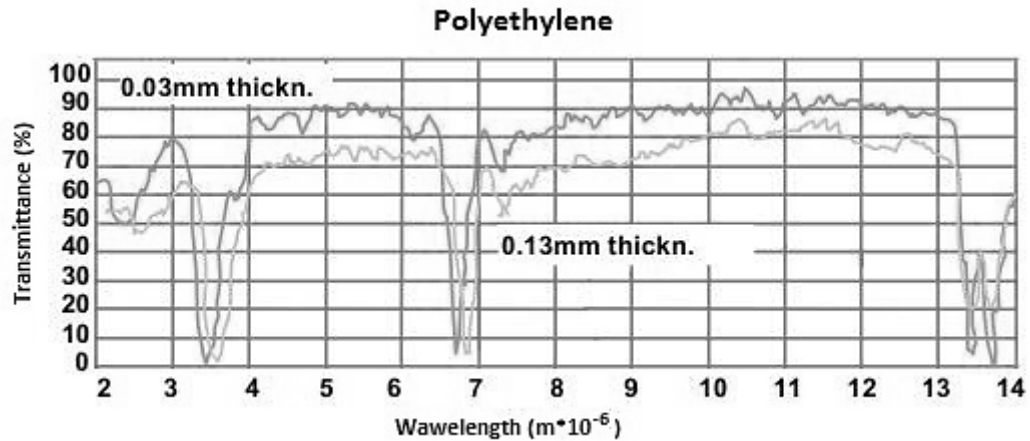


Figure 23. The dependency between transmittance and wavelength values of a polyethylene film [39].

5.4 Advantages of the IR thermometers

Temperature has very important role in industry, when the conditions of a product are examined in manufacturing process as well as in quality control. When temperature monitoring is done accurately and the results are exploited to improve the process, product quality and productivity can be increased. IR temperature monitoring helps to optimize the process conditions without interruptions, which decreases downtimes. IR based technology is not a new invention and it has been used for decades in industry. However new innovations have led to smaller IR sensors and measurement units which have reduced costs and improved reliability. These improvement steps have resulted in IR temperature monitoring to become an interesting and useful tool for new kinds of applications [39].

IR temperature measurement has several key advantages, which support its use. IR based temperature measurement is very suitable device for automatized processes because of its short response time. The elapsed time is in millisecond range, which enables to collect large amounts of data in short period of time [38, 39]. IR thermometers allow temperature measurement of moving objects, which is key especially in process industry where interruptions are highly undesirable [39]. IR temperature measurements can be done in very high temperatures without any problems because of its noncontact method. Consequence of that, IR temperature measurement can also be done from inaccessible or hazardous spots. For example, high-voltage or explosive places are not a problem [38, 39]. IR thermometers do not contaminate or damage the surface of object. This allows risk-free measurement of highly finished products. IR measurement technique is accurate and there is no energy dissipation from the object. In case of poor heat conductors such as plastics, the measured value is highly accurate compared to contact thermometers [39].

5.5 Sources of error

Temperature measurement using IR thermometers is exposed to multiple sources of error. This is an implication of the complicated transfer process of thermal radiation from the target to the measuring device. Various errors of IR thermometry can be classified into three groups. Firstly, characterization of the radiation process, which is associated to surface emissivity and reflections. Secondly, transmission path errors, which include absorption and size of target effects. Finally, signal processing errors, which occur in the measuring device [37].

One of the most important factors when executing IR temperature measurements is to recognize the surface material and condition of target so that the emissivity can be adjusted to the IR thermometer [37]. Surface emissivity varies according to the wavelength and the surface of target. In practice, the emissivity is not necessarily a problem because usually measured materials are identified and emissivity values can be found in tables or manufacturer's instructions. In addition, tables usually provide the corresponding wavelengths for each material [37, 39]. However, the quality of the surface is sometimes ambiguous, because it can be i.e. polished, rough or oxidized. Therefore, proper calibration of the equipment is usually the best way to ensure exact results [37].

In practical measurement of thermal radiation, it is not possible to separate the radiation of target surface from other sources of radiation that are at the range of IR thermometer. Radiation that is emitted or reflected from other sources than the target is called background radiation. Problems caused by background radiation are dependent on its intensity. High intensity radiation, in comparison to the target, over the desired waveband can increase the temperature that is indicated by the device and consequently distort the results. Background radiation is not always easy to observe and therefore consideration should be done on occasion [37]. Positioning of the equipment needs to be designed in a way that optics is not exposed to background radiation, which can distort the results [37, 38]. Avoiding background radiation is in some cases impossible. Therefore, the temperature of other emitting or reflecting object needs to be measured and using that information correct the measurement signal [38]. Few general but important precepts can be executed to minimize the error caused by background radiation. Verify that the viewing range of the IR thermometer is completely covered by the target. Choose the wavelength area to correspond the range where the target has high emissivity and low transmittance. Place the IR thermometer on location that minimizes reflections [37].

The principle of IR temperature measurement causes that the radiation must travel through a medium. Consequently, few factors may lead to problems and complicate the measurement. Those factors include absorption, scattering and fluorescence. Air along with most other gases is not totally transparent and it can absorb emitting radiation at specific wavelengths [37]. It contains small amount of carbon dioxide and variable quan-

tivity of water vapor, which can distort the results [38]. Transmittance of a medium is quantity that defines the proportion of transmitted radiation across the specified distance. Transmittance of air over a 300 m distance is shown in figure 24. Air is opaque in the black areas and transparent in the white areas [37].

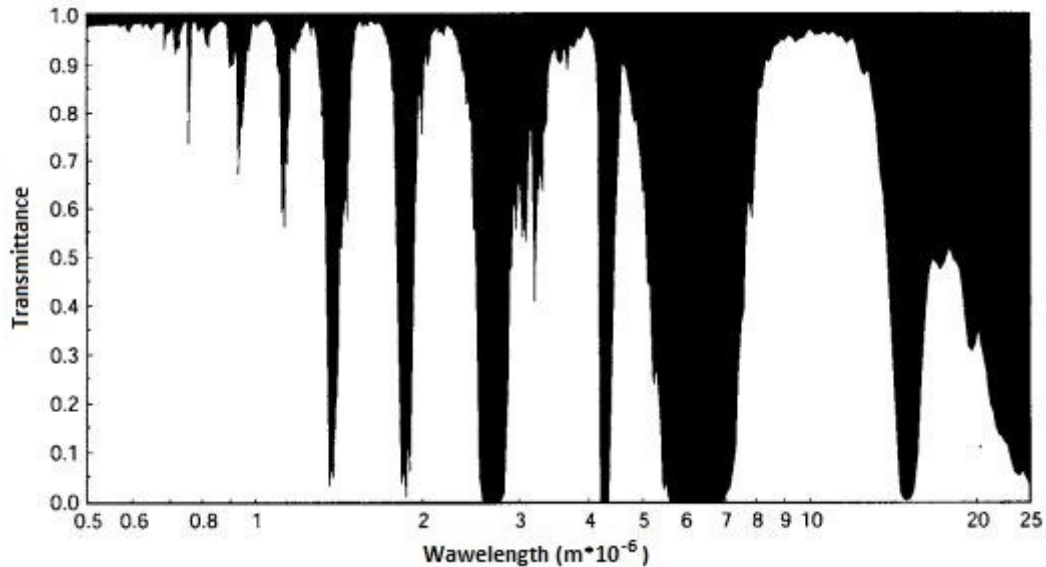


Figure 24. *Transmissivity of air as a function of wavelength [37].*

To ensure reliable measurement and results, it is important to use detector that is sensitive at the same wavelength area where the transmittance is as high as possible. As mentioned above, majority of the absorbed radiation in air is caused by carbon dioxide and water vapor. Because of the absorption of radiation, the temperature value indicated by IR thermometer is too low compared to real value. Similarly, the effects of other mediums need to be considered depending on the circumstances [37].

Some applications need protective cases and windows between the detector and target. In those cases, the reflection of window material can cause losses along with the transmission [37]. Protective cases are also needed if the surroundings is unclean [37, 38]. Solid particles such as dust can cause error to the results and the environment between the target and detector must be kept clean [37, 38, 39]. Equipment can also be protected against dirt and dust by airflow, which keeps the electronics cool [38]. In very hot applications, the equipment requires circulating water cooling system, which prevents overheating [38, 39].

In practice, IR thermometers collect radiation from cone shaped or tubular in front of the optics. That is not a point measurement but an average temperature value of the concerned zone. The spot size of target, or the field of view, is determined by the angle and detector aperture. The field of view is characteristic to every device and it depends on the model and manufacturer. In ideal situation, the edges of target zone are sharp and distinguishable and therefore outside radiation does not disturb the results. However, in practice several

factors can blur the target and complicate the measurement such as weak focus and optical aberrations [37]. It is crucial that the field of view is totally filled by the target but it is recommended that the diameter of target is twice as large [37, 38]. Size of the target increases with increasing distance, since the measurement zone is cone shaped. This is illustrated in figure 25. The spot size increases linearly as a function of distance, hence it is possible to determine with random target distance [39].

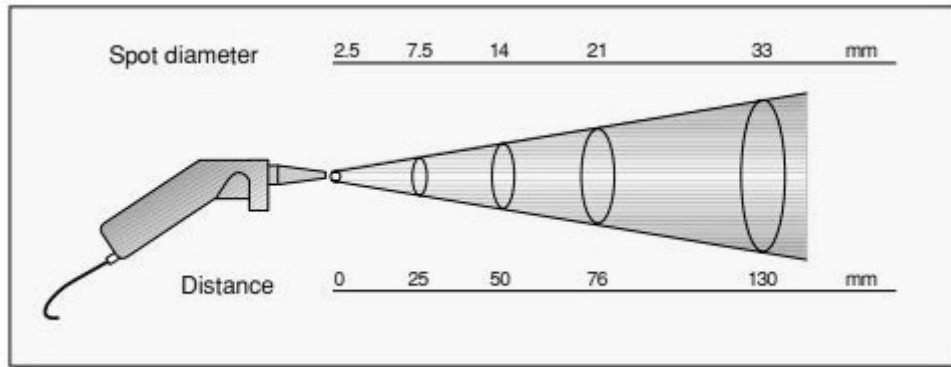


Figure 25. The dependency between the spot size and the target distance [39].

5.6 Thermal imagers

Generally, thermal imagers consist of optical system, detector, processing electronics and display components [37]. All the components are not necessarily present in every camera type rather the certain design is dependent on detector element and output format. The detector is the most essential component of thermal camera and it converts IR radiation into electrical signal that is measured [40]. It is possible to form two-dimensional image of the temperature distribution using single detector in thermal imager [37]. However, array of detectors, staring arrays or focal plane arrays, are much more common [37, 38]. There are two types of array detectors, which are cooled and uncooled ones. Generally, uncooled array detectors have more problems including random thermal noise and long response time. Thermal imagers operate at specific wavelength bands, which can be roughly divide into short (or medium) and long wavelength IR radiation bands [38, 40]. Amplification and signal processing form an electronic image from a target. Differences in measured voltage correspond intensity and consequently temperature differences of a target. The electronics of detector have to match the detector characteristics and output. It is important to format the signal so that it is consistent with monitor requirements [40]. Thermal imagers do not need any visible light to form an image of the target, which expand their applications further [37]. An example of thermal imaging data, received from thermal imager at TUT extrusion coating line, is shown in figure 26.

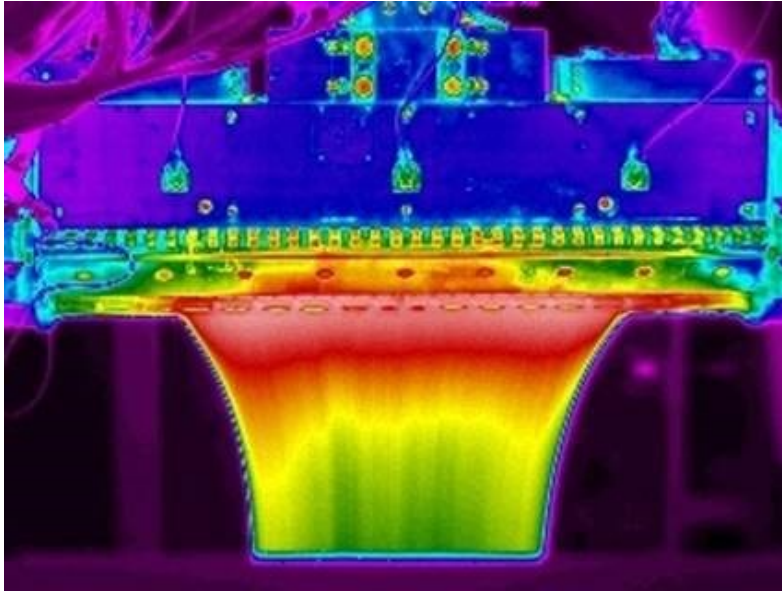


Figure 26. *Thermal image of the extrusion coating die and film.*

Thermal imaging is a special application of IR temperature measurement [38]. Thermal imaging measurement system focuses to determine the spatial distribution of thermal radiation that is emitted from the surface of target object. By means of that information, data from the temperature distribution of surface can be defined [37]. As in other IR temperature measurements, the thermal imagers do not necessarily predicate the actual temperature due to non-contact measurement method [40]. The device might measure the radiation that originates outside of the target. The total radiation that reaches to detector contains emitted radiation of the target, reflected ambient radiation and radiance of the environment [37, 40]. Thermal imaging system needs to be calibrated in a way that the output is proportional to the temperature of target. Exact calibration requires knowledge from the emissivity of target, the ambient temperature and radiation and transmittance of the environment [40].

The problems that are related to thermal imagers are similar as in other IR thermometers. Although the emissivity value of the target is known or it can be determined, the quality of surface has a great affect too. The surface can be oxidized, wet or unclean and the quality may change during the measurement [40]. Furthermore, the ambient conditions and the transparency of environment can be unknown and affect the results causing inaccuracy. Environmental effect to the total radiation can be decreased, if the used wavelength band is in the area where the atmosphere is as transparent as possible [37, 40]. Thermal imaging of the surface that consist of multiple materials must be carefully and accurately measured since each material have specific emissivity values and the same value doesn't necessarily apply to the whole image [37]. Thermal imagers are generally used to gather qualitative information. Research of temperature distribution or determination of temperature difference are widely used functions for thermal imagers. However, quantitative values such as exact temperature values are also possible to determine [37, 38, 40].

5.7 Correlation between theory and practical IR temperature measurements

Polymer film cools simultaneously as it proceeds in the air gap and the cooling starts immediately after the die lip. Lower film temperature increases viscosity, which reduces penetration to the substrate. Oxidation of the film is also decreased in lower temperature. [29] Moreover, thinner polymer layers cool more in the air gap than thicker layers, which raises the viscosity and weakens penetration. All the previous factors induce reduction of the adhesive strength and therefore the temperature decrease in the air gap is advantageous to know. [25] Cooling in the air gap can be estimated with differential heat balance equation, which is presented in equation (5) Equation (5) is indicating a heat balance on a differential element of the molten web at the distance dz from the die exit. The left and right side of the heat balance equation are expressing heat in (conduction) and out (convection) of the molten curtain, respectively [10, 14, 27].

$$MC_p dT = -2hw(T - T_{air})dz, \quad (5)$$

where M is mass flow rate, C_p is heat capacity, T is temperature of the film, h is heat transfer coefficient, w is width of the film, T_{air} is ambient temperature and z is distance from the die exit. The film temperature is solved as a function of the distance from die exit in equation (6). Equation (6) shows that the film temperature is dependent on the coating thickness, line speed and material [25, 42].

$$\frac{T - T_{air}}{T_0 - T_{air}} = \exp\left(\frac{-2hz}{\rho_f g_f C_p v_f}\right), \quad (6)$$

where T_0 is temperature of the film at the die exit, ρ_f is density of the polymer, g_f is coating thickness and v_f is line speed [25, 42].

The theoretical temperature decrease in the air gap can be derived by applying the previous equations (5) and (6). The cooling is described in figure 27, where the temperature is shown as a function of TIAG and with different coating thicknesses. The ambient temperature is assumed 25°C and the temperature at the die exit is 300°C. Figure 27 shows the distinct temperature decrease when the TIAG is increased or the coating thickness is decreased. Moreover, the cooling effect intensifies, when the coating thickness is reduced from 50 μm to 6 μm [29]. It is important to notice that although equation (6) takes the line speed into account, in practice the increase of the line speed causes also the gain of the airflow, which decreases the film temperature [42].

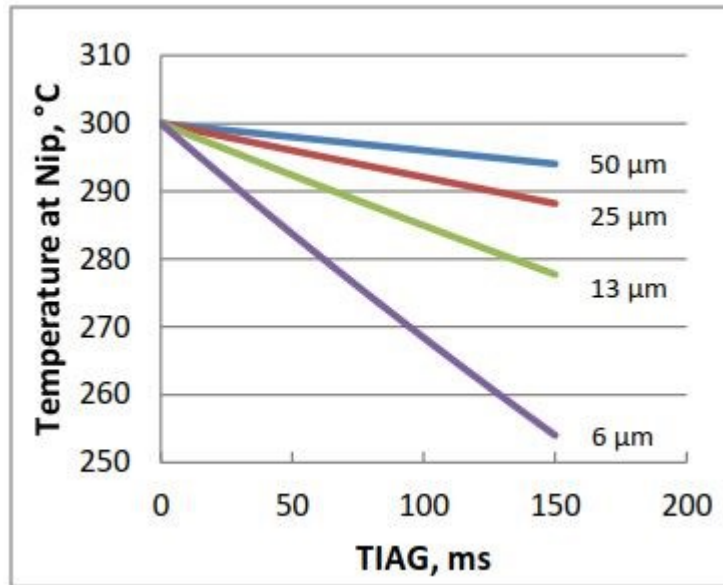


Figure 27. *Temperature decrease in the air gap as a function of TIAG and coating thickness [29].*

Equation (6) indicates that the temperature decreases according to an exponential function with decreasing film thickness [25, 42]. Although the equation (6) is exponential function, the temperature decreases almost linearly in the air gap. This results from the fact that distance from air gap is much smaller than rest of the exponent ($z \ll 2h/\rho_f g c_p v_f$), so the change is almost linear [42]. Challenge of equation (6) is related to the heat transfer coefficient h , which is hard to estimate. In theory, the heat transfer coefficient consists of convective and radiant heat transfer and some values can be found in literature, but the values are not necessarily exact and they vary on occasion. The actual temperature of the polymer film have significant effect to the properties of the product e.g. adhesion and therefore practical measurement of the film temperature in the air gap is beneficial [25].

Some earlier studies show that the actual temperature reading, measured with IR thermometer is higher than the theoretical models predict. Early models overestimate the temperature drop in the air gap due to the difficulty of determining the exact heat transfer coefficient [25]. The theoretical models can correlate with the experimental data in spite of the complexity of the heat transfer coefficient. For instance, in 2014 Foederer, B. M. et al. showed with extrusion coating studies of PE-LD that when the radiant heat transfer is ignored and the convective heat transfer coefficient is set at certain value applying least square analysis, the theoretical model fits well with the experimental data. The principle is illustrated in figure 28, where the convective heat transfer coefficient (h) is $9.9 \text{ W/m}^2\text{-K}$. Consequently, the experimental data and the model prediction of the temperature drop in the air gap are nearly the same [42]. The similar principle is shown in figure 29, where $h = 5.7 \text{ W/m}^2\text{-K}$, based on the IR temperature measurements of PE-LD film done by Morris, B. A. in 2008 [25]. These two recent models predict the temperature drop rather well, which can be seen in figures 28 and 29 [25, 42].

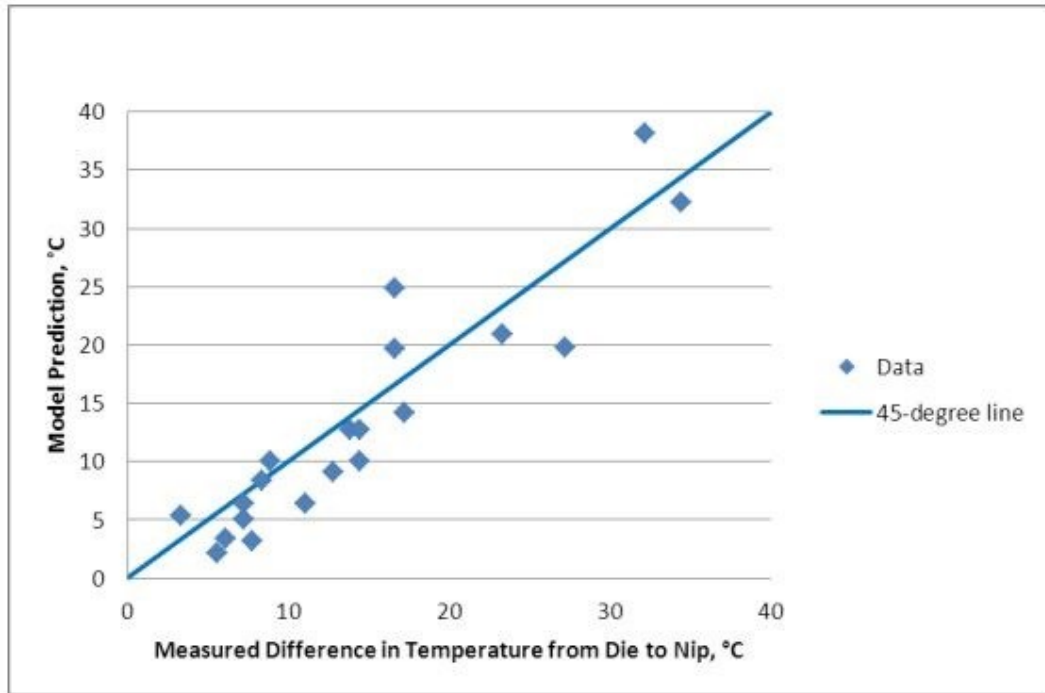


Figure 28. Comparison of theoretical and measured temperature drop, convective heat transfer coefficient $h=9.9 \text{ W/m}^2\text{-K}$ [42].

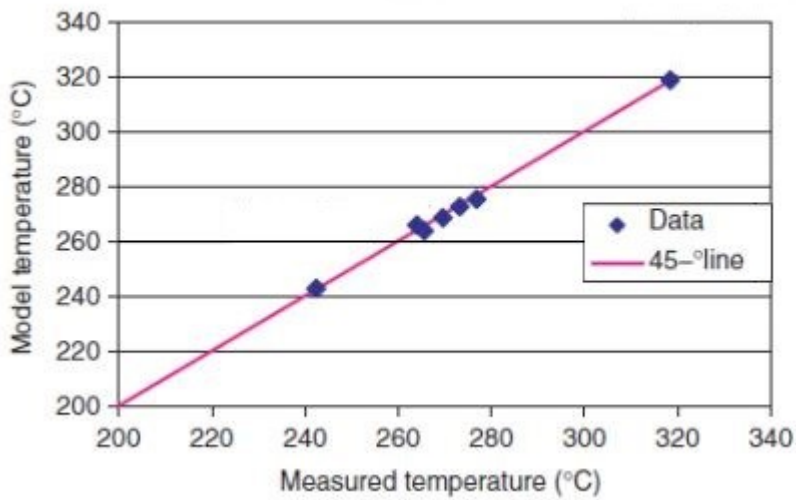


Figure 29. Comparison of theoretical and measured temperature value, convective heat transfer coefficient $h=5.7 \text{ W/m}^2\text{-K}$ [25].

6. EXPERIMENTAL MATERIALS AND METHODS

This section includes information about the materials, extrusion coating pilot line and process parameters. Furthermore, the methods of IR temperature measurements, hot air sealing measurements and pinhole measurements are discussed in detail.

6.1 Materials

The extrusion coating substrate material is the same throughout all trial runs and measurements. In addition to the extrusion coating of the samples, the same substrate material is used as uncoated in the hot air sealing measurements, where the samples are sealed against the uncoated paperboard. The main extrusion coating polymer of all trial runs and measurements is Polyethylene 1 (PE1). It is the reference material, which forms a baseline for all the results. Furthermore, it is the main component in PE blends, which include different proportions of Additive 1 and Additive 2 resins. The compositions of test materials are presented in table 10.

Table 10. Compositions of the test materials.

		Resin content		
		PE1	Additive 1	Additive 2
Coating material	Reference (PE1)	x		
	PE2 blend ratio 1 (high)	x	x	
	PE3 blend ratio 2 (low)	x	x	
	PE4 blend	x		x

In addition to PE1 and Additives 1 and 2, three resins are used in the co-extrusion temperature measurements. These resins form the other layer in the two-layer film structure, which temperature is metered on both sides. The co-extrusion materials are Functional 1, Functional 2 and Functional 3.

6.2 Pilot line and process parameters

Extrusion coating pilot line at TUT is the process line, where all the test materials and samples are manufactured. The trial runs are executed from low to high line speed or to

the breaking point of the film. The sample points are marked for further analysis. The coating weight of the sample points decreases as the line speed increases since screw speed and consequently output of the extruder is kept constant during a single trial run. TUT pilot line is illustrated in figure 30.

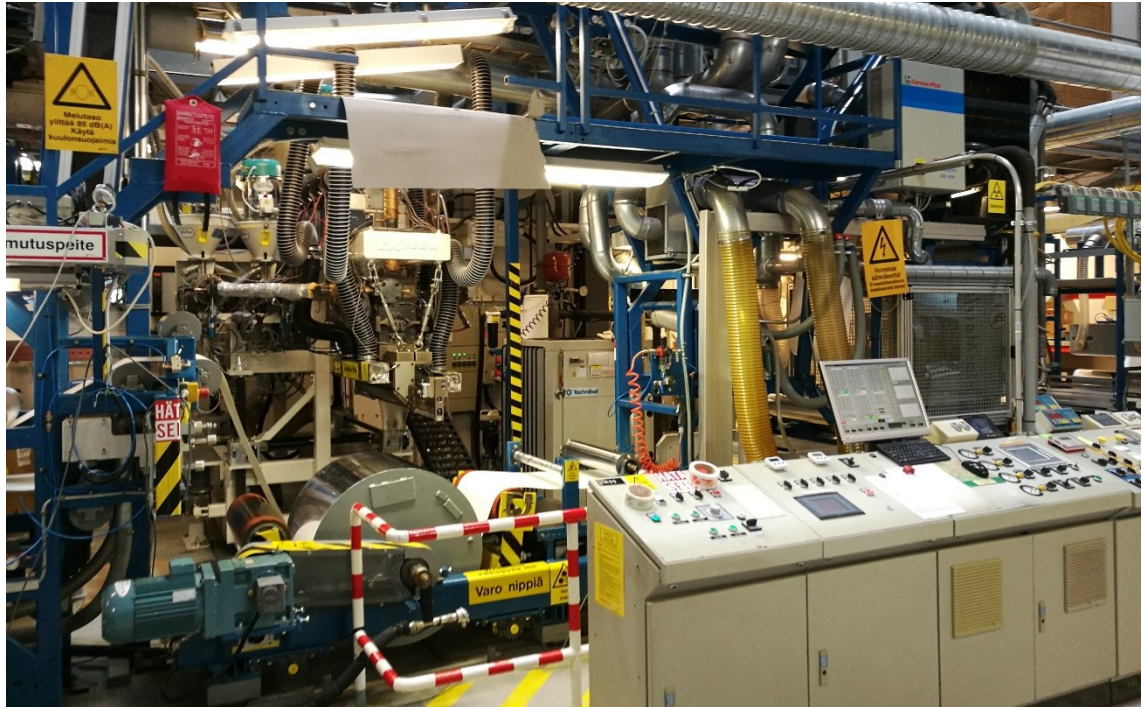


Figure 30. TUT pilot line.

The pilot line consist of few main units, which are unwinding, extruders, laminator and rewinding. Furthermore, the line includes several different surface treatment stations such as corona, post corona, flame and plasma. The extrusion equipment contains four extruders (A, B, C and D), internally deckled T-type die and 5-layer dual plane feedblock. The basic properties of the extruders are presented in table 11 [18].

Table 11. Basic properties of pilot line extruders [18].

	Extruder A	Extruder B	Extruder C	Extruder D (encapsulation)
Diameter (mm)	60	40	30	30
L/D ratio	30	24	25	25
Max output (kg/h) (PE-LD)	90	30	20	20

6.3 Process parameters

The extrusion coating process contains multiple different parameters, which have an influence to the properties of the final product. In this thesis, the most important parameters are the melt temperature and the air gap distance, because they are varied during the trial runs in order to achieve the best possible results. Furthermore, two different screw speed settings are used during the trial runs. All other process parameters are kept constant in order to invalidate their effect on the final product.

The experimental part includes ten trial runs, which focus on the effect of the melt temperature and the air gap distance. Furthermore, two co-extrusion trial runs are performed in order to examine the temperature of two-layer film. All of the materials and the melt temperature, screw speed and air gap settings are collected in the processing table, which is presented in table 12. This table shows the specific material and process parameter combinations for each trial run, which are numbered based on the trial date.

Table 12. Processing table of the trial runs.

Trial run	Coating material	Substrate material	Melt temperature (°C)	Screw speed (rpm)	Air gap (mm)
20170125	PE1	Substrate 1	T1 T2 T3	low high	AG2
20170131-B17	PE2 blend (Ratio 1)	Substrate 1	T1 T2 T3	low high	AG2
20170216-B18	PE3 blend (Ratio 2)	Substrate 1	T1 T2 T3	low high	AG2
20170223-B19	PE4 blend	Substrate 1	T1 T2 T3	low high	AG2
20170302	PE1	Substrate 1	T2	low high	AG1 AG2 AG3
20170308	PE1	Substrate 1	T3	low high	AG1 AG2 AG3
20170309-B20	PE2 blend (Ratio 1)	Substrate 1	T2	low high	AG1 AG2 AG3
20170404-B21	PE4 blend	Substrate 1	T2	low high	AG1 AG2 AG3
20170406-B22	PE2 blend (Ratio 1)	Substrate 1	T3	low high	AG1 AG2 AG3
20170411-B23	PE4 blend	Substrate 1	T3	low high	AG1 AG2 AG3
Co-extrusion					
20170315	Extruder A: PE1	Substrate 1	T2 (medium)		
20170321	Extruder B: Functional 1 Functional 2 Functional 3				

6.4 Temperature measurement set-up

Temperature measurement of the molten polymer film is executed with a pyrometer. The main components of the pyrometer are the measuring probe that meters the film temperature and the monitor that shows the reading in degrees Celsius. Raytek Corporation is the manufacturer of the pyrometers that are used in the temperature measurements of this thesis. The model of both pyrometers is RAYRHP3SF, which is designed especially for the temperature measurement of plastics. Prior to the measurements, the manufacturer has calibrated the pyrometers and adjusted to the exact wavelength that matches PE film. The most important properties of the pyrometer are presented in table 13 and the measuring device including the probe and the monitor is shown in figure 31 [43, 44].

Table 13. *The most important properties of RAYRHP3SF pyrometer [43, 44].*

Parameter	Value
Wavelength area (μm)	3.43
Temperature area ($^{\circ}\text{C}$)	30-340
Accuracy ($^{\circ}\text{C}/\%$)	$\pm 3^{\circ}\text{C}$ (to 65°C) $\pm 2^{\circ}\text{C}$ (from 66°C to 93°C) $\pm 1\%$ (from 94°C to 340°C)
Repeatability of measurements ($^{\circ}\text{C}/\%$)	$\pm 1^{\circ}\text{C}$ or $\pm 0,5\%$
Response time (s)	≤ 2
Ambient temperature ($^{\circ}\text{C}$)	0-65 (without cooling) 0-120 (air cooling) 0-175 (water cooling) 0-315 (thermo jacket)
Relative humidity (%)	10-95

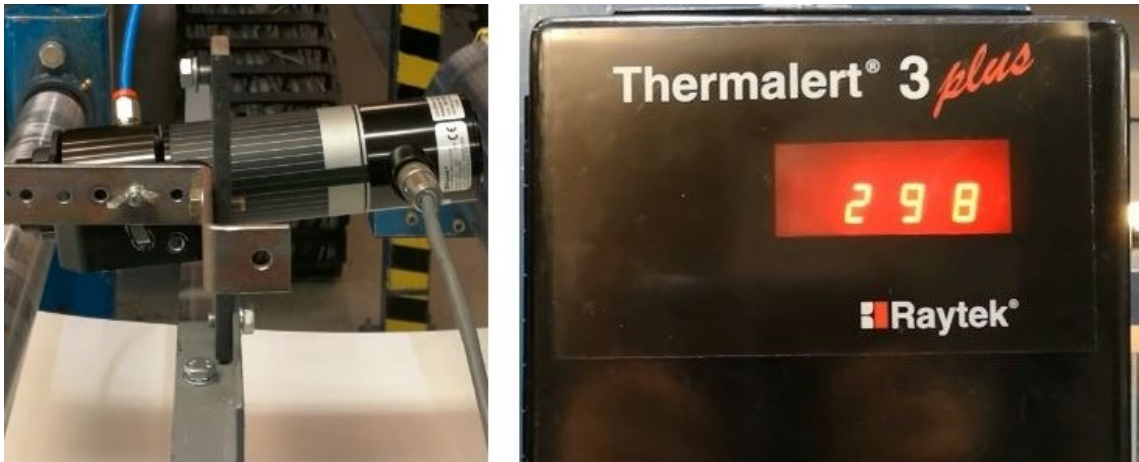


Figure 31. *Measuring device: pyrometer and monitor.*

In IR temperature measurement, the right measurement set-up is as important as the suitable measurement equipment to achieve exact results. It is due to non-contact measurement method, which causes some challenges in addition to many advantages. Both pyrometers are mounted over and in the middle of the extrusion coating line. One is positioned before the extruder (unwinding side) and the other after the extruder (rewinding side), which allows temperature measurement of both layers in two-layer structure. The temperature measurement set-up of extrusion coating trial runs is illustrated in figure 32.

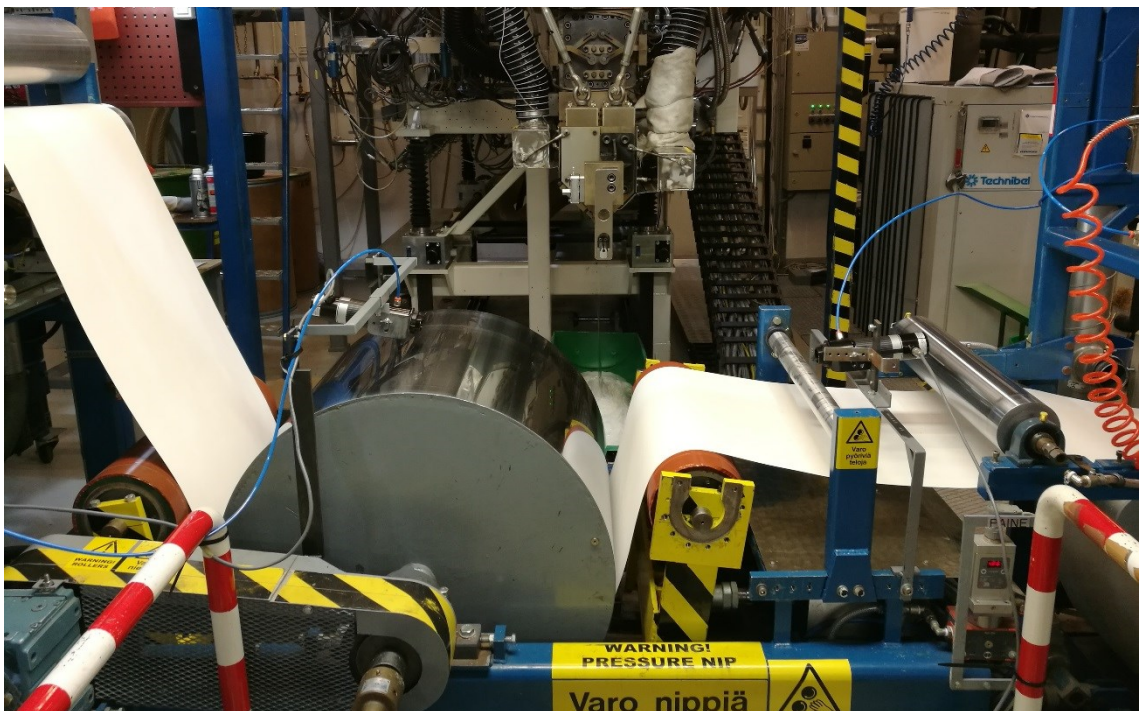


Figure 32. *IR temperature measurement set-up.*

The most important factor in the positioning of the pyrometers is unrestrained field of view to the target. The field of view in conjunction with possible mounting points determine the locations of the pyrometers. The pyrometers are cooled by airflow that enables

their use close to the hot film. Both pyrometers can be placed approximately 50 cm distance away from the target. The spot size of the pyrometer expands as the distance between target and pyrometer is increased. The technical data of the manufacturer presents that the minimum spot diameter is 2.5 mm and it increases linearly as the distance increases. Using that information, the spot diameter of pyrometers can be calculated and it is approximately 122 mm. The calculations and corresponding linear regression is shown in table 14 and figure 33.

Table 14. Correlation between target distance and spot diameter.

Target distance (mm)	Spot diameter (mm)
0	2.5
25	7.5
50	14
76	21
130	33
Actual values	
(Spot diameter = 0.2388 * Target distance + 2.1806)	
500	122

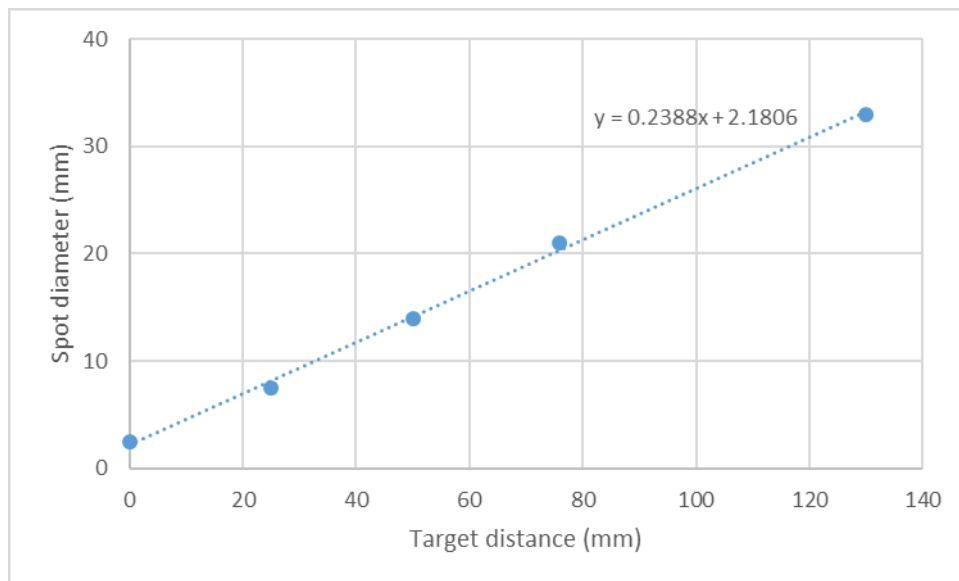


Figure 33. Linear regression between target distance and spot diameter.

The whole spot must fit on the target to receive exact results. The mounting of pyrometers allows adjustment of the angle, which moves the spot in vertical direction. It is crucial for the temperature measurements of the film with low air gap distances. Every time the temperature measurements are conducted, the operator must be certain that the pyrometer spot is entirely on the film and the reading is reliable.

6.5 Hot air sealing measuring method

Heat sealing measurements of the samples is done by using the hot air sealing equipment at TUT. The hot air sealing measuring method differs slightly from the traditional hot bar sealing method. It utilizes the hot air blowers to heat the samples, and the heat and pressure are applied on the samples consecutively at the different stations. Furthermore, the heating and cooling of the machine is very fast, which is advantageous, when numerous sample points are sealed. The hot air sealing equipment is shown in figure 34.

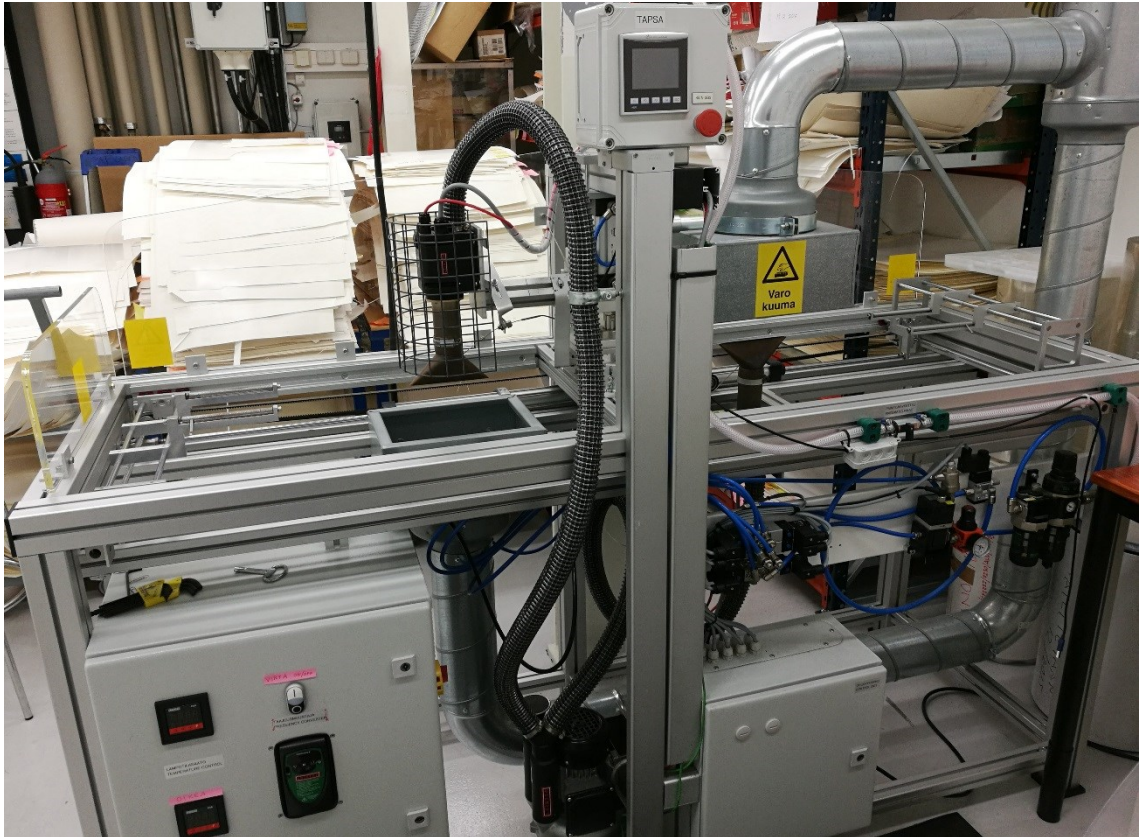


Figure 34. Hot air sealing equipment.

In this thesis, hot air sealing measurements are conducted by pressing the extrusion coated sample against the uncoated paperboard, which is the same material as the extrusion coating substrate. Furthermore, all the samples are sealed in the machine direction. The process starts with the manual attachment of the samples. The coated sample is attached to the right side clamp and the uncoated paperboard to the left side clamp of the machine. The process is automated and when the samples are attached, the sealing is started from the monitor. The machine moves the samples next to the blowers, where they are heated for a certain time. Since the heating is accomplished via hot air and the samples are not in direct contact with the blowers, the temperature setting is much higher than the actual temperature on the surface of the samples. After the heating, the samples are moved one on the other between the clamping unit, where a certain amount of pressure is applied for a certain time to form a tight seal. The dimensions of the seal is determined by the sealing

bars size. The most important properties and parameters of hot air sealing equipment are presented in table 15. This table provides both the possible range of the equipment and the setting used in every measurement [30].

Table 15. *Parameters of the hot air sealing equipment [30].*

Parameter	Range
Hot air blower temperature (°C)	Up to 550
Hot air blower speed (Hz)	20-60
Heating time (s)	Up to 5
Open time (s)	Up to 5
Pressing time (s)	Up to 5
Sealing force (N)	100-1000
Sealing bar size (cm)	0.3 x 15 (upside) 1 x 15 (underside)
Sample size (cm)	11 (machine direction) x 15.5 (cross direction)

As the sealing process is completed, the sealed sample is manually released from the clamps and the machine is returned back to the initial position from the monitor. Thereafter, the strength of the seal is examined, which is the most important phase of the measurements. The sample is manually torn perpendicularly to the seal direction in order to define how tightly the sides are adhered together. The procedure should be performed similarly every time so that the variation caused by the measurer is minimal. The adhesion of the seal is graded by values from 0 to 5 and the value is qualified by visually analyzing the tear of the seal. The value is determined according to the percentage of fiber tear. The value 5 corresponds to 100% fiber tear and it is the goal for every sample. If the fiber tear is less than 100% and consequently the result of measurement is other than 5, the measurement is repeated with the same sample point and higher temperature setting. As the value 5 is achieved three times in a row with the same sample point, the corresponding temperature value can be considered the minimum sealing temperature and the result is documented. The scale of hot air sealing measurement results is shown in table 16 [45].

Table 16. Seal grading scale of hot air sealing [45].

Value	Description
0	No seal
1	Weak adhesion
2	Adhered but no tear
3	Under 50% fiber tear
4	Over 50% fiber tear
4.5	Over 90% fiber tear
5	100% fiber tear

6.6 Pinhole measuring method

Pinhole measurements of the samples are conducted to examine the amount of tiny holes, tears or other defects in the polymer film. These discontinuity points in the coating impair e.g. barrier properties and collapse the quality of the final product. The measurement principle is rather straightforward. Ethanol-turpentine solution is applied on the test surface by brush. The solution is left to take effect briefly whereupon it penetrates any holes in the coating and colors the substrate below. The measurement principle is illustrated in figure 35.

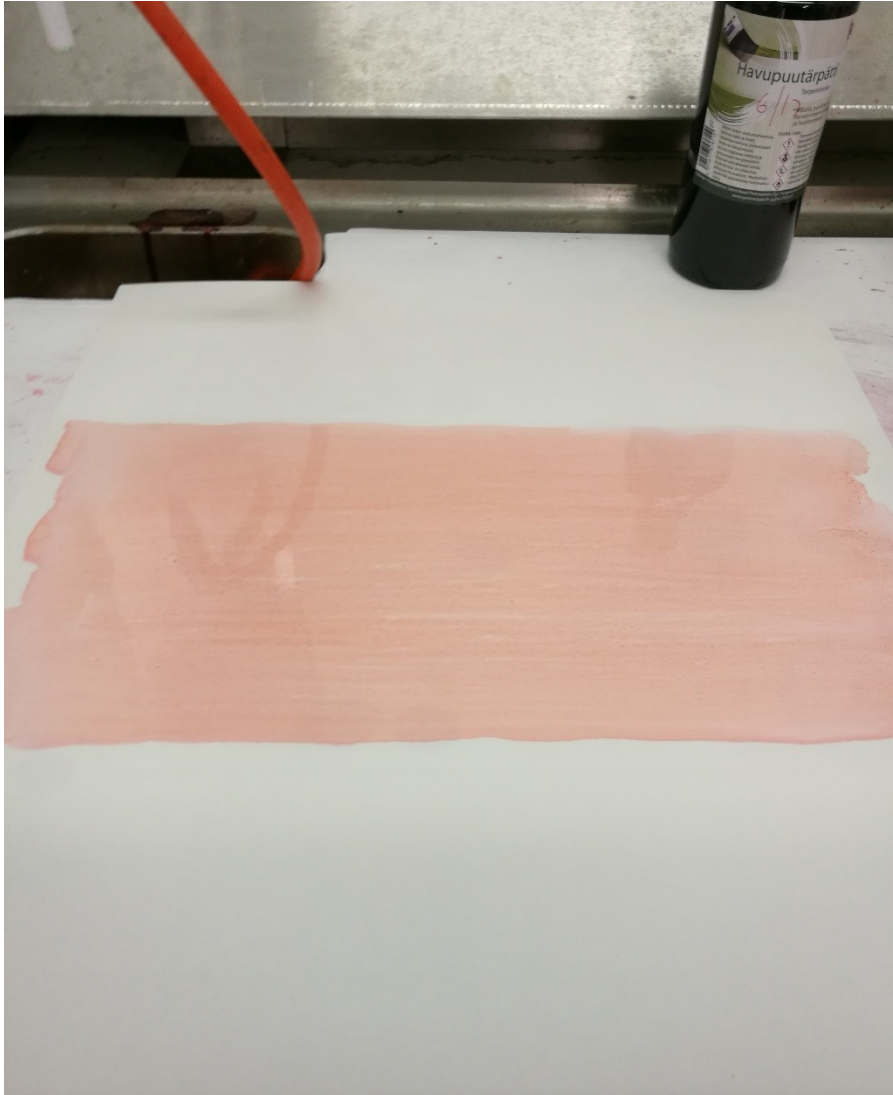


Figure 35. *Pinhole measuring method.*

If the polymer film is continuous, the solution stays on top of the coating and the substrate remains clean. Otherwise, the number of colored spots overlaid are counted and the results are documented. The results can be expressed as a number of pinholes per square meter. In this thesis, the term off refers to zero pinholes and the term on refers to number of pinholes over two. Borderline cases i.e. values 1 and 2 are recorded as such. The size of the pinhole measurement sample is set to the constant length of 50 cm in the machine direction. In the cross direction, the size of the sample is dependent on the width of the film and consequently on neck-in value.

7. RESULTS AND DISCUSSION

In this section of the thesis, all the measurement data and results are discussed. The measurement data is reviewed in chronological order based on the trial runs that are performed at the pilot line. In the first part of the measurements, the effect of melt temperature and material choice is considered. In the second part, the influence of air gap distance is examined with limited material choices and melt temperature values, which are based on the first set of the measurements. Lastly, the temperature measurements of co-extrusion applications are discussed briefly. The temperature measurements are performed with pyrometer at pilot line in real time with the trial runs. Hot air sealing and pinhole measurements are conducted in laboratory after the trial runs. The sample points of hot air sealing and pinhole measurements are located at various line speed regions of the trial run, and consequently the effect of coating weight reduction can be examined.

7.1 Effect of melt temperature and material on product properties

The first part of the results focuses on the influences of PE material and melt temperature to the specified product properties, which are hot air sealing and pinholes. The melt temperature setting is modified in order to examine the thermos-mechanical degradation in the extruder barrel. This part consists of four trial runs, and corresponding hot air sealing and pinhole measurements in the laboratory. The research include four different PE materials, which are processed with three temperature and two screw speed settings. The reference material of the measurements is PE1. Other material choices are PE blends, which include contents of Additives 1 and 2. The melt temperatures are set to low (T1), medium (T2) and high (T3) and all temperature settings are operated with low and high screw speeds and with the constant air gap setting (AG2).

7.1.1 Trial runs 20170125

The coating material of the trial runs 20170125 is the reference PE1. The specific process parameters and the materials of the trial runs 20170125 are presented in table 12.

The laboratory measurement of the trial runs contain determination of coating weight average including standard deviation, adhesion and width and neck-in of the film. The laboratory measurement results of the trial runs 20170125 are listed in appendix A. Adhesion is enhanced, when the melt temperature is increased. At the highest melt temperature (T3), adhesion is excellent (value 5) even with the lowest coating weights, when under 10 g/m² values are reached. Width and neck-in of the film are not relevant factors,

because the air gap distance is the constant (AG2), which doesn't cause significant neck-in.

I Temperature measurements

In this first trial run (20170125), IR temperature measurements of the film were not accomplished. Although IR temperature measurement set-up was not used in this first trial run, the material comparison can be performed later as planned. Temperature values of the film that correspond T2 and T3 melt temperature settings with AG2 setting, can be received from the subsequent temperature measurements concerning the air gap distance.

II Hot air sealing measurements

Hot air sealing measurement results of the trial runs 20170125 are presented in appendix B. Each line speed is listed with the corresponding coating weight and sealing temperature. Some of the low line speed sample points are left out from the hot air sealing measurements, since the corresponding coating weights are very high and they are located outside the most significant coating weight area. The measurement results are shown in figure 36. Sealing temperature is presented as a function of coating weight and each data series is connected with fitted curve, which adapt to the data series as closely as possible.

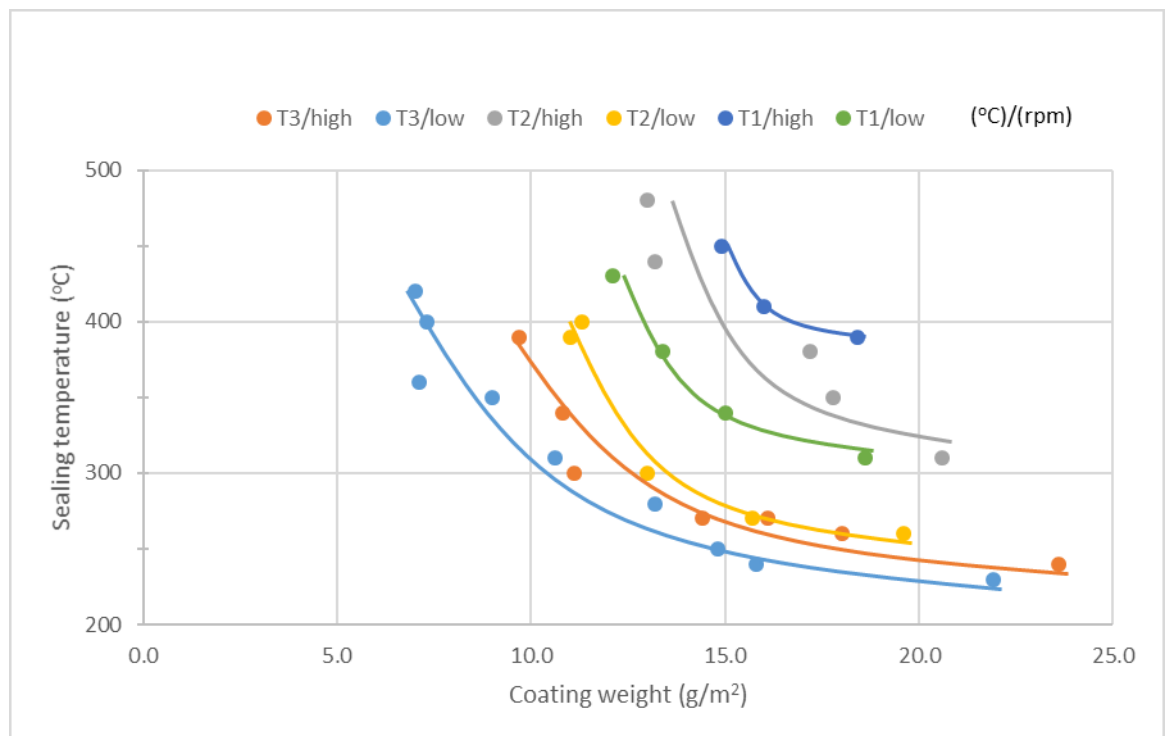


Figure 36. Hot air sealing temperature as a function of coating weight, trial runs 20170125.

Figure 36 shows that the sealing temperature increases as the coating weight decreases. Thicker layer of coating material seals more easily and at lower temperature, if the layer

is not excessive. As the sealing temperature increases over too high temperatures, the seal starts to darken and the paperboard burns because of the excessive high temperature. The higher melt temperature improves the sealability and consequently decreases the sealing temperature. As the melt temperature inside the barrel increases, degradation of PE increases, which generates more active chain ends. These chain ends enhance the oxidation and consequently increase the bonding between the molten PE and the paperboard. However, excessive temperatures and degradation should be avoided, since they can deteriorate the sealing properties. Since the melt temperature is higher with the lower screw speed, low rpm trial run samples are sealed much better compared to high rpm trial run samples with same temperature setting.

III Pinhole measurements

Pinhole measurement results of the trial runs 20170125 are presented in table 17. The coating weight limit, where pinholes appear, is highlighted with yellow color. In contrast to hot air sealing measurements, all sample points are examined in the case of pinholes are generated during the extrusion coating process.

Table 17. Pinhole results of trial runs 20170125.

20170125-1 (T1/low)			20170125-2 (T1/high)			20170125-3 (T2/low)		
Line speed	Coating weight (g/m ²)	Pin-holes	Line speed	Coating weight (g/m ²)	Pin-holes	Line speed	Coating weight (g/m ²)	Pin-holes
low1	20.76	off	low1	36.14	off	low1	21.8	off
low2	18.56	off	low2	28.26	off	low2	19.62	off
low3	15.02	off	low3	24.38	off	low3	15.74	off
low4	13.36	off						
medium1	12.06	off	medium1	18.4	off	medium1	13	1
			medium2	16	off	medium2	11.02	on
			medium3	14.92	off	medium3	11.28	on
20170125-4 (T2/high)			20170125-5 (T3/low)			20170125-6 (T3/high)		
Line speed	Coating weight (g/m ²)	Pin-holes	Line speed	Coating weight (g/m ²)	Pin-holes	Line speed	Coating weight (g/m ²)	Pin-holes
low1	35.86	off	low1	21.94	off	low1	33.42	off
low2	29.34	off	low2	15.78	off	low2	26.42	off
low3	25.78	off	low3	14.78	off	low3	23.58	off
medium1	20.56	off	medium1	13.24	off	medium1	17.96	off
medium2	17.78	off	medium2	10.64	1	medium2	16.14	off
medium3	17.24	off	medium3	9.04	1	medium3	14.4	off
high1	13.24	off	high1	7.12	on	high1	11.08	off
high2	12.96	1	high2	7.28	on	high2	10.8	1
			high3	6.96	on	high3	9.74	on

Pinhole measurement results show that pinholes start to appear between coating weights of 13 g/m² and 10 g/m². Higher melt temperature decreases pinhole limit to slightly lower coating weights but the effect enhances only after the melt temperature exceeds T2 and the best results are achieved at the highest melt temperature (T3). At the lowest melt temperature (T1), draw down and melt strength of the material are poor and the film breaks at low line speeds. Therefore, low coating weights are not reached and the pinholes does not appear at all.

7.1.2 Trial runs 20170131-B17

The coating material of the trial runs 20170131-B17 is PE2 blend. The specific process parameters and the material composition of the trial runs 20170131-B17 are presented in table 12.

The laboratory measurement results of the trial runs 20170131-B17 are listed in appendix A. Adhesion is excellent throughout the measurements. Only at the lowest melt temperature (T1), adhesion is below maximum (value 5) with high line speeds. Compared to the previous trial runs, adhesion is enhanced slightly. The width and neck-in of the film are not significant factors, because air gap is set to the constant value (AG2) that does not cause notable neck-in.

I Temperature measurements

In trial runs 20170131-B17, IR temperature measurement equipment including the pyrometer was used for the first time. Temperature curves of the trial runs 20170131-B17 are illustrated in figure 37. The temperature value of the molten film is presented as a function of time. The corresponding line speeds are also shown in this figure, because the line speed value has an influence on the film temperature in practice.

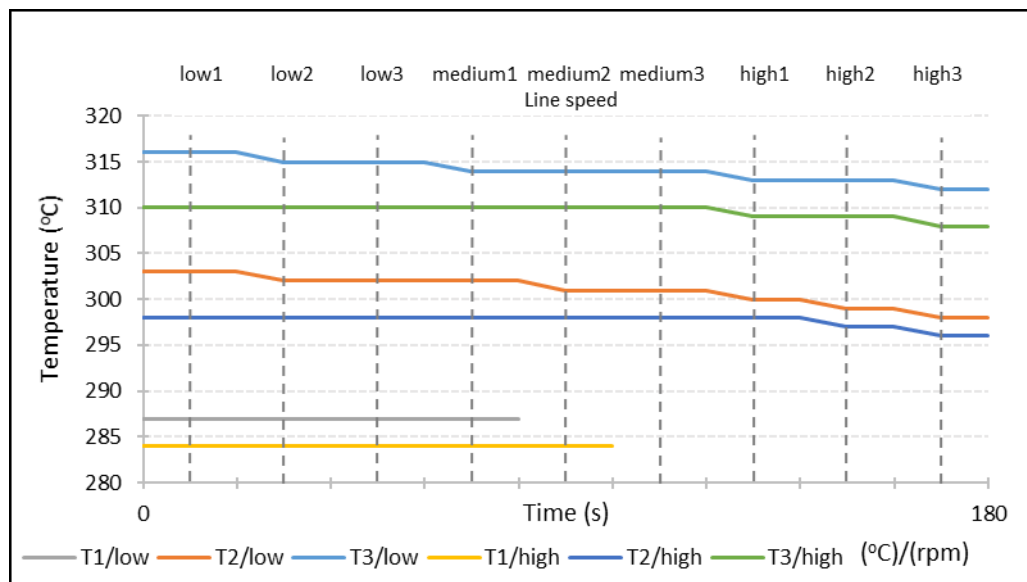


Figure 37. *Film temperature as a function of time, trial runs 20170131-B17.*

Cooling of the film during the trial runs is the most important result of the IR temperature measurements. Cooling is mainly caused by the increasing line speed and consequently increasing airflow as well as the decreasing of film thickness. In these trial runs, cooling is not significant overall due to relatively low air gap distance (AG2), but minor temperature decrease is noticed. At the lowest melt temperature (T1) value, the film do not cool at all until the melt breakdown occurs. At the higher screw speed, cooling does not starts prior to medium3 line speed, when the effect of airflow intensifies. Therefore, the temperature drop is only a few degrees. At the lower screw speed, the film starts to cool slightly earlier due to the lower throughput, but overall the cooling is still small.

II Hot air sealing measurements

Hot air sealing measurement results of the trial runs 20170131-B17 are presented appendix B, where each line speed is listed with the corresponding coating weight and sealing temperature. Some of the sample points are left out from the measurements, since corresponding coating weights are very high. The measurement results are shown in figure 38. Sealing temperature is presented as a function of coating weight and each data series is combined with fitted curve.

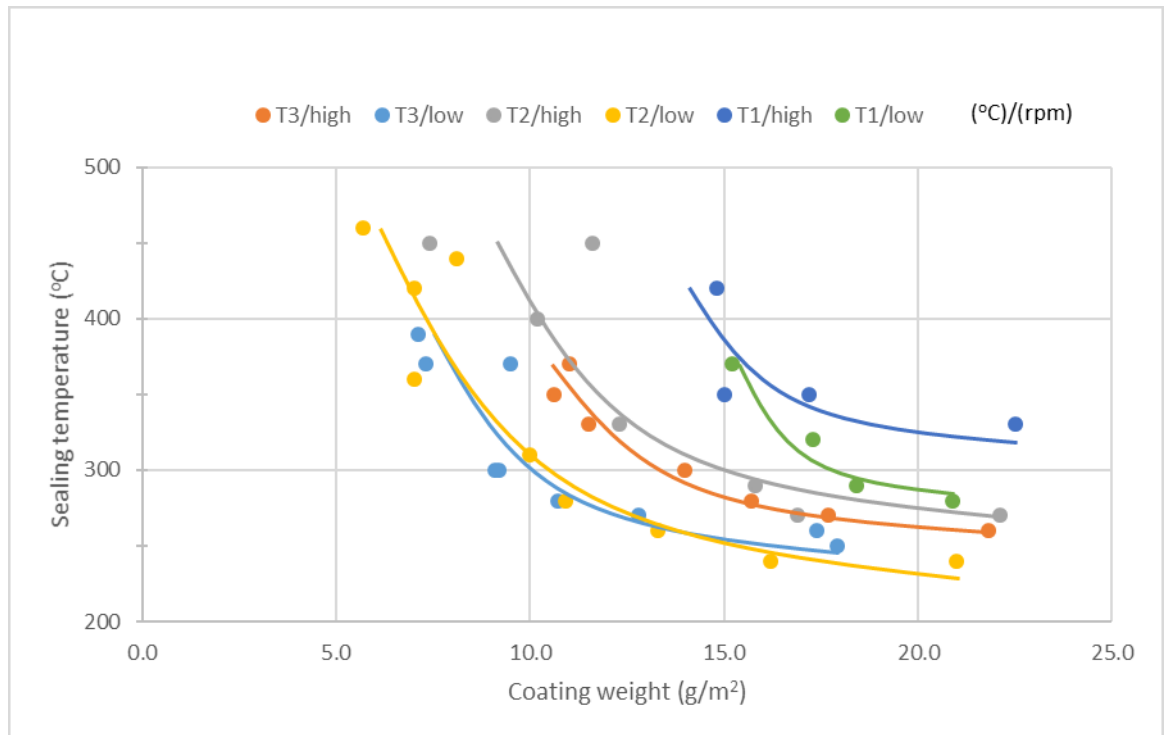


Figure 38. Hot air sealing temperature as a function of coating weight, trial runs 20170131-B17.

Figure 38 illustrates that the sealing temperature increases as the coating weight decreases, if the coating thickness is not excessive. The sealing temperature is decreasing due to high melt temperatures prevailed in extrusion coating. However, the difference between T2 and T3 melt temperature is minor. The highest melt temperature does not provide as great advantage as in the previous measurements. Furthermore, the scatter of results is rather large at the low coating weights. Therefore, T3 is not necessarily the optimal melt temperature considering hot air sealing and it may locate between T2 and T3.

III Pinhole measurements

Pinhole measurement results of the trial runs 20170131-B17 are presented in table 18. The coating weight limit, where pinholes appear, is highlighted with yellow color. All

sample points are examined to make sure that pinholes are not generated in any part of the extrusion coating process.

Table 18. Pinhole results of trial runs 20170131-B17.

20170131-B17-1 (T1/low)			20170131-B17-2 (T1/high)			20170131-B17-3 (T2/low)		
Line speed	Coating weight (g/m ²)	Pin-holes	Line speed	Coating weight (g/m ²)	Pin-holes	Line speed	Coating weight (g/m ²)	Pin-holes
low1	20.88	off	low1	31.64	off	low1	21.02	off
low2	18.36	off	low2	26.54	off	low2	16.18	off
low3	17.3	off	low3	22.48	off	low3	13.34	off
low4	15.18	off	low4	17.16	off	medium1	10.88	off
			medium1	15	off	medium2	9.98	off
			medium2	14.78	1	medium3	7.02	1
						high1	6.98	2
						high2	8.1	on
						high3	5.66	on
20170131-B17-4 (T2/high)			20170131-B17-5 (T3/low)			20170131-B17-6 (T3/high)		
Line speed	Coating weight (g/m ²)	Pin-holes	Line speed	Coating weight (g/m ²)	Pin-holes	Line speed	Coating weight (g/m ²)	Pin-holes
low1	31.9	off	low1	17.94	off	low1	32.44	off
low2	25.78	off	low2	17.44	off	low2	25.56	off
low3	22.14	off	low3	12.84	off	low3	21.78	off
medium1	16.9	off	medium1	10.66	off	medium1	17.68	off
medium2	15.82	off	medium2	9.06	1	medium2	15.74	off
medium3	12.26	off	medium3	9.24	on	medium3	14.02	off
high1	10.24	off	high1	9.46	on	high1	11.54	off
high2	11.56	off	high2	7.3	on	high2	10.56	1
high3	7.42	on	high3	7.12	on	high3	11.02	1

Pinhole results show that pinholes start to appear between coating weights of 11 g/m² and 7 g/m², if the lowest melt temperature samples are not included. At the lowest melt temperature (T1), draw down is poor and the melt breakdown occurs at low line speeds. Consequently, low coating weights are not reached and only one sample point contains a pinhole. Pinhole results between T2 and T3 melt temperature setting are very similar and the distinct difference cannot be observed. Therefore, the optimal melt temperature considering pinholes is not definitive.

7.1.3 Trial runs 20170216-B18

The coating material of the trial runs 20170216-B18 is PE3 blend. The specific process parameters and the material composition are presented in table 12.

The laboratory measurement results of the trial runs 20170216-B18 are listed in appendix A. Adhesion is enhanced distinctly as the melt temperature is increased. Only the highest melt temperature (T2) provides the maximum adhesion (value 5) throughout all the line speeds. As the melt temperature is decreased, the adhesion starts to deteriorate simultaneously. Consequently, adhesion is worse at lower temperatures compared to the previous trial runs.

I Temperature measurements

The temperature curves of the trial runs 20170216-B18 are illustrated in figure 39. Temperature value of the film is presented as a function of time and the corresponding line speeds are also shown in the figure.

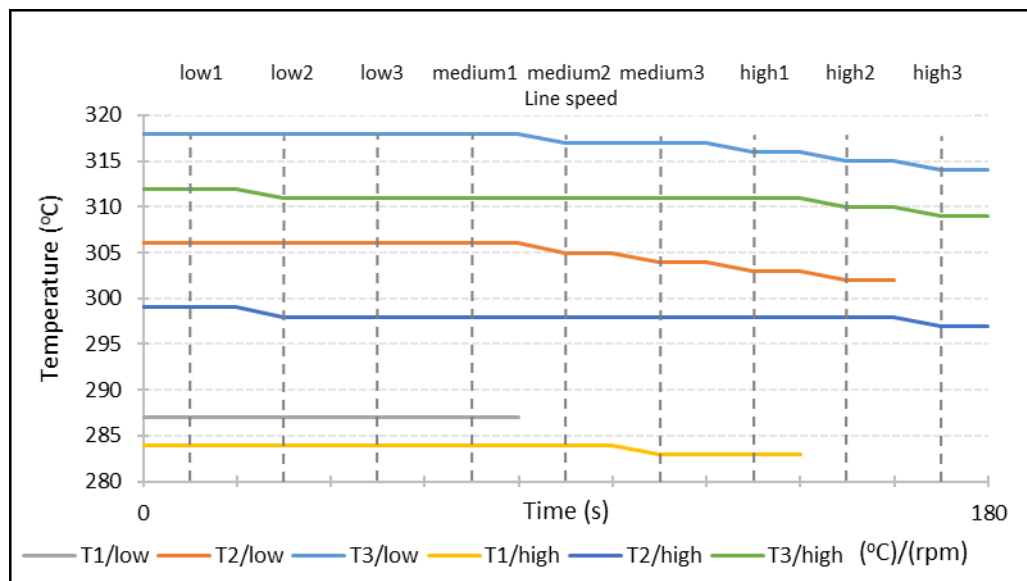


Figure 39. *Film temperature as a function of time, trial runs 20170216-B18.*

The temperature data presents that the film cooling is not significant due to relatively low air gap distance (AG2), but some temperature decrease is observed. At the low screw speed, cooling is slightly faster compared to the high screw speed due to lower throughput. However, the largest temperature drop is still a few degrees at most. The cooling intensifies after medium2 line speed, when the effect of airflow intensifies. The differences between different melt temperature values are minor. At T1 melt temperature and high screw speed setting, the film does not cool at all, since the melt breakdown occurs so early.

II Hot air sealing measurements

Hot air sealing results of the trial runs 20170216-B18 are presented in appendix B. The measurement results are also shown in figure 40.

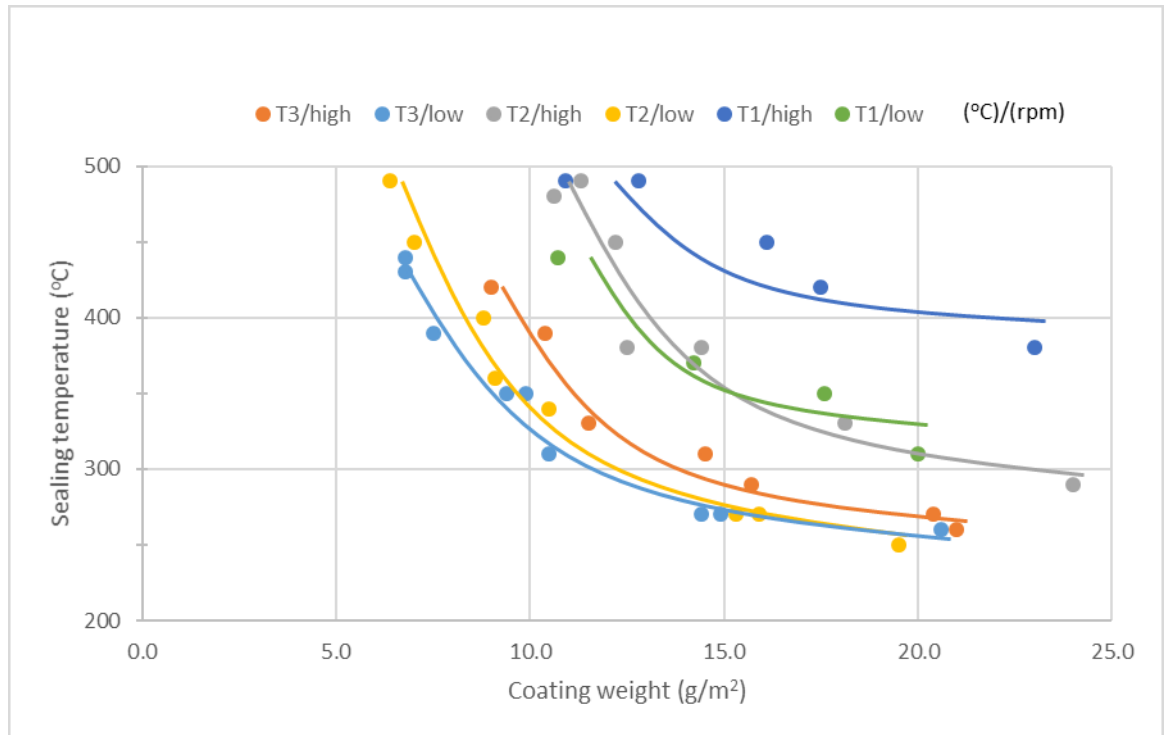


Figure 40. Hot air sealing temperature as a function of coating weight, trial runs 20170216-B18.

Figure 40 illustrates the distinct trend that the sealing temperature increases as the coating weight decreases. Higher melt temperature decreases the sealing temperature, but T2 melt temperature and low screw speed setting is also performing well. The similar results are noticed in the previous measurements, where the same materials are used with the different blending ratio. Therefore, the optimal melt temperature setting considering hot air sealing results is not obvious for Additive 1 blends, although T3 setting provides the best results.

III Pinhole measurements

Pinhole measurement results of the trial runs 20170216-B18 are presented in table 19 and the coating weight limit, where pinholes appear, is highlighted with yellow color.

Table 19. Pinhole results of trial runs 20170216-B18.

20170216-B18-1 (T1/low)			20170216-B18-2 (T1/high)			20170216-B18-3 (T2/low)		
Line speed	Coating weight (g/m ²)	Pin-holes	Line speed	Coating weight (g/m ²)	Pin-holes	Line speed	Coating weight (g/m ²)	Pin-holes
low1	19.98	off	low1	32.86	off	low1	19.46	off
low2	17.64	off	low2	28.12	off	low2	15.94	off
low3	14.22	off	low3	22.98	off	low3	15.34	off
medium1	10.74	off	medium1	17.48	off	medium1	10.52	off
			medium2	16.08	off	medium2	9.06	off
			medium3	12.84	off	medium3	8.84	off
			high1	10.9	off	high1	7.04	on
						high2	6.44	on
20170216-B18-4 (T2/high)			20170216-B18-5 (T3/low)			20170216-B18-6 (T3/high)		
Line speed	Coating weight (g/m ²)	Pin-holes	Line speed	Coating weight (g/m ²)	Pin-holes	Line speed	Coating weight (g/m ²)	Pin-holes
low1	34.36	off	low1	20.64	off	low1	32.18	off
low2	28.42	off	low2	14.94	off	low2	25.48	off
low3	24	off	low3	14.36	off	low3	20.96	off
medium1	18.1	off	medium1	10.5	off	medium1	20.38	off
medium2	14.36	off	medium2	9.9	off	medium2	15.74	off
medium3	12.5	off	medium3	9.4	1	medium3	14.46	1
high1	12.2	off	high1	7.46	on	high1	11.48	off
high2	10.58	off	high2	6.82	on	high2	10.36	off
high3	11.32	1	high3	6.78	on	high3	8.98	on

Pinhole results present that pinholes start to appear between coating weights of 11 g/m² and 7 g/m². At the lowest melt temperature (T1), the melt breakdown occurs before the highest line speeds are reached and pinholes do not appear at all. As in the previous measurements with the same materials and different blending ratio, pinhole results between T2 and T3 melt temperature setting are very similar. The best result is achieved with T2 and high screw speed settings and therefore the optimal melt temperature setting considering pinholes is not evident.

7.1.4 Trial runs 20170223-B19

The coating material of the trial runs 20170223-B19 is PE4 blend. These are the final runs, where the effect of melt temperature and thermo-mechanical degradation in extruder barrel are examined. The specific process parameters and the material composition are presented in table 12.

The laboratory measurement results of the trial runs 20170223-B19 are listed in appendix A. Adhesion of the samples is excellent throughout every melt temperature and screw speed combination. Only few sample points are below the maximum adhesion level (value 5) and the melt temperature has no significant effect to the adhesion values. High line speeds were not met, because the blend was not homogenous. Therefore, the melt strength was not high enough in extrusion coating phase.

I Temperature measurements

The temperature curves of the trial runs 20170223-B19 are illustrated in figure 41. Temperature value of the film is presented as a function of time and with the corresponding line speed values.

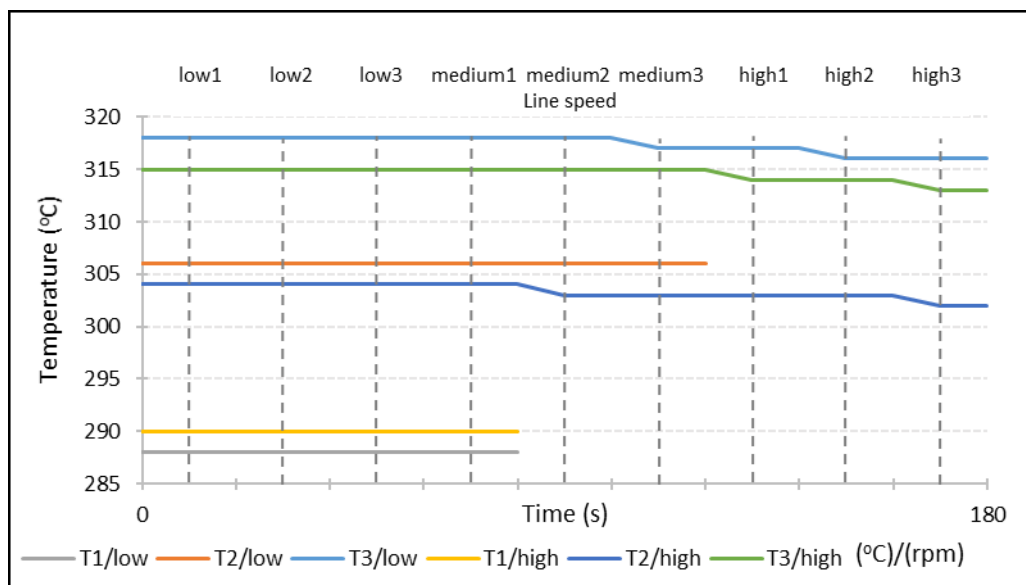


Figure 41. *Film temperature as a function of time, trial runs 20170223-B19.*

The film cooling during the trial runs is observable but it is not significant due to the medium air gap distance setting (AG2). The temperature drop is only few degrees at most. The film cooling begins actually above medium2 line speed, when the effect of airflow intensifies. The lowest melt temperature trial runs are not finished because of the melt breakdown occurs, before any temperature drop can be observed.

II Hot air sealing measurements

Hot air sealing results of the trial runs 20170223-B19 are presented in appendix B. The measurement results are also shown in figure 42.

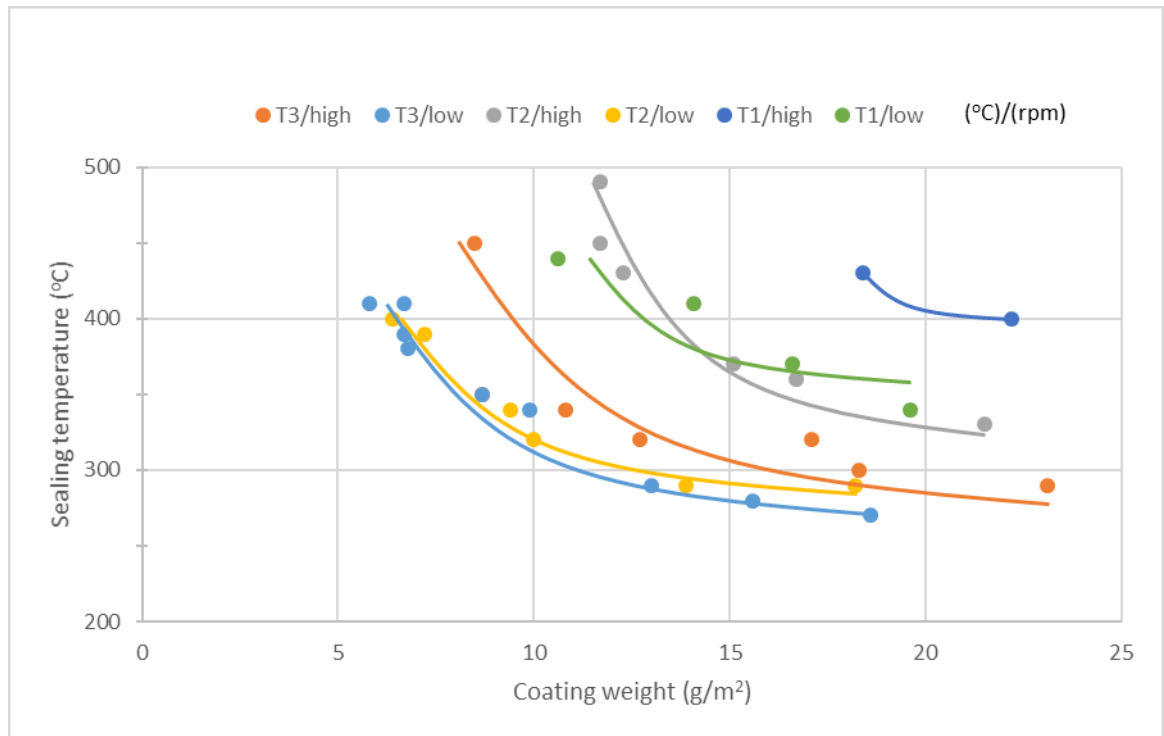


Figure 42. Hot air sealing temperature as a function of coating weight, trial runs 20170223-B19.

Figure 42 illustrates the trend, where the sealing temperature increases as the coating weight decreases. Extremely high sealing temperatures are limited to the lower melt temperature samples and the samples of T3 setting are sealed fine. Higher melt temperature decreases the sealing temperature, although the difference between T2 and T3 melt temperature setting is minor with lower screw speed. The highest melt temperature can be considered as the best alternative concerning the sealing properties. The lowest temperature setting in extrusion coating has been distinctly worst throughout every hot air sealing measurement and the trial runs 20170223-B19 does not make exception.

III Pinhole measurements

Pinhole measurement results of the trial runs 20170223-B19 are presented in table 20 and the coating weight limit, where pinholes appear, is highlighted with yellow color.

Table 20. Pinhole results of trial runs 20170223-B19.

20170223-B19-1 (T1/low)			20170223-B19-2 (T1/high)			20170223-B19-3 (T2/low)		
Line speed	Coating weight (g/m ²)	Pin-holes	Line speed	Coating weight (g/m ²)	Pin-holes	Line speed	Coating weight (g/m ²)	Pin-holes
low1	19.62	off	low1	32.1	off	low1	18.22	off
low2	16.56	off	low2	27.26	off	low2	13.9	off
low3	14.14	off	low3	22.16	off	low3	10.04	off
medium1	10.64	off	medium1	18.36	off	medium1	9.44	off
						medium2	7.2	on
						medium3	6.4	on
20170223-B19-4 (T2/high)			20170223-B19-5 (T3/low)			20170223-B19-6 (T3/high)		
Line speed	Coating weight (g/m ²)	Pin-holes	Line speed	Coating weight (g/m ²)	Pin-holes	Line speed	Coating weight (g/m ²)	Pin-holes
low1	35.36	off	low1	18.56	off	low1	32.94	off
low2	29.42	off	low2	15.58	off	low2	26.1	off
low3	24.56	off	low3	13.02	off	low3	23.06	off
medium1	21.46	off	medium1	9.9	off	medium1	18.32	off
medium2	16.72	off	medium2	8.66	off	medium2	17.14	off
medium3	15.06	off	medium3	6.76	on	medium3	12.72	off
high1	12.26	off	high1	6.74	on	high1	10.76	off
high2	11.66	on	high2	6.68	on	high2	8.72	1
high3	11.72	on	high3	5.76	on	high3	8.48	on

Pinhole results present that pinholes start to appear between coating weights of 12 g/m² and 7 g/m². Higher melt temperature decreases pinhole limit to slightly lower coating weights but distinct difference between T2 and T3 melt temperature settings is not noticed with the lower screw speed. However, the higher screw speed setting indicates that the highest melt temperature (T3) provides the best results. The lowest melt temperature (T1) causes melt breakdown at such low line speeds, that pinholes do not appear at all.

7.2 Effect of air gap distance and material on product properties

The second part of the results focuses on the influences of PE material and air gap distance to the hot air sealing and pinhole properties. The air gap setting is modified in order to analyze the oxidation in the air gap region. This part consists of six trial runs including film temperature measurements, and corresponding hot air sealing and pinhole measurements in the laboratory. In these trial runs, the research include three different PE mate-

rials, which are determined by previous results. PE3 blend is left out from the measurements, because the lower Additive 1 content causes slight weakening of the hot air sealing and pinhole results. The materials are processed with two temperature and screw speed settings. The lowest melt temperature is excluded from the examination, since the results of the first part of measurements are unsatisfactory and the processing temperature is clearly too low for good results. The reference material of the measurements is the same PE1, but the manufacturing batch is changed. Other two materials are PE2 and PE4 blends. The melt temperatures are set to medium (T2) and high (T3), and the temperatures are operated with low and high screw speeds. The air gap distance settings are low (AG1), medium (AG2) and high (AG3).

7.2.1 Trial runs 20170302

The coating material of the trial runs 20170302 is the reference PE1. The process parameters and the materials are shown in table 12.

The laboratory measurement results of trial run 20170302 are listed in appendix A. Adhesion is excellent (value 5) almost at every sample point. The only exceptions are two lower air gap trial runs with the higher screw speed, where adhesion is slightly decreased at the high line speeds. Lower melt temperature results in decreased oxidation depending on the processing parameter set-ups. The highest air gap distance (AG1) and consequently longer oxidation time results in excellent adhesion. The width and neck-in of the film are considerably important factors than in the previous trial runs. Because the air gap distance is varied, the width decreases and neck-in increases with the higher air gap. This can be seen from the laboratory results. Neck-in of the film is over three times larger with the highest air gap compared to the lowest setting. This causes increase of the uncoated area and thicker edge beads.

Temperature measurements

The temperature curves of the trial runs 20170302 are illustrated in figure 43. Temperature value of the film is presented as a function of time and with the corresponding line speed values. The importance of film temperature measurement is increased, because the air gap is varied and the film cooling changes depending on the air gap distance.

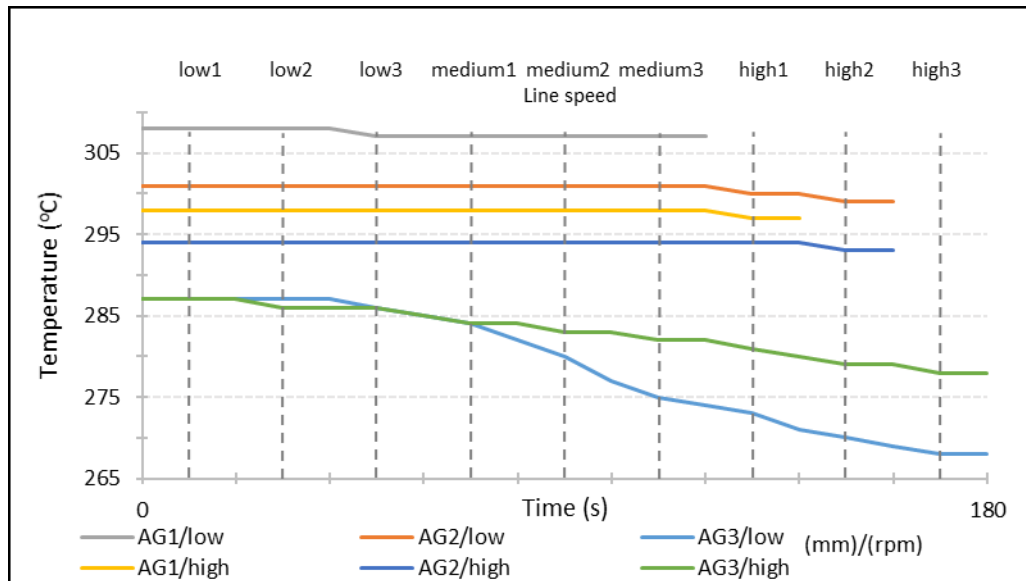


Figure 43. Film temperature as a function of time, trial runs 20170302.

The most important goal of the temperature measurements is to monitor the film cooling during the trial runs, because the air gap is varied. The cooling is not significant with the low and medium air gap settings (AG1 and AG2). Moreover, the difference between AG1 and AG2 settings is minor, because the angle of the pyrometer must be modified for the lowest air gap distance so that the whole spot of pyrometer is within the film. Therefore, the distances from the die exit to the measuring point are close to each other and consequently the cooling is similar. The most interesting temperature curves are accomplished with the highest air gap setting (AG3). In these curves, the cooling of the film is observed clearly. Temperature starts to decrease significantly right after low3 line speed and the decrease is rather linear. At this line speed, the effect of airflow starts to intensify, and the cooling is assisted by the decreasing film thickness. The final temperature drop is around 20°C with the low rpm setting and around 10°C with the high rpm setting.

II Hot air sealing measurements

Hot air sealing measurement results of trial runs 20170302 are shown in appendix B, where every sample point is listed with corresponding coating weights and sealing temperatures. As previously, some of the sample points are left out from measurements, since corresponding coating weights are very high and they do not affect to the final conclusions. The effect of the air gap distance on the hot air sealing temperature is analyzed with figure 44.

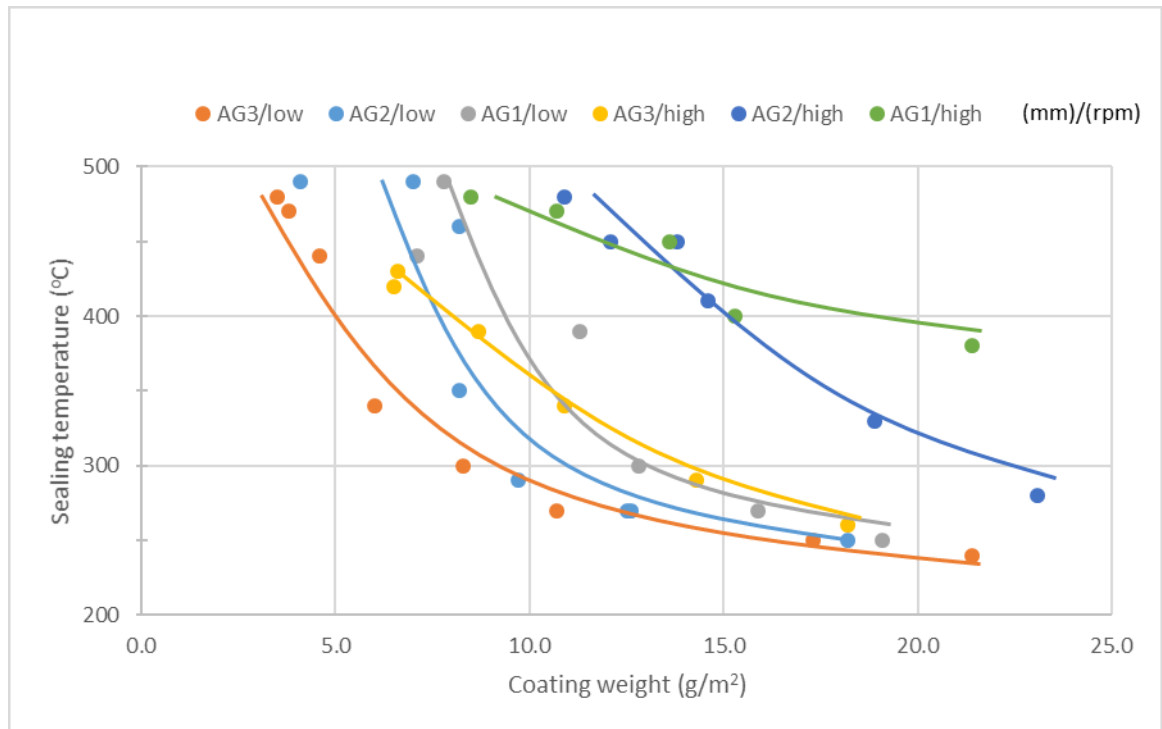


Figure 44. Hot air sealing temperature as a function of coating weight, trial runs 20170302.

Examination of the hot air sealing results of the trial runs 20170302 shows the distinct trend between the curves of the different air gap distances. At the low screw speed, as the air gap distance increases, the hot air sealing curves move towards lower sealing temperatures, if the coating weight is equal. Higher air gap distance result in increasing oxidation of the film, which in turn enhances the bonding between materials and eventually lowers the sealing temperature. Similar trend can be observed at the high screw speed, although the slope of hot air sealing curves is more gentle. The only exception is AG1 and high screw speed setting, which differs from the trend most. This is due to the high sealing temperature of the highest coating weight sample point, which affects to the slope of curve.

III Pinhole measurements

Pinhole measurement results of the trial runs 20170302 are presented in table 21 and the coating weight limits, where first pinholes appear, are highlighted with yellow. Contrary to hot air sealing measurements, all sample points are still examined to make sure that any pinholes are not generated during the extrusion coating.

Table 21. Pinhole results of trial runs 20170302.

20170302-1 (T2/low/AG1)			20170302-2 (T2/low/AG2)			20170302-3 (T2/low/AG3)		
Line speed	Coating weight (g/m ²)	Pin-holes	Line speed	Coating weight (g/m ²)	Pin-holes	Line speed	Coating weight (g/m ²)	Pin-holes
low1	19.08	off	low1	18.18	off	low1	27.8	off
low2	15.9	off	low2	12.64	off	low2	21.42	off
low3	12.82	off	low3	12.46	off	low3	17.3	off
medium1	11.26	1	medium1	9.72	off	medium1	10.68	off
medium2	7.08	on	medium2	8.24	on	medium2	8.28	off
medium3	7.82	on	medium3	8.2	on	medium3	6.02	off
			high1	7.02	on	high1	4.56	on
			high2	4.1	on	high2	3.76	on
						high3	3.5	on
20170302-4 (T2/high/AG1)			20170302-5 (T2/high/AG2)			20170302-6 (T2/high/AG3)		
Line speed	Coating weight (g/m ²)	Pin-holes	Line speed	Coating weight (g/m ²)	Pin-holes	Line speed	Coating weight (g/m ²)	Pin-holes
low1	30.94	off	low1	32.82	off	low1	50.14	off
low2	24.6	off	low2	27.98	off	low2	37.62	off
low3	21.38	off	low3	23.14	off	low3	27.38	off
medium1	15.28	off	medium1	18.86	off	medium1	18.16	off
medium2	13.62	off	medium2	14.56	off	medium2	14.26	off
medium3	10.68	2	medium3	13.8	off	medium3	10.88	off
high1	8.5	on	high1	12.1	off	high1	8.7	off
			high2	10.86	on	high2	6.54	off
						high3	6.58	off

Pinhole measurement results of the trial runs 20170302 show that overall pinholes start to appear between coating weights of 11 g/m² and 5 g/m². The highest air gap distance decreases pinhole limit to distinctly lower coating weights but distinct difference between AG1 and AG2 settings cannot be noticed. The effect is similar with both screw speed settings. The results of two lower air gap settings are at similar level as previously, but AG3 setting provides excellent results and the last trial run avoids pinholes totally.

7.2.2 Trial runs 20170308

The coating material of the trial runs 20170302 is the reference PE1. The process parameters and the materials are shown in table 12.

The laboratory measurement results of trial run 20170308 are listed in appendix A. Every sample point has excellent (value 5) adhesion. This is due to high melt temperature, which provides great bonding between the film and substrate, even with the lowest air gap distance setting. The width and neck-in of the film are significant factors, because the air gap distance is varied. The width decreases and neck-in increases with the higher air gap, which is seen from the laboratory results. Neck-in of the film is over three times larger with the highest air gap compared to the lowest value.

I Temperature measurements

The temperature curves of the trial runs 20170308 are illustrated in figure 45. Temperature value of the film is presented as a function of time and with the corresponding line speed values.

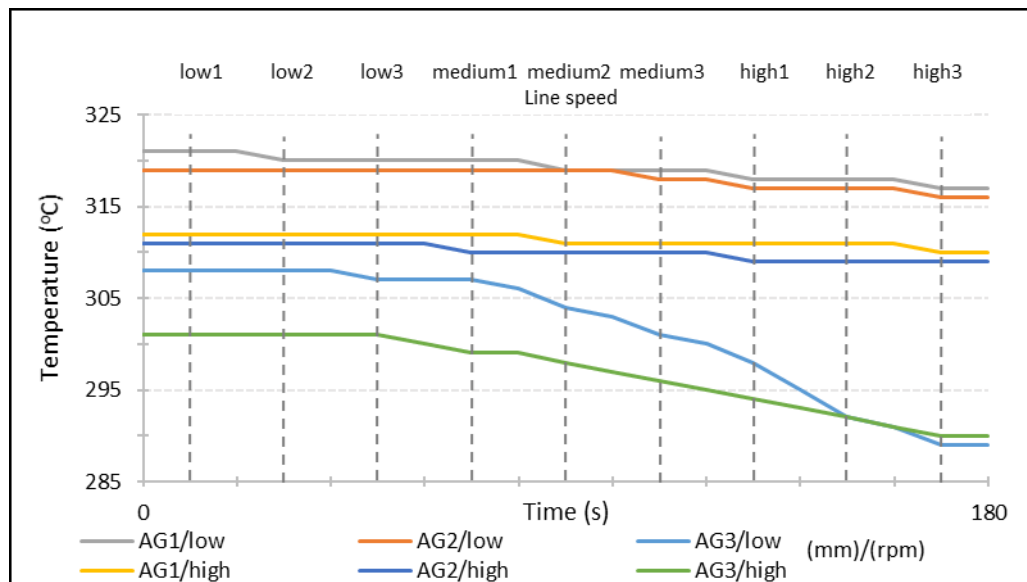


Figure 45. *Film temperature as a function of time, trial runs 20170308.*

The temperature data shows that the film cooling is almost negligible with the low and medium air gap settings (AG1 and AG2). The highest air gap setting (AG3), produce the most uneven temperature data and the temperature drop is significant. Temperature starts to decrease powerfully around medium1 line speed and the decrease is rather linear with both screw speed settings. The lower screw speed setting has higher initial temperature but the cooling is faster due to lower throughput and the final temperature is at lower level. Altogether, the temperature drop is around 20°C with the low rpm setting and around 10°C with the high rpm setting.

II Hot air sealing measurements

Hot air sealing measurement results of the trial runs 20170308 are shown in appendix B. The effect of the air gap distance on the sealing temperature is analyzed with figure 46..

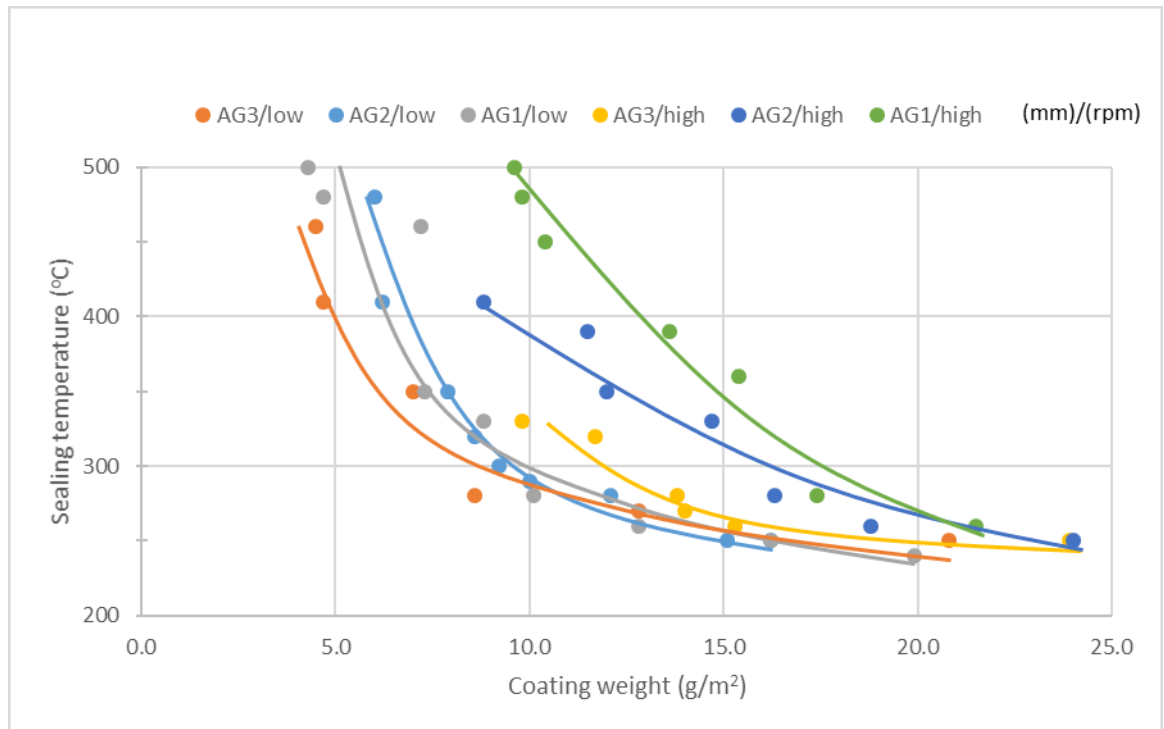


Figure 46. Hot air sealing temperature as a function of coating weight, trial runs 20170308.

Analysis of the hot air sealing results 20170308 present similar trend as the first set of the air gap related measurements. Generally as the air gap distance increases, the hot air sealing curves move towards lower sealing temperatures, if the coating weight is equal. The effect is observable with both screw speed settings. The only exceptions are the lower air gap settings at the lower screw speed. The lowest air gap setting (AG1) provides slightly better results than AG2 setting, but the difference is minor and any conclusions cannot be made based on this.

III Pinhole measurements

Pinhole measurement results of the trial runs 20170308 are presented in table 22 and the coating weight limits, where first pinholes appear, are highlighted with yellow.

Table 22. Pinhole results of trial runs 20170308.

20170308-1 (T3/low/AG1)			20170308-2 (T3/low/AG2)			20170308-3 (T3/low/AG3)		
Line speed	Coating weight (g/m ²)	Pin-holes	Line speed	Coating weight (g/m ²)	Pin-holes	Line speed	Coating weight (g/m ²)	Pin-holes
low1	19.86	off	low1	16.18	off	low1	46.92	off
low2	16.18	off	low2	15.06	off	low2	38.74	off
low3	12.84	off	low3	12.14	off	low3	31.52	off
medium1	10.08	off	medium1	10.04	off	medium1	20.84	off
medium2	8.82	on	medium2	9.2	on	medium2	12.8	off
medium3	7.32	on	medium3	8.56	on	medium3	8.62	off
high1	7.18	on	high1	7.92	on	high1	6.98	off
high2	4.74	on	high2	6.16	on	high2	4.7	on
high3	4.28	on	high3	5.98	on	high3	4.48	on
20170308-4 (T3/high/AG1)			20170308-5 (T3/high/AG2)			20170308-6 (T3/high/AG3)		
Line speed	Coating weight (g/m ²)	Pin-holes	Line speed	Coating weight (g/m ²)	Pin-holes	Line speed	Coating weight (g/m ²)	Pin-holes
low1	30.96	off	low1	32.56	off	low1	63.1	off
low2	26.8	off	low2	27.88	off	low2	49.22	off
low3	21.52	off	low3	23.98	off	low3	36.46	off
medium1	17.44	off	medium1	18.82	off	medium1	23.94	off
medium2	15.42	off	medium2	16.28	off	medium2	15.3	off
medium3	13.64	off	medium3	14.7	off	medium3	14.04	off
high1	10.36	off	high1	11.98	off	high1	13.78	off
high2	9.84	on	high2	11.54	off	high2	11.7	off
high3	9.6	on	high3	8.8	1	high3	9.76	off

Pinhole measurement results of the trial runs 20170308 present that overall pinholes start to appear between coating weights of 10 g/m² and 5 g/m². As in the previous results, the highest air gap distance decreases the pinhole limit to distinctly lower coating weights but clear difference between AG1 and AG2 air gap settings cannot be observed. The results of two lower air gap settings are at the typical level but AG3 setting produces again excellent results and the last trial run avoids pinholes completely.

7.2.3 Trial runs 20170309-B20

PE2 blend is the coating material of the trial runs 20170309-B20. The process parameters and the material composition are shown in table 12.

The laboratory measurement results of the trial runs 20170309-B20 are listed in appendix A. Overall, adhesion of the sample points is mainly excellent (value 5). The lower melt temperature setting (T2) causes slight weakening of adhesion especially with the higher screw speed. This can be noticed from trial runs of AG1 and AG2 settings. However, the highest air gap enhance oxidation so much that the adhesion remains excellent. The width and neck-in of the film are again varied along the air gap settings. Neck-in of AG1 setting is over doubled with AG2 setting and over tripled with AG3 setting.

I Temperature measurements

The temperature data of the trial runs 20170309-B20 is illustrated in figure 47. Temperature value of the film is presented as a function of time and the line speed of the pilot line is shown in the figure.

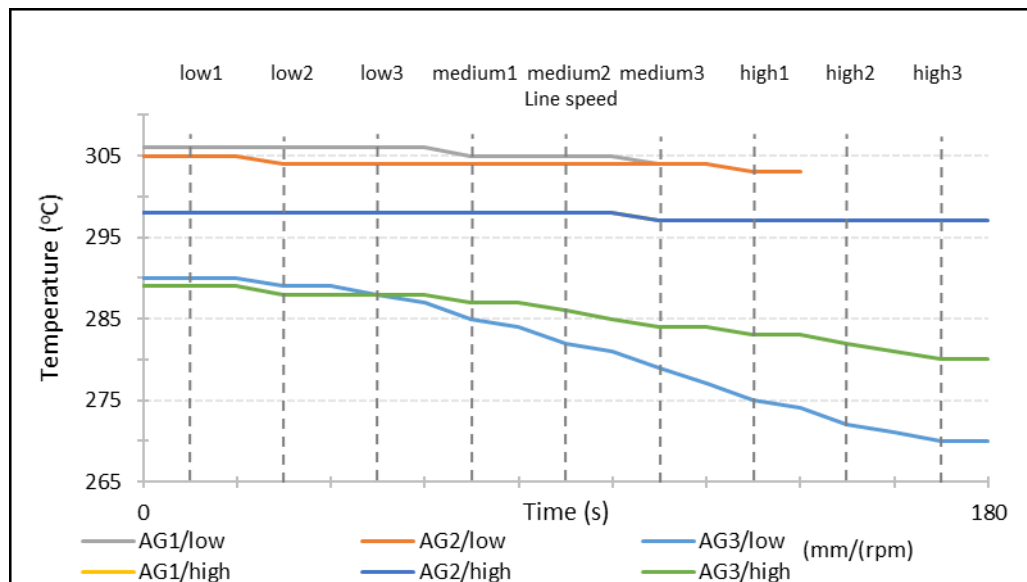


Figure 47. Film temperature as a function of time, trial runs 20170309-B20.

The temperature drop of the film is very small throughout the trial runs with low and medium air gap settings (AG1 and AG2). The higher screw speed decreases the initial film temperature distinctly, although the difference moderates with the highest air gap setting (AG3). The highest air gap setting causes significant temperature drop as noticed in the previous trial runs. The temperature starts to decrease more rapidly around low3 line speed and the decrease is rather linear with both screw speed settings. The final temperature of the lower screw speed setting ends up distinctly lower level, because the cooling is faster with the lower throughput. Altogether, the temperature drop is around 10°C with the high rpm setting and twice as much with the low rpm setting.

II Hot air sealing measurements

Hot air sealing measurement results of the trial runs 20170309-B20 are shown in appendix B and in figure 48.

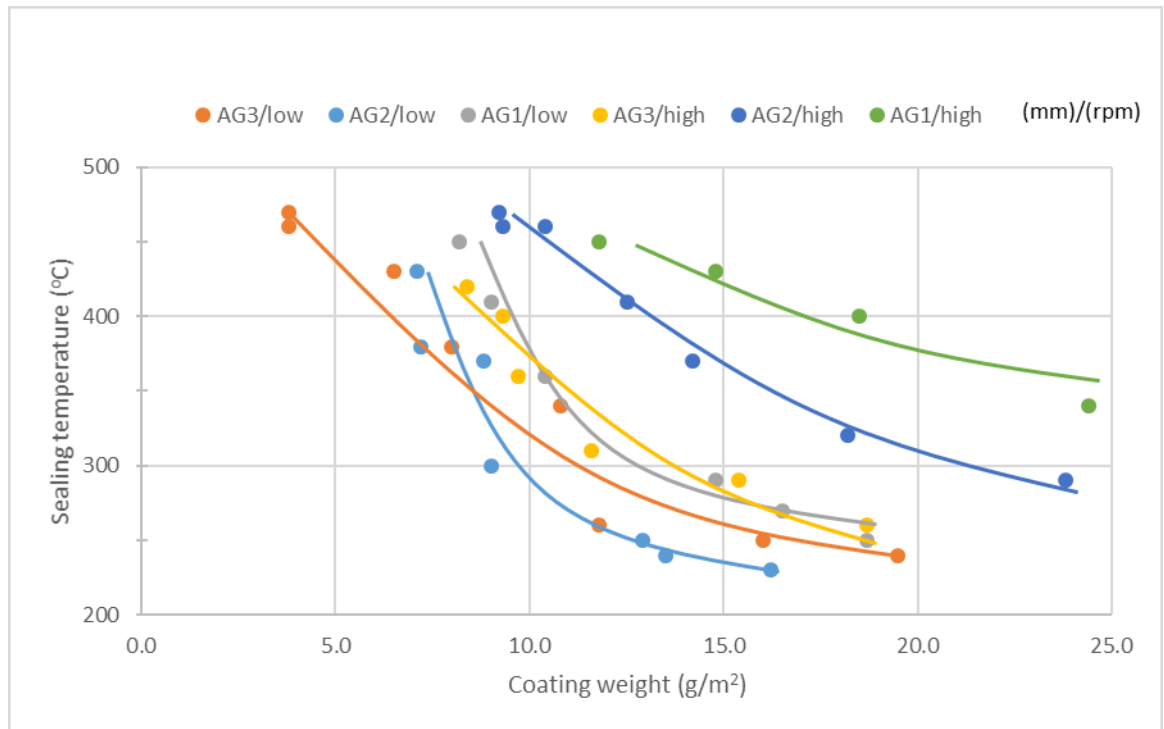


Figure 48. Hot air sealing temperature as a function of coating weight, trial runs 20170309-B20.

Hot air sealing results of the trial runs 20170309-B20 indicate the same trend that is noticed in the previous measurement results. Increasing air gap distance decreases the sealing temperature, if the coating weight is equal and the material change to PE2 blend does not have an influence on the trend. The effect of air gap distance can be noticed with both screw speed settings but the sealing temperature difference is even larger with the higher screw speed. The medium and high air gap settings at lower screw speed cause minor exception to the results. Initially, AG3 setting causes higher sealing temperatures than AG2 setting, but the difference turns around, when lower coating weights are reached.

III Pinhole measurements

Pinhole measurement results of the trial runs 20170309-B20 are presented in table 23, where the pinhole limits are highlighted with yellow.

Table 23. Pinhole results of trial runs 20170309-B20

20170309-B20-1 (T2/low/AG1)			20170309-B20-2 (T2/low/AG2)			20170309-B20-3 (T2/low/AG3)		
Line speed	Coating weight (g/m ²)	Pin-holes	Line speed	Coating weight (g/m ²)	Pin-holes	Line speed (m/min)	Coating weight (g/m ²)	Pin-holes
low1	18.66	off	low1	16.18	off	low1	29.02	off
low2	16.46	off	low2	13.48	off	low2	19.54	off
low3	14.8	off	low3	12.86	off	low3	15.96	off
medium1	10.44	off	medium1	9.02	off	medium1	11.82	off
medium2	9	on	medium2	8.84	off	medium2	10.76	off
medium3	8.24	on	medium3	7.24	on	medium3	8	off
			high1	7.1	on	high1	6.48	on
						high2	3.82	on
						high3	3.84	on
20170309-B20-4 (T2/high/AG1)			20170309-B20-5 (T2/high/AG2)			20170309-B20-6 (T2/high/AG3)		
Line speed	Coating weight (g/m ²)	Pin-holes	Line speed	Coating weight (g/m ²)	Pin-holes	Line speed	Coating weight (g/m ²)	Pin-holes
low1	35.18	off	low1	31.9	off	low1	49.7	off
low2	27.84	off	low2	27.22	off	low2	35.16	off
low3	24.4	off	low3	23.8	off	low3	25.16	off
medium1	18.48	off	medium1	18.24	off	medium1	18.68	off
medium2	14.82	off	medium2	14.24	off	medium2	15.36	off
medium3	11.8	off	medium3	12.52	off	medium3	11.62	off
			high1	10.42	off	high1	9.68	off
			high2	9.34	off	high2	9.26	off
			high3	9.18	off	high3	8.44	off

Pinhole results of the trial runs 20170309-B20 show that pinholes appear between coating weights of 9 g/m² and 6 g/m². The difference between the highest and lowest air gap value is smaller than in the previous pinhole measurements. Furthermore, the high screw speed sample points does not contain any pinholes, although the low coating weights are reached. The results are great with all process parameter combinations, and pinhole limit is at relatively low coating weights.

7.2.4 Trial runs 20170404-B21

PE4 blend is the coating material of the trial runs 20170404-B21. The process parameters and the material composition are shown in table 12.

The laboratory measurement results of trial run 20170404-B21 are listed in appendix A. The first impression of adhesion is excellent but closer examination reveal some issues. The worst adhesion values are measured from the low screw speed and higher air gap sample points. These sample points have the lowest and the most desired coating weights and other process parameters produce rather high coating weights. Therefore, adhesion of the material cannot be considered excellent. This is mainly caused by the lower melt temperature setting, which does not work properly with this blend. The same issue was noticed in the first part of the measurements, where the effect of melt temperature was examined. Width and neck-in of the film vary typically along the air gap settings. Neck-in at AG1 setting approximately doubles with AG2 setting and triples with AG3 setting.

I Temperature measurements

The temperature data of the trial runs 20170404-B21 is illustrated in figure 49. Temperature value of the film is presented as a function of time and the line speed of the pilot line is shown in the figure.

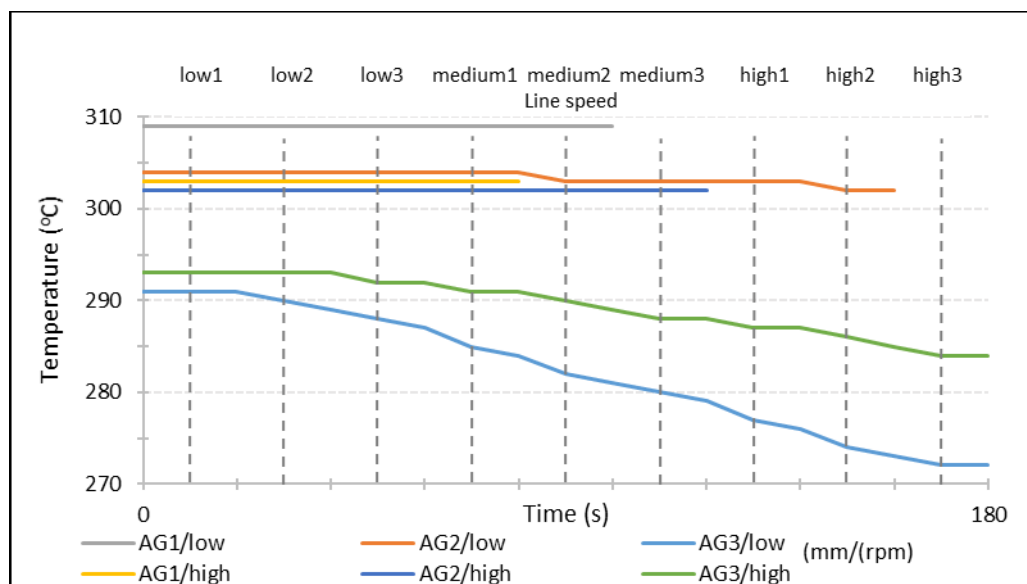


Figure 49. *Film temperature as a function of time, trial runs 20170404-B21*

The temperature drop of the film is extremely small throughout the trial runs with the low and medium air gap settings (AG1 and AG2), which is typical. The most significant deviation is in AG3 setting results, where the high screw speed has higher initial temperature than the low screw speed. Normally, the extruder produces higher melt temperature with the lower screw speed, due to the long residence time. However, the temperature decrease and the rate of decrease are at similar level with earlier measurements. The temperature drop accelerates around low3 line speed and the final temperature drop is around 10°C with the high rpm setting and twice as much with the low rpm setting.

II Hot air sealing measurements

Hot air sealing measurement results of the trial runs 20170404-B21 are presented in appendix B and in figure 50.

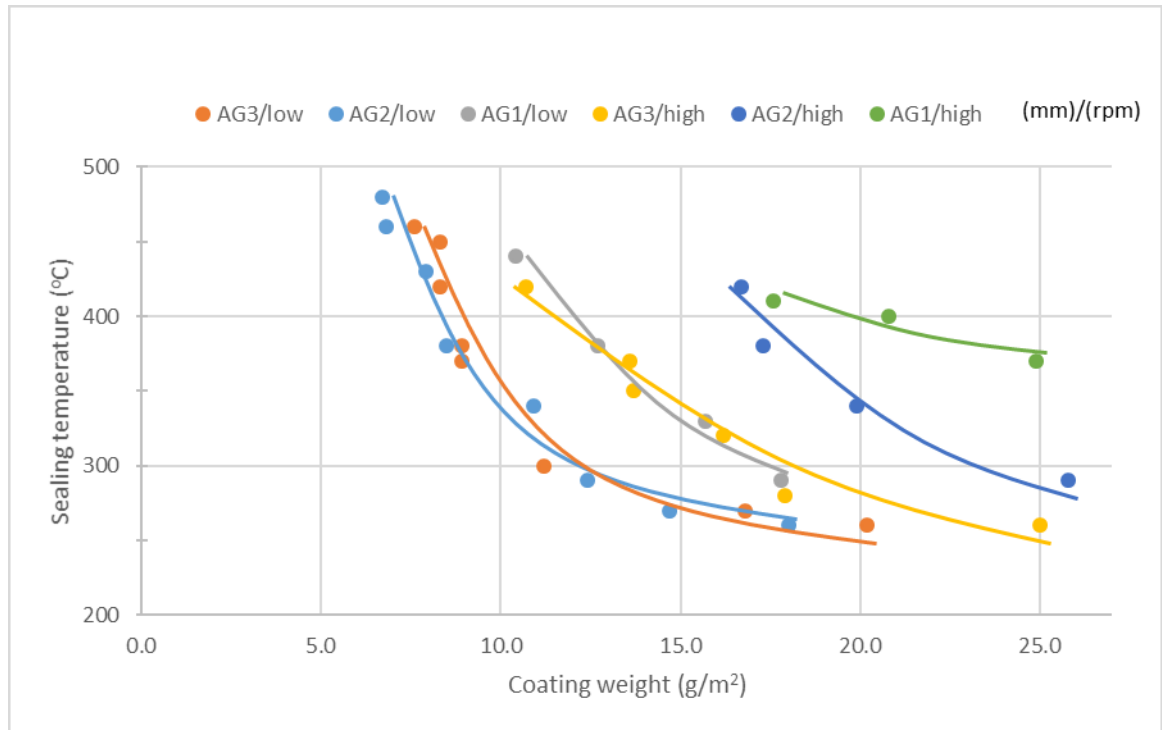


Figure 50. Hot air sealing temperature as a function of coating weight, trial runs 20170404-B21.

Hot air sealing results of the trial runs 20170404-B21 indicate the similar trend as the previous measurement results, although some exceptions are noticed. Generally, increasing air gap distance decreases the sealing temperature, if the coating weight is equal. The results of AG2 setting are equal or even better than the results of AG3 setting at the low screw speed, which refers to excessive cooling of the material with the highest air gap value. However, the sealing temperatures are very close to each other and valid conclusions cannot be made based on few sample points. Furthermore, the higher screw speed causes significant difference between the sealing temperatures of AG2 and AG3 settings.

III Pinhole measurements

Pinhole measurement results of the trial runs 20170404-B21 are shown in table 24, where the pinhole limit are highlighted with yellow.

Table 24. Pinhole results of trial runs 20170404-B21.

20170404-B21-1 (T2/low/AG1)			20170404-B21-2 (T2/low/AG2)			20170404-B21-3 (T2/low/AG3)		
Line speed	Coating weight (g/m ²)	Pin-holes	Line speed	Coating weight (g/m ²)	Pin-holes	Line speed	Coating weight (g/m ²)	Pin-holes
low1	21.1	off	low1	18.04	off	low1	27.54	off
low2	17.82	off	low2	14.68	off	low2	20.16	off
low3	15.66	off	low3	12.38	off	low3	16.78	off
medium1	12.68	off	medium1	10.92	off	medium1	11.24	off
medium2	10.42	on	medium2	8.5	off	medium2	8.94	2
			medium3	7.94	on	medium3	8.86	1
			high1	6.82	on	high1	8.3	on
			high2	6.7	on	high2	8.28	on
						high3	7.64	on
20170404-B21-4 (T2/high/AG1)			20170404-B21-5 (T2/high/AG2)			20170404-B21-6 (T2/high/AG3)		
Line speed	Coating weight (g/m ²)	Pin-holes	Line speed	Coating weight (g/m ²)	Pin-holes	Line speed	Coating weight (g/m ²)	Pin-holes
low1	36.16	off	low1	37.26	off	low1	56.3	off
low2	29.52	off	low2	30.04	off	low2	41.18	off
low3	24.9	off	low3	25.76	off	low3	32.94	off
medium1	20.8	off	medium1	19.86	off	medium1	25.04	off
medium2	17.64	off	medium2	17.32	off	medium2	17.92	off
			medium3	16.72	off	medium3	16.2	off
						high1	13.72	off
						high2	13.56	off
						high3	10.7	off

Pinhole results of the trial runs 20170404-B21 show that pinholes appear between coating weights of 11 g/m² and 8 g/m². With the lower screw speed, the difference between the highest and the lowest air gap value is rather low and AG2 setting provides better results than AG3 setting. As suggested in hot air sealing measurements, the results indicate that the melt temperature is too low with AG3 setting and therefore the blend does not work successfully. Higher screw speed sample points does not contain any pinholes, because the low coating weights are not reached and therefore valid conclusions cannot be made.

7.2.5 Trial runs 20170406-B22

The trial runs 20170406-B22 are performed with PE2 blend. The process parameters and the material information are presented in table 12.

The laboratory measurement results of trial run 20170406-B22 are listed in appendix A. Adhesion of the sample points is excellent throughout the measurements and only two 4.5 values are measured. Both of them are produced with the lowest air gap setting (AG1) that is noticed inadequate also in the previous measurements. The width and neck-in of the film are in typical level and they vary along the air gap settings as in previous measurements i.e. higher air gap increases neck-in and decreases width of the film.

I Temperature measurements

The temperature data of the trial runs 20170406-B22 is presented in figure 51.

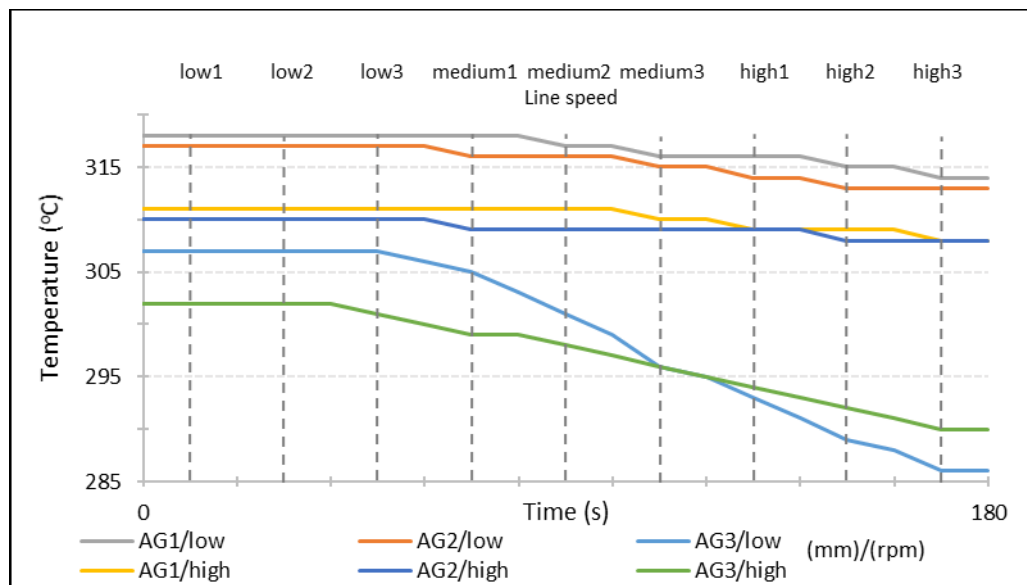


Figure 51. *Film temperature as a function of time, trial runs 20170406-B22.*

The temperature data of trial runs 20170406-B22 does not offer dissimilar results compared to the previous temperature measurements. Temperature drop of the film is negligible with the low and medium air gap, which is normal since the cooling time is short. Furthermore, the film temperatures act normally with the highest air gap setting (AG3). The initial film temperature is higher and the cooling is faster with the low screw speed. Moreover, the rate and amount of cooling are at typical level with the highest air gap. The cooling accelerates around low3 line speed with both screw speed settings and thereafter proceeds almost linearly until the end of trial run. The final temperature drops are similar compared to the previous results.

II Hot air sealing measurements

Hot air sealing measurement results of the trial runs 20170406-B22 are shown in appendix B and in figure 52.

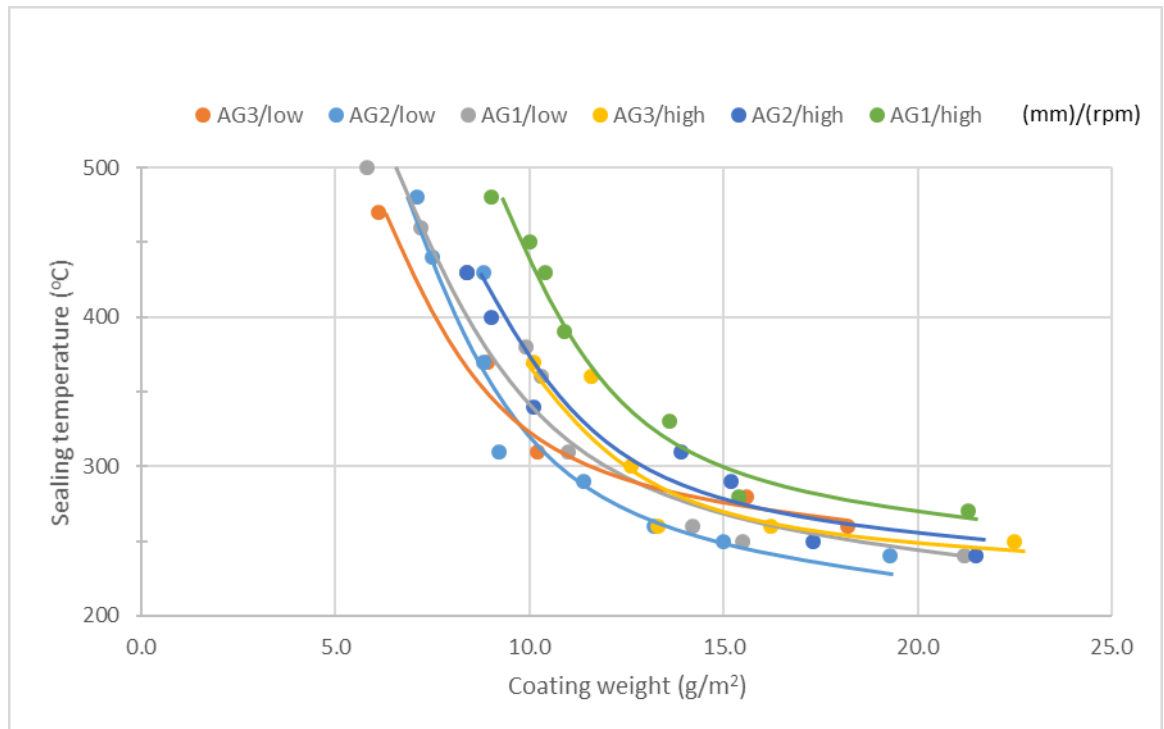


Figure 52. Hot air sealing temperature as a function of coating weight, trial runs 20170406-B22.

Hot air sealing results of the trial runs 20170406-B22 display that the sealing temperatures and consequently the curves are closer to each other than before. This can be originated from the highest melt temperature setting (T3). In the first part of the measurements, the highest melt temperature was noticed improper for PE2 blend and the properties start to weaken at the excessive temperature. However, the closer examination reveals that the higher air gap decreases slightly the sealing temperature, if the coating weight is equal and therefore the results are rather level with the previous measurements. The highest air gap and lower screw speed setting (AG3/low) is the only distinct exception from the trend at high coating weights.

III Pinhole measurements

Pinhole measurement results of the trial runs 20170406-B22 are presented in table 25.

Table 25. Pinhole results of trial runs 20170406-B22.

20170406-B22-1 (T3/low/AG1)			20170406-B22-2 (T3/low/AG2)			20170406-B22-3 (T3/low/AG3)		
Line speed	Coating weight (g/m ²)	Pin-holes	Line speed	Coating weight (g/m ²)	Pin-holes	Line speed	Coating weight (g/m ²)	Pin-holes
low1	21.18	off	low1	19.26	off	low1	44.42	off
low2	15.46	off	low2	15.04	off	low2	33.62	off
low3	14.16	off	low3	13.18	off	low3	27.04	off
medium1	11.04	off	medium1	11.38	1	medium1	18.16	on
medium2	10.32	on	medium2	9.16	1	medium2	15.62	on
medium3	9.94	on	medium3	8.8	on	medium3	10.22	on
high1	8.42	on	high1	8.82	on	high1	8.88	on
high2	7.22	on	high2	7.5	on	high2	8.4	on
high3	5.84	on	high3	7.12	on	high3	6.1	on
20170406-B22-4 (T3/high/AG1)			20170406-B22-5 (T3/high/AG2)			20170406-B22-6 (T3/high/AG3)		
Line speed	Coating weight (g/m ²)	Pin-holes	Line speed	Coating weight (g/m ²)	Pin-holes	Line speed	Coating weight (g/m ²)	Pin-holes
low1	32.38	off	low1	31	off	low1	58.64	off
low2	26.2	off	low2	25.26	off	low2	43.56	off
low3	21.34	off	low3	21.54	off	low3	34.64	off
medium1	15.44	off	medium1	17.28	off	medium1	22.52	off
medium2	13.64	off	medium2	15.18	off	medium2	16.16	off
medium3	10.94	off	medium3	13.86	off	medium3	13.34	off
high1	10.36	off	high1	10.08	off	high1	12.62	off
high2	10.04	off	high2	9	off	high2	11.58	off
high3	8.98	on	high3	8.44	off	high3	10.08	off

Pinhole results of trial runs 20170406-B22 present that pinholes appear between coating weights of 18 g/m² and 9 g/m². With the higher screw speed setting, the material works rather well, but serious problems are noticed, when the lower screw speed results are examined. The low and medium air gap settings provide moderate results, but the highest air gap (AG3) causes the worst result among all the pinhole measurements considering air gap distance. As suggested during the hot air sealing measurements, the results indicate that the melt temperature is too high and PE2 blend does not work successfully because of Additive 1.

7.2.6 Trial runs 20170411-B23

The trial runs 20170411-B23 are executed with PE4 blend. These are the final runs, where the effect of oxidation in the air gap region are examined. The process parameters and the material information are presented in table 12.

The laboratory measurement results of trial run 20170411-B23 are listed in appendix A. Adhesion of the sample points is almost perfect and only two 4.5 values are measured with the lowest air gap setting (AG1). As noticed in all the previous measurements, this setting is distinctly the worst considering the measured product properties. The width and neck-in of the film are in typical level and they vary along the air gap settings as in the previous measurements, i.e. the higher air gap causes the larger neck-in and narrower film.

I Temperature measurements

The temperature data of the trial runs 20170411-B23 is presented in figure 53.

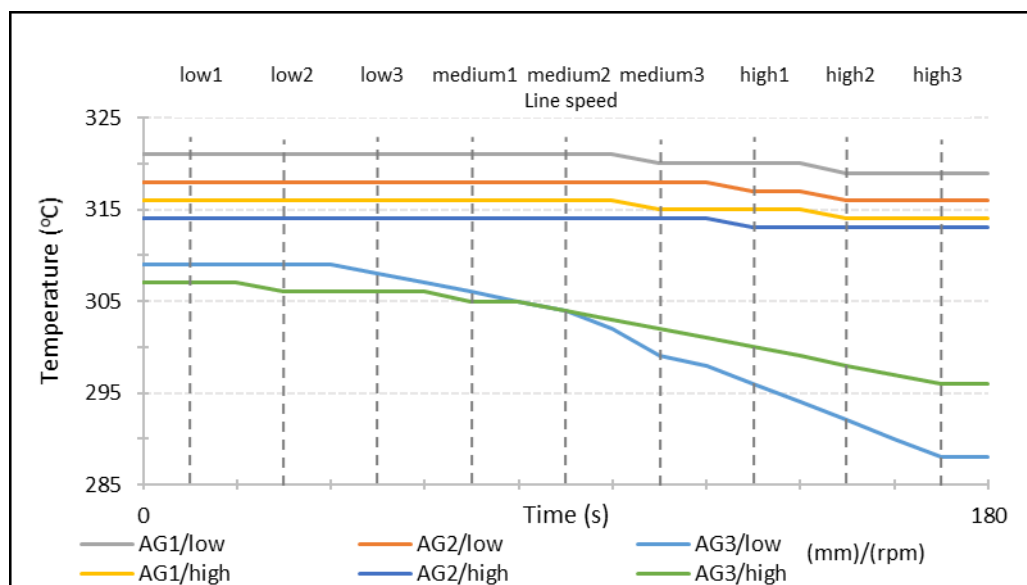


Figure 53. *Film temperature as a function of time, trial runs 20170411-B23.*

The temperature data of trial runs 20170411-B23 does not differ from the temperature measurements of the previous trial runs and the cooling of the film occurs similarly. The temperature drop is negligible with the low and medium air gap settings and the film temperatures decreases normally with the highest air gap setting (AG3). The rate and amount of cooling are at the typical level with the highest air gap. The cooling accelerates around low3 line speed with both screw speed settings, and thereafter proceeds rather constantly. The final temperature drops are similar compared to the previous results.

II Hot air sealing measurements

Hot air sealing measurement results of the trial runs 20170411-B23 are presented in appendix B and in figure 54.

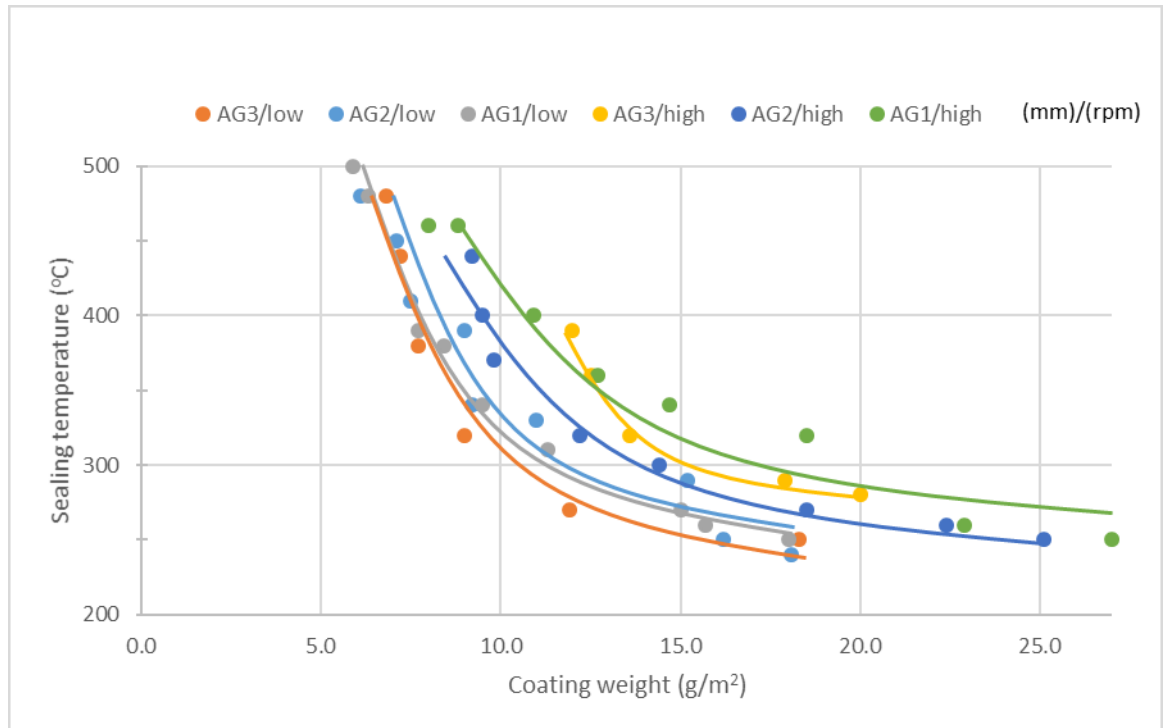


Figure 54. Hot air sealing temperature as a function of coating weight, trial runs 20170411-B23.

Hot air sealing results of the trial runs 20170411-B23 are similar as the previous results (20170406-B22), and the sealing curves are closer to each other than normally. However, this cannot be resulted from the highest melt temperature (T3), because PE3 blend should work best with the T3 setting as noticed in the first part of the measurements. Therefore, it is plausible that the material cools too much with the highest air gap setting, which compensates the improved oxidation and bonding. Especially the higher screw speed causes poor results with AG3 setting. However, this is partly result from narrow coating weight range, which can distort the trend of the plotted curve.

III Pinhole measurements

Pinhole measurement results of the trial runs 20170411-B23 are shown in table 26.

Table 26. Pinhole results of trial runs 20170411-B23.

20170411-B23-1 (T3/low/AG1)			20170411-B23-2 (T3/low/AG2)			20170411-B23-3 (T3/low/AG3)		
Line speed	Coating weight (g/m ²)	Pin-holes	Line speed	Coating weight (g/m ²)	Pin-holes	Line speed	Coating weight (g/m ²)	Pin-holes
low1	17.96	off	low1	18.1	off	low1	42.16	off
low2	15.68	off	low2	16.2	off	low2	33.14	off
low3	15.04	off	low3	15.22	off	low3	26.72	off
medium1	11.32	1	medium1	11	off	medium1	18.26	off
medium2	9.52	1	medium2	9.16	1	medium2	11.86	off
medium3	8.4	on	medium3	9.02	on	medium3	9.04	off
high1	7.7	on	high1	7.48	on	high1	7.72	1
high2	6.26	on	high2	7.06	on	high2	7.18	on
high3	5.92	on	high3	6.06	on	high3	6.8	on
20170411-B23-4 (T3/high/AG1)			20170411-B23-5 (T3/high/AG2)			20170411-B23-6 (T3/high/AG3)		
Line speed	Coating weight (g/m ²)	Pin-holes	Line speed	Coating weight (g/m ²)	Pin-holes	Line speed	Coating weight (g/m ²)	Pin-holes
low1	32.72	off	low1	33.72	off	low1	66.98	off
low2	26.98	off	low2	25.08	off	low2	49.96	off
low3	22.86	off	low3	22.4	off	low3	40.72	off
medium1	18.54	off	medium1	18.5	off	medium1	28.78	off
medium2	14.74	off	medium2	14.36	off	medium2	19.98	off
medium3	12.74	off	medium3	12.22	off	medium3	17.88	off
high1	10.94	1	high1	9.76	off	high1	13.64	off
high2	8.8	1	high2	9.48	off	high2	12.54	off
high3	8	on	high3	9.2	2	high3	12	off

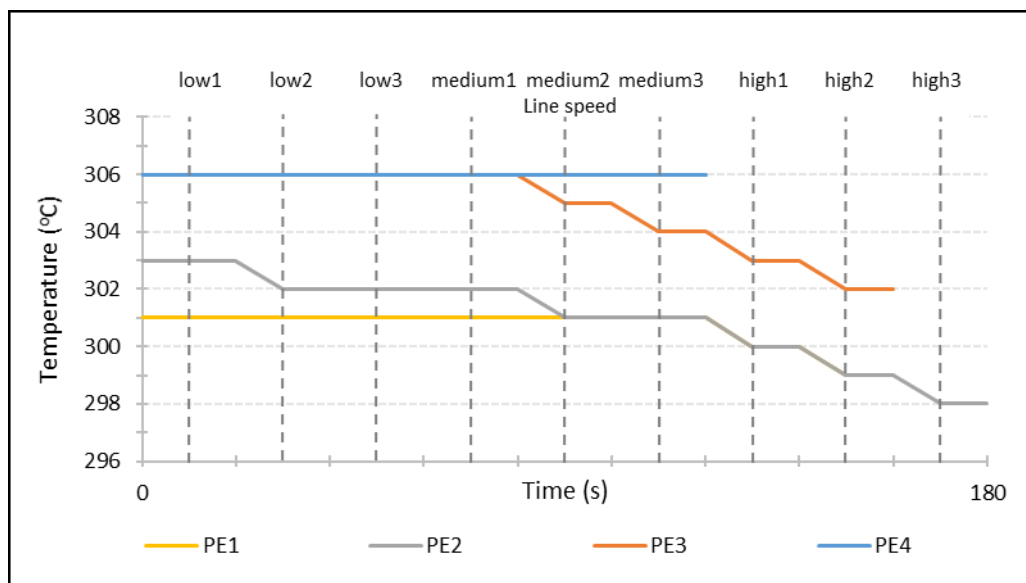
Pinhole measurement results of trial runs 20170411-B23 present that pinholes appear between coating weights of 11 g/m² and 8 g/m². The coating weight limit of pinholes is around the typical level. Increasing the air gap decreases the pinhole limit slightly towards the lower coating weights, excluding the final trial run, where coating weights are large and no pinholes appear. As considered during the hot air sealing measurements, an excessive cooling of the material with the highest air gap setting does not weaken pinhole properties similarly. Therefore, the optimization of air gap distance needs more measurements with PE4 blend.

7.3 Comparison of melt temperatures and materials

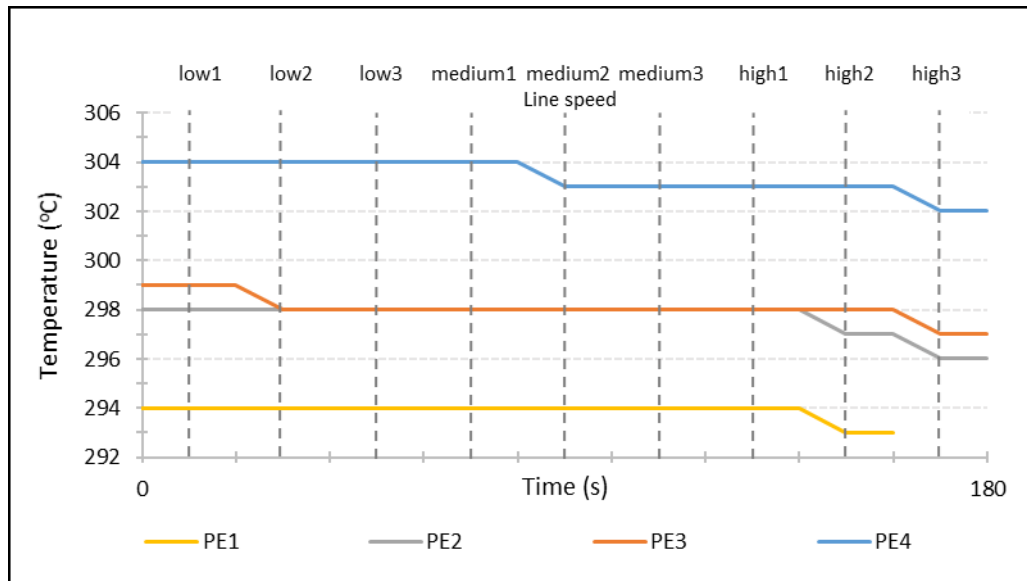
The first part of the measurements focuses on the melt temperature and thermo-mechanical degradation inside the extruder barrel. The other main goal of the measurements is to compare the hot air sealing and pinhole results of PE blends to the reference. The comparison of temperature data include an essential factor that must be noticed. The film temperature of the reference (PE1) is measured during the subsequent examination of air gap distance.

I Temperature comparison

The first part of analysis is the comparison of the temperature measurement results between the trial runs and consequently between different materials. The film temperature comparison of materials is executed with T2 and T3 melt temperature settings. The lowest melt temperature setting (T1) is excluded from the comparison because it caused improper results in the hot air sealing and pinhole measurements. The film temperature data of the materials with T2 setting are presented in figures 55a and 55b.



a) T2 and low rpm setting.

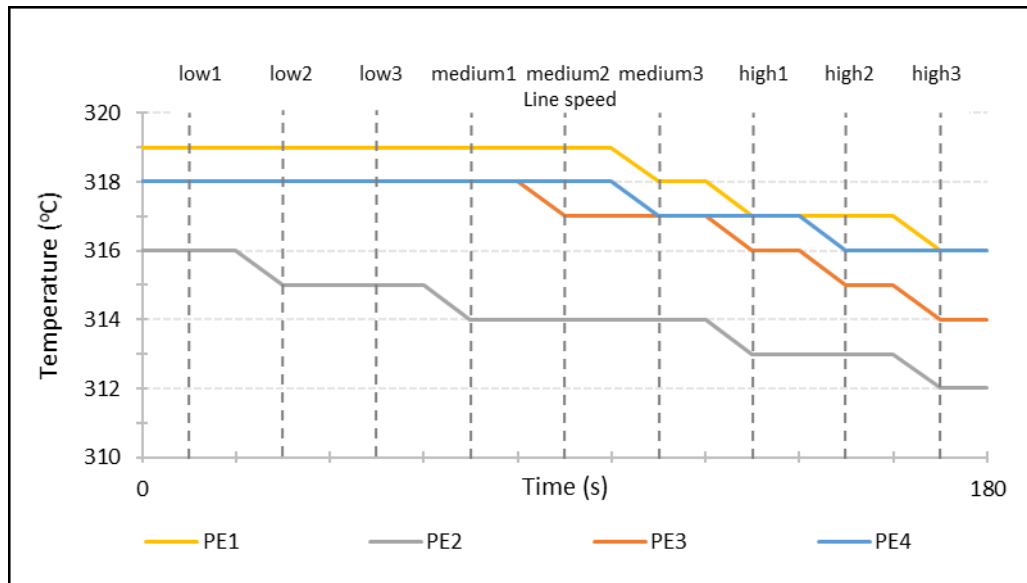


b) T2 and high rpm setting.

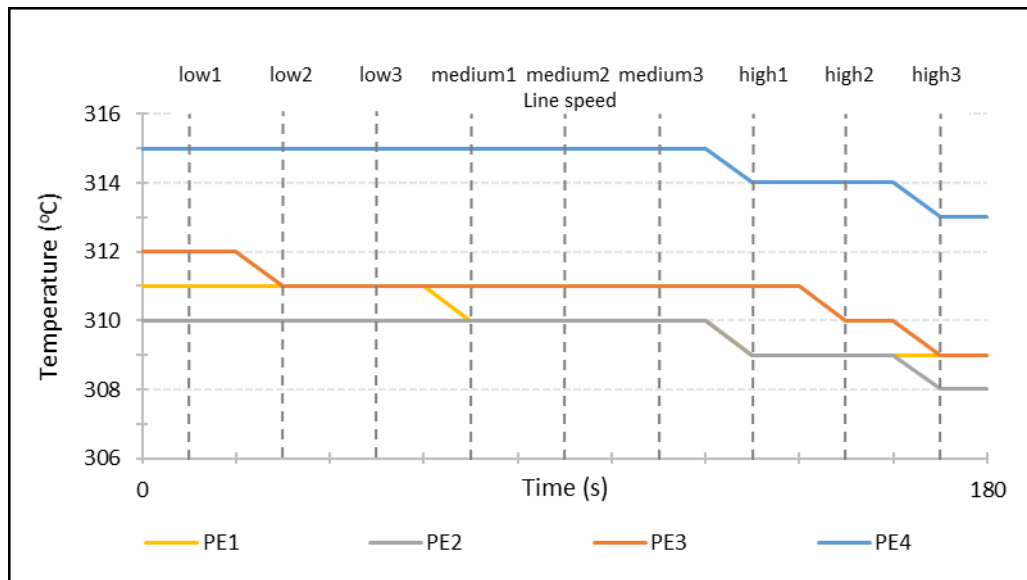
Figure 55. *Film temperature as a function of time for used PE materials.*

Figure 55 presents important information from the film temperatures of the materials. The figure 55a shows that the lower screw speed and consequently the lower throughput causes the melt breakdown of most materials and only PE2 blend withstands throughout the trial runs. Therefore, the comparison of temperature decrease is not possible for all the materials with these settings, although PE2 and PE3 blends seem to behave similarly. A significant difference can be observed from the initial temperatures of the films. PE4 blend has the highest film temperature at the start of the trial runs. Furthermore, the initial temperature of the reference (PE1) is the lowest with both screw speed settings, which is usually weakening factor in hot air sealing and pinhole measurements. The temperature drop of different materials can be noticed in figure 55b. The trend of all temperature curves is very similar. The temperature decrease is not significant with medium air gap distance (AG2) and the majority of cooling occurs with the high line speed values.

Similar comparison between the film temperature data of the materials is done with the results of T3 melt temperature setting. The film temperatures are shown in figures 56a and 56b.



a) T3 and low rpm setting.



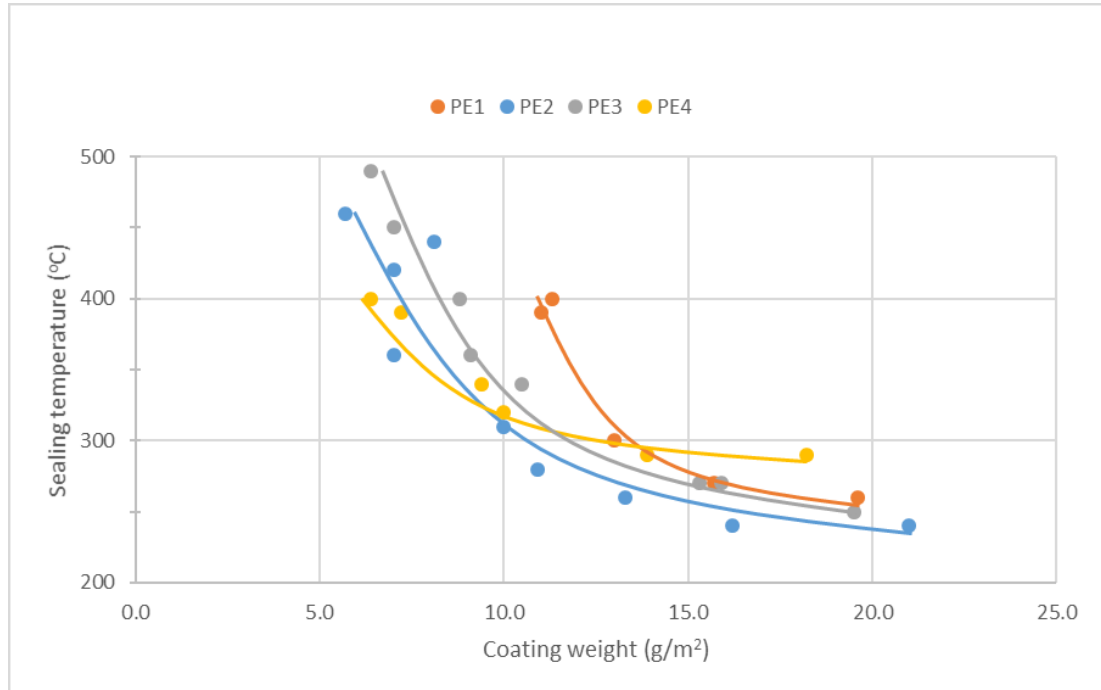
b) T3 and high rpm setting.

Figure 56. Film temperature as a function of time for used PE materials.

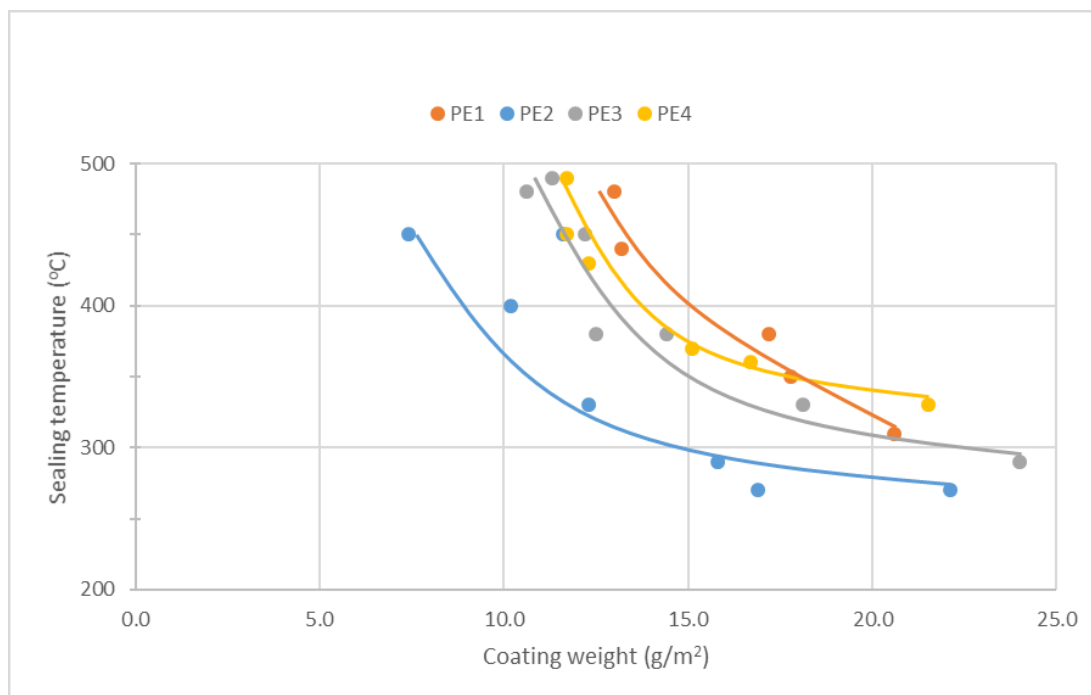
The results are rather similar compared to T2 setting. The trend of temperature curves correspond very well to the previous figure 55, although the temperature drop is slightly more intense. However, majority of the cooling occurs likewise at the higher line speeds. Furthermore, comparison of the initial film temperatures show that the PE4 blend has again the highest film temperature with the high screw speed setting. The only distinct difference between T2 and T3 settings is the exceptionally high film temperature of the reference (PE1) with the low screw speed setting. The temperature value stays at higher level than corresponding value of PE4 almost throughout the whole trial run.

II Hot air sealing comparison

The second part of material and melt temperature comparison is the analysis of the hot air sealing results between the trial runs and consequently between different materials. The comparison is performed with T2 and T3 melt temperature settings. The hot air sealing data with T2 melt temperature setting is presented in figures 57a and 57b.



a) T2 and low rpm setting.

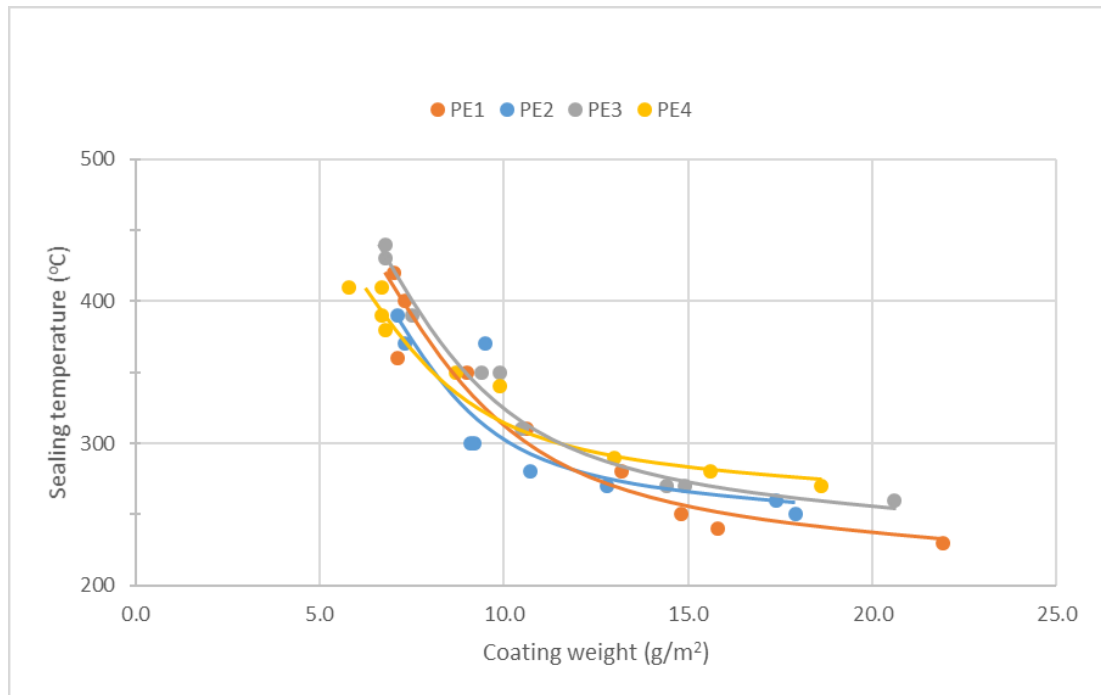


b) T2 and high rpm setting.

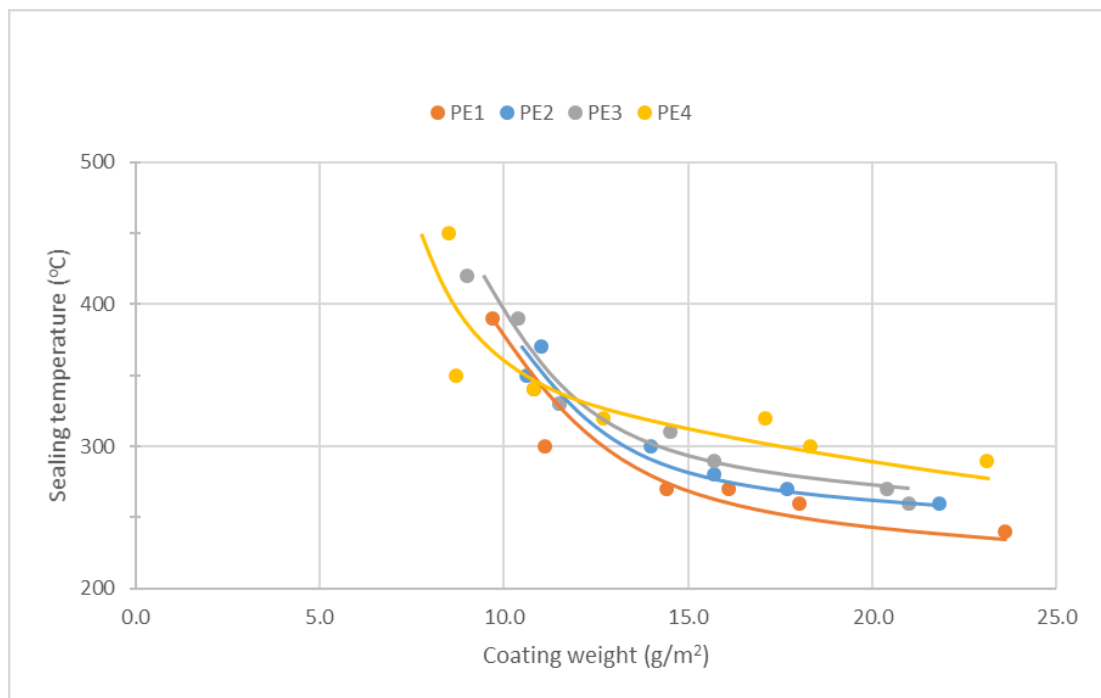
Figure 57. Hot air sealing temperature as a function of coating weight for used PE materials.

Based on the figures 57a and 57b, the blending improves the hot air sealing with T2 temperature setting. The reference material (PE1) has overall the worst hot air sealing results and the sealing curves steepen at the higher coating weights compared to the blends. PE2 blend is superior with the higher screw speed but on the other hand, it is also the only material, which reaches under 10 g/m² coating weight. Reduction of Additive 1 ratio increase the sealing temperatures with both screw speeds. The most interesting material is PE4 blend, which works poorly with the higher screw speed but the performance improves considerably, when the lower screw speed is applied and consequently the lower throughput is received. Furthermore, as noticed earlier, the lower screw speed causes the longer residence time and the higher film temperature, which can contribute the improvement of PE4 blend sealing properties.

Similar comparison of the hot air sealing results between the materials is done with T3 melt temperature setting. The hot air sealing data is shown in figures 58a and 58b.



a) T3 and low rpm setting.



b) T3 and low rpm setting.

Figure 58. Hot air sealing temperature as a function of coating weight for used PE materials.

The curves in the figures 58a and 58b show that the differences between the resin types are moderated with T3 temperature setting, and distinct difference is harder to observe.

Especially, the sealing results of the reference (PE1) are improved considerably. Furthermore, PE4 blend seems to work better with the higher temperature setting. It has the best results, when the sealing temperatures of the lowest coating weights are examined. Therefore, the optimal melt temperature of PE1 and PE4 blend can be considered closer to T3 than T2. On the other hand, PE2 blend has lost the advantage at the highest melt temperature and the material works distinctly better with T2 melt temperature setting.

III Pinhole comparison

The final part of material and melt temperature comparison is the examination of the pinhole results. The comparison between materials is executed by searching the limit, where pinholes start to appear. Each trial run has the sample point and corresponding coating weight value (g/m^2), where the first pinholes are observed. The coating weight limits of pinholes are presented in table 27.

Table 27. *Coating weight limits (g/m^2) of pinholes for used PE materials.*

	PE1	PE2	PE3	PE4
T2 low	13.00	7.02	7.04	7.20
T2 high	12.96	7.42	11.32	11.66
T3 low	10.64	9.06	9.40	6.76
T3 high	10.80	10.56	8.98	8.72

The comparison of the pinhole results favors the observations that are made during the analysis of the hot air sealing results. The properties of the reference (PE1) are not level with the PE blends with T2 setting, but the results improve, as in hot air sealing, when T3 setting is used. PE4 blend functioned better in hot air sealing with the highest melt temperature setting, and this is supported by the pinhole measurements as well. PE2 blend has low pinhole limit compared to other materials with T2 melt temperature setting. However, the advantage diminishes, when the melt temperature is increased.

Overall, based on the hot air sealing and pinhole measurements, PE2 blend is the best alternative with T2 melt temperature setting and PE4 blend with T3 melt temperature setting. However, valid conclusions cannot be made based on the first part of the measurements. Therefore it's crucial to get more information from the air gap distance analysis, which also includes the best melt temperature alternatives.

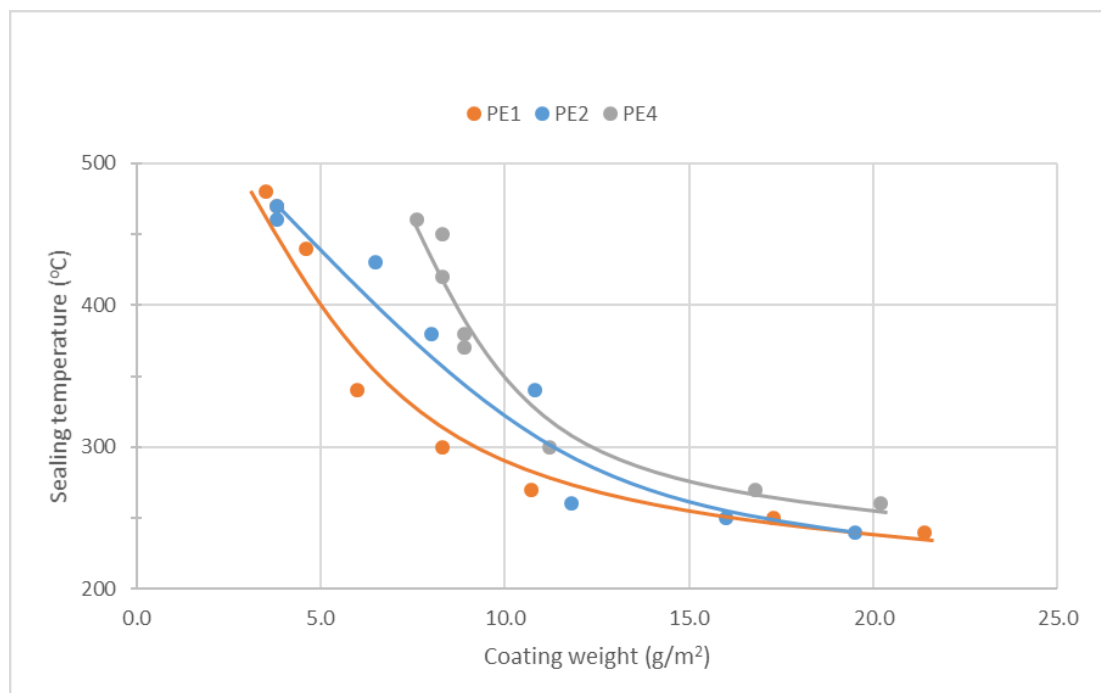
7.4 Comparison of air gap distances and materials

The second part of the measurements focuses on the air gap distance and oxidation in the air gap region. The other main goal is to continue the material comparison between the reference (PE1) and PE blends.

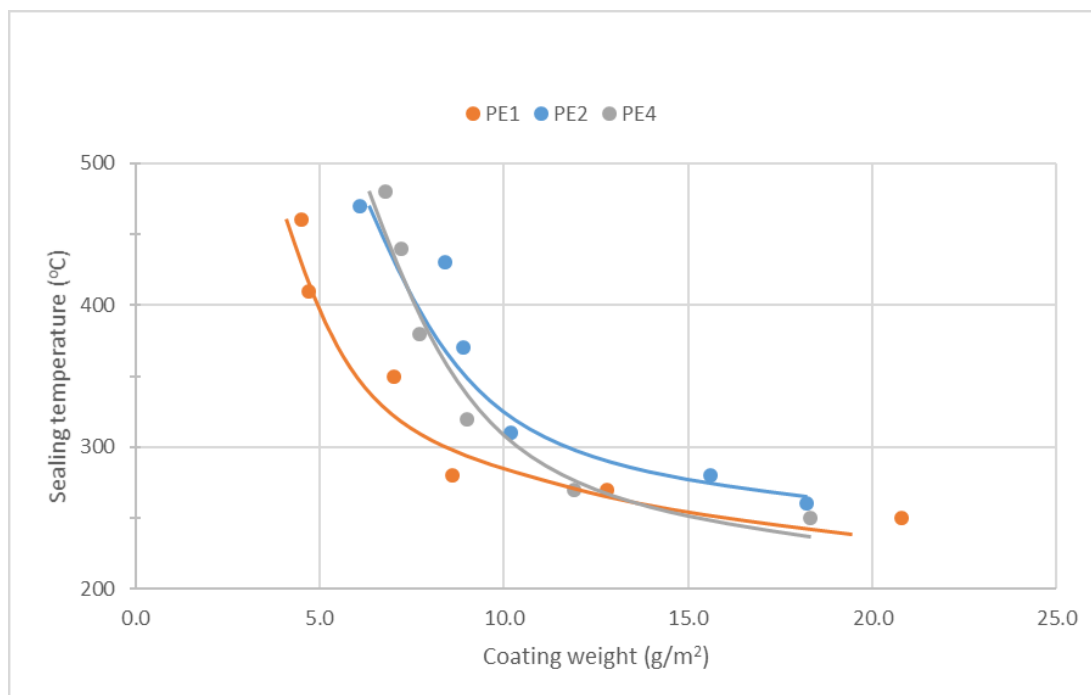
The temperature data of air gap examination is not discussed comprehensively at this point, because the materials cool in the air gap region similarly regardless of the air gap distance. The low and medium air gap settings (AG1 and AG2) cause negligible film cooling during the trial runs. The highest air gap setting (AG3) produces notable temperature drop, but the initial and final temperatures as well as rate of cooling are rather similar with every material.

Hot air sealing comparison

The first part of material and air gap distance comparison is the analysis of hot air sealing results between the material choices. The comparison is executed with AG2 and AG3 settings. The lowest air gap (AG1) is excluded from the comparison because the results are distinctly the worst. Hot air sealing measurement data with AG3 air gap and low screw speed setting is presented in figures 59a and 59b. The hot air sealing figures of the high screw speed setting are shown in appendix C.



a) T2/low/AG3 setting.

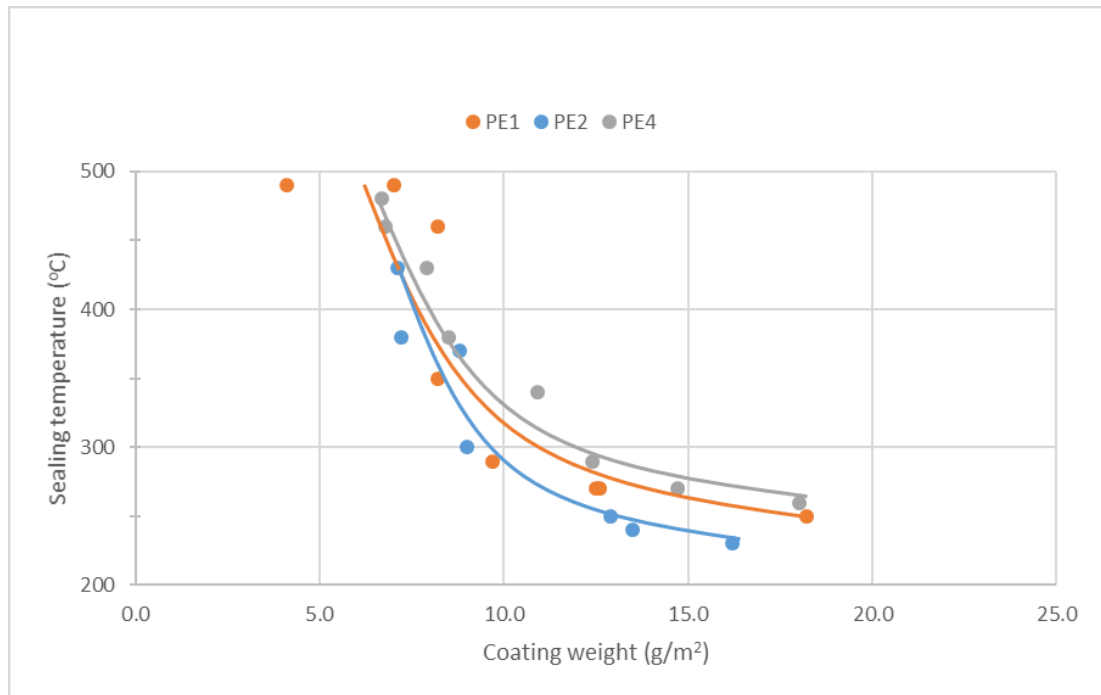


b) T3/low/AG3 setting.

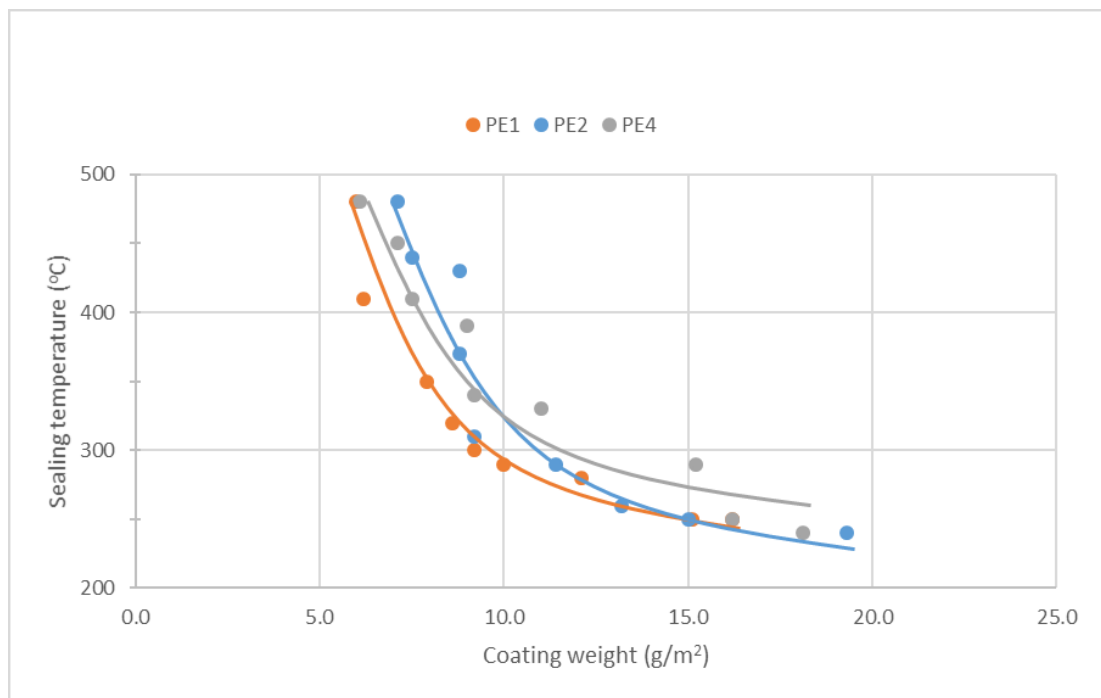
Figure 59. Hot air sealing temperature as a function of coating weight for used PE materials.

The first observation from the figure 59a and 59b is the excellent performance of the reference (PE1) with AG3 setting. It has distinctly lower sealing temperatures than both PE blends especially at the low coating weights. These results differ considerably from the material comparison of the melt temperature part. However, the reference PE batch was not the same as in the melt temperature part. The hot air sealing results of PE blends are similar to the melt temperature part despite the higher air gap distance. PE2 blend has very good performance at T2, but it decreases radically, when the temperature is increased to T3. This confirms further that the optimal melt temperature is closer to T2. PE4 blend works conversely and the performance is poor at T2, but it improves as the melt temperature is increased to T3.

Similar comparison between the hot air sealing results is done with AG2 and low screw speed setting. The hot air sealing data is shown in figures 60a and 60b. The hot air sealing figures of 150 rpm screw speed setting are presented in appendix C.



a) T2/low/AG2 setting.



b) T3/low/AG2 setting.

Figure 60. Hot air sealing temperature as a function of coating weight for used PE materials.

The curves in the figures 60a and 60b indicate the excellent performance of the reference (PE1) also with AG2 setting, although the advantage to PE blends is decreased distinctly compared to the results of AG3 setting. The hot air sealing curves of PE blends are rather

similar between AG2 and AG3 settings and the increase of air gap doesn't improve the hot air sealing performance as much as the performance of the reference. However, the melt temperature has the same effect on the hot air sealing of PE blends as in all the previous measurements. PE2 blend works better at T2 setting, and PE4 blend has better performance at T3 setting.

II Pinhole comparison

The second part of material and air gap distance comparison is the examination of the pinhole results. The coating weight limits of pinholes for each PE material are presented in table 28.

Table 28. *Coating weight limits (g/m²) of pinholes for used PE materials.*

	PE1	PE2	PE4
T2 low AG2	8.24	7.24	7.94
T2 low AG3	4.56	6.48	8.94
T2 high AG2	10.86	off	off
T2 high AG3	off	off	off
T3 low AG2	9.2	11.38	9.16
T3 low AG3	4.7	18.16	7.72
T3 high AG2	8.8	off	9.2
T3 high AG3	off	off	off

The examination of the pinhole results support the consideration that is made during the analysis of hot air sealing results. The increase of air gap decreases the amount of pinholes almost invariably with both melt temperature settings. Especially AG3 setting decreases the coating weight limits of pinholes to very low level or excludes pinholes entirely. The

only major exception is PE blend, which works poorly with T3 setting. When the materials are compared, the performance of the reference is excellent and the pinhole limits are partly lower than corresponding values of PE blends. The results of PE2 blend match excellently the previous hot air sealing results. The material provides the best pinhole results with T2 setting, but the pinhole limit increases radically, when the melt temperature is raised to T3. The improvement of PE4 blend performance at high temperatures does not appear in the pinhole results similarly to hot air sealing and the previous measurements. The results are almost equal with both melt temperature settings. However, the pinhole limits are at low level. Despite the pinhole results does not show that PE4 works better in higher temperatures, this can be noticed in the melt temperature part of the study.

7.5 IR temperature measurements of co-extrusion

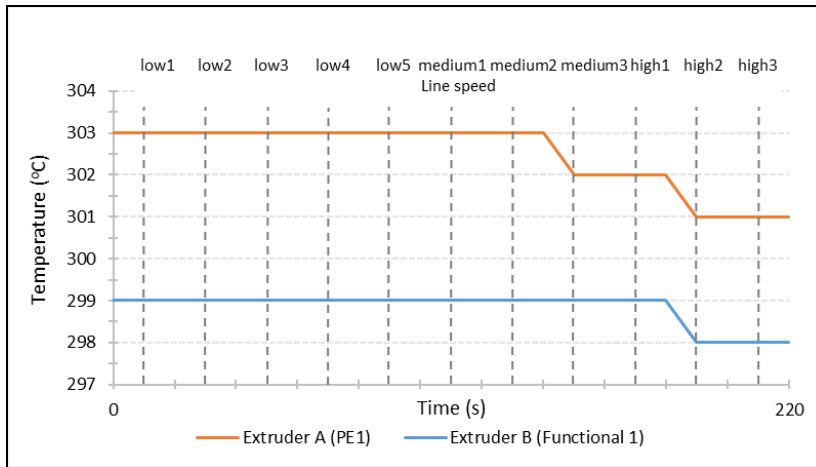
The final part of the practical results and discussion covers IR temperature measurements of co-extrusion applications. These measurements are the separate part of the examination and not related to the previous melt temperature and air gap distance analysis. The goal of these measurements is to exploit two pyrometers in the IR temperature measurement set-up, in order to examine and define the temperature values from both sides of two-layer film structure. Furthermore, the measurement set-up enables determination of temperature difference between the sides of the film. These measurements does not include further analysis of the material properties as previously. Therefore, laboratory results as well as hot air sealing and pinhole measurements are excluded from the analysis and the main focus is only in the film temperature.

The temperature measurements are performed similarly to the previous trial runs. The only difference is that second equal pyrometer is mounted over the chill roll i.e. the re-winding side of the extruder. The most important factor in the set-up is to adjust both pyrometer spots to the same point and height on the film. Consequently, the air gap distance is equal and the effect of cooling is similar on both sides of the film.

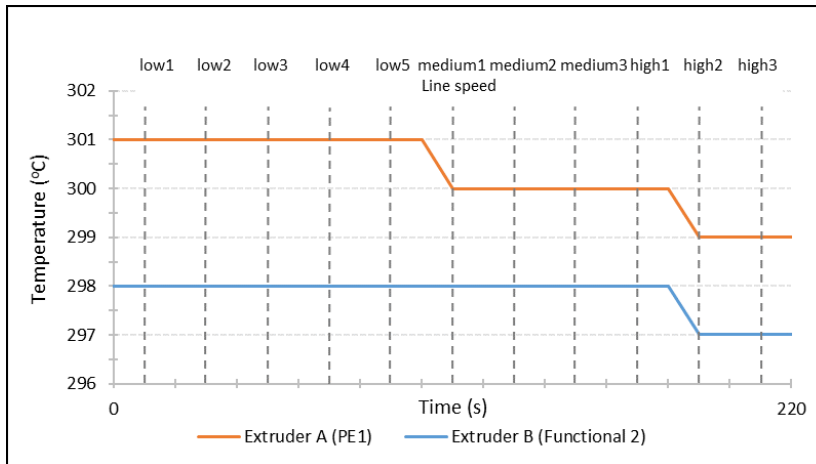
IR temperature measurements of co-extrusion include two trial runs 20170315 and 20170321. Both of the trials contain four runs, but examination of all measurement data is not necessary because each material is processed twice to coat two different substrates. Consequently, the temperature data is similar because the substrate has no influence on the film temperature. PE1 forms one layer of the film in all trial runs. The other layer is varied between different resins, which are Functional 1, Functional 2 and Functional 3.

PE1 is processed with the extruder A and Functional 1, 2 and 3 resins are processed with the extruder B in every trial runs. The similar melt temperature set-up is used in both extruders. However, this does not invalidate the temperature difference between the layers, because the material structures and melt indexes are not equal and the extruders produce slightly variable melt temperatures despite the same setting. The temperature data of the co-extrusion films is illustrated in figure 61. All figures (61a, 61b, and 61c) include

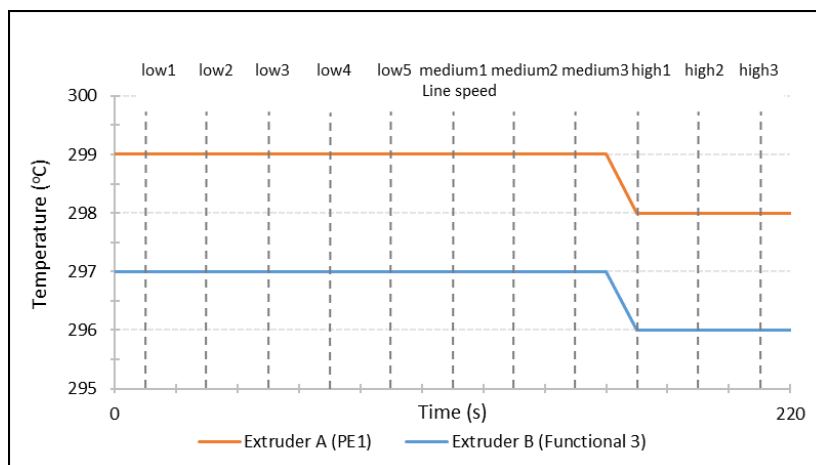
the temperature curves from both sides of the film and the corresponding material layer is shown in the chart legend.



a) PE1 and Functional 1 materials.



b) PE1 and Functional 2 materials.



c) PE1 and Functional 3 materials.

Figure 61. Film temperature as a function of time for co-extrusion films.

The general appearance of all three figures (61a, 61b and 61c) is almost identical. The initial temperature of the PE1 is higher in every graph. One reason is that normally the extruder A produces slightly higher melt temperature although the temperature settings are equal. However, the temperature differences between the different materials and trial runs are not very significant. Furthermore, the temperature difference between the two layers remains similar during the trial runs. Levelling of the layer temperatures would be more likely, and easier to notice, if the initial temperature difference were higher.

The temperature drop during the trial runs is very similar to the previous measurements, which are performed with the monolayer films. The cooling is not observable until medium1 line speed when the airflow increases and the film thickness decreases more significantly. However, the amount of cooling is minor and the overall temperature drop is only 1-2°C depending on the material and trial run. This is due to the medium air gap setting (AG2), which does not cause significant cooling as noticed previously. Furthermore, the temperature of both film layers decreases almost simultaneously, which indicates that the co-extrusion film acts similarly to monolayer film.

Examination of the film temperature include one essential factor that must be noticed, when the temperature values are compared to each other. The pyrometers have 1% margin of error, which signifies 3°C at concerned temperature. Therefore, most of the temperature differences fits inside the measurement error. However, the exact temperature value isn't generally the main goal of the measurements, and extreme precision doesn't provide further advantage. In these measurements, the main focus is in the measurement set-up evaluation and the temperature difference observation. Therefore, the results can be considered adequate, and the set-up can be used in further co-extrusion applications.

8. CONCLUSIONS

The focus of this study is specified at the start of the examination, and the ultimate goal is source reduction that defines the guidelines for all measurements and conclusions. In extrusion coating, source reduction signifies retrenchment of coating material consumption and consequently decrease of costs. However, the reduction of polymer film thickness is not possible without affecting many essential product properties. Heat sealability and pinholes are some of the most important properties that are influenced by the film thickness and coating weight. Generally, heat sealing temperature increases as the coating weight decreases, which complicates manufacturing of the final product. Furthermore, the amount of pinholes increases as the coating weight decreases, which deteriorates the quality of product. Therefore, heat sealability and pinholes are determined as the most essential properties, which are examined and measured in this study.

In order to achieve the reduction of coating weight without damaging the heat sealing and pinhole properties excessively, the extrusion coating process must be optimized. This denotes the adjustment of the process parameters that enhance heat sealing and pinhole properties. Based on the theoretical examination, the molten curtain temperature and air gap distance between the die and nip are the key parameters that affect the product properties. These parameters are one of the main reasons to introduce and utilize non-contact, IR thermometer i.e. pyrometer in the temperature examination. The melt temperature setting inside the extruder does not correspond to the value in the air gap, since the film starts to cool immediately after the die lip. Furthermore, cooling increases as a function of air gap distance, which increases the temperature difference between the die and nip. In extrusion coating line, temperature metering is challenging with traditional contact thermometers, which supports the use of IR thermometer further.

Increase of melt temperature and air gap distance enhance the oxidation of the polymer and consequently bonding between coating and the substrate. Furthermore, the material is degraded more at the higher temperature, which modifies the structure and physical properties. Since melt temperature and air gap distance have significant effect on the product properties, they were selected as the main variables of the measurements. The third main variable of the experiments was the coating material. The reference material (PE1) was used as the baseline in all measurements. Other materials included Additive 1 and 2 resins, which were blended to the reference in order to improve heat sealing and pinhole properties.

The first part of the practical measurements contained the examination of melt temperature and material choice. Three melt temperature settings were applied and the influences were analyzed based on the hot air sealing and pinhole results. The three melt temperatures are set to process four materials and their performance were researched on the

grounds of the measurement results. The main goal was to discover the best melt temperature and material combinations concerning hot air sealing and pinholes.

The results of the first part of the measurements indicated some distinct guidelines to further examination. The lowest melt temperature setting (T1) was noticed to be insufficient to successful processing of the material not to mention measurement results. Melt breakdown occurred at relatively low line speeds and low coating weights were not reached. Furthermore, hot air sealing and pinhole results were clearly the worst. These factors excluded the lowest melt temperature setting from the further analysis. The comparison of the higher temperatures (T2 and T3) revealed that the optimal melt temperature is dependent on the material.

The highest melt temperature (T3) was the best setting for the reference (PE1) and PE4. The material performance, including hot air sealing and pinhole results, improved distinctly as the melt temperature increases. Conversely, PE2 and PE3 blends performed worse at the highest temperature, and the properties started to decrease between T2 and T3 settings. Therefore, medium (T2) melt temperature setting can be considered optimal concerning hot air sealing and pinhole results. The amount of Additive 1 resin had also clear influence on the measurement results, and reducing of the content (from high to low) weakened the product properties. Therefore, there was no basis for the use of smaller content and PE3 was excluded from the further air gap distance analysis.

The second part of the measurements involved the analysis of air gap distance as well as continuation of material choice consideration. Three air gap distance settings were applied along with two melt temperature settings that were based on the first results. These process parameters were set to process three materials in order to compare hot air sealing and pinhole results. Based on the results, the goal was to examine the best process parameters and material combinations.

The results of the second set of measurements confirmed most of the previous conclusions but new observations and a few contradictory results were also discovered. The main variable of the analysis was the air gap distance and it had clear effect on the hot air sealing and pinhole results. Higher air gap distance improved the measurement results almost every time, although the melt temperature simultaneously decreased. Hot air sealing curves changed towards lower sealing temperatures and pinhole limits shifted towards lower coating weights as the air gap distance increased. The lowest air gap distance (AG1) resulted the worst measurement results and therefore the further analysis was groundless. The only slight exception was PE4 blend, which required very high melt temperature. The highest air gap distance (AG3) caused excessive cooling of the material and the properties did not improve compared to medium (AG2) air gap setting.

As the material comparison is expanded further, the previous conclusions considering melt temperature setting are still valid. PE2 performed better than other two materials at

lower temperatures and it produced the best results at medium (T2) melt temperature. Moreover, the properties of PE4 remained poor until the melt temperature was increased to the highest setting (T3). However, the air gap study results were not as promising as previously even at T3 melt temperature. The most exceptional result was the better performance of the reference, which can be seen by comparing the results of melt temperature and air gap distance examination. Hot air sealing of the reference was improved significantly at T2 and it performed distinctly the best at T3 melt temperature. Furthermore, the pinhole limit changed towards lower coating weights. The improved performance of the reference cannot be explained with process parameters, because apart from air gap distance variation, they are standardized and therefore result are comparable with medium (AG2) air gap setting. As indicated in the results and discussion, the most significant difference between the measurements is the different PE1 resin batches. The batch was changed before the air gap distance examination, which contributed the conclusion that the resin was the main source of the variable results. Therefore, the resin properties including oxidation and structure must be examined further to ensure the ultimate reason behind the performance of the reference.

Overall, when all the measurement results and conclusions from melt temperature and air gap distance analysis are combined, some important outcomes can be confirmed. Higher melt temperature mainly improves hot air sealability and reduces pinholes, but the individual differences can be noticed. These differences appear at very high temperatures, when the degradation of the material structure accelerates, and the excessive heating start to decrease the properties. The similar trend is observed concerning the effect of air gap distance. Higher air gap distance improves almost invariably hot air sealing and pinhole properties. However, higher air gap distance decreases the width of film and increases neck-in, which must be noticed, when benefits of the improved properties are considered. Finally, the effect of Additives 1 and 2 remains partially uncertain. In the first part of the measurements, the hot air sealing and pinhole properties of the PE2 and PE4 blends were improved compared to the reference (PE1). However, the second part of the measurements revealed that the performance of reference was at higher level, which might eliminate the advantage of PE blends. Moreover, if the material cost are included to the comparison, the position of the reference (PE1) is emphasized even more.

REFERENCES

- [1] L. H. Sperling, Introduction to Physical Polymer Science, Fourth Edition, Wiley-Interscience, USA, 2005, 845 p.
- [2] A Guide to Polyolefin Extrusion Coating, LyondellBasell Industries, USA, 61 p. Available https://www.lyondellbasell.com/globalassets/documents/polymers-technical-literature/a_guide_to_polyolefin_extrusion_coating.pdf
- [3] R. Mikkonen, T. Hukka, Polymeerikemia, Luku 5: Kestomuovot, Tampere University of Technology, Tampere, Finland, 2015.
- [4] W. M. Karszes, Extrusion Coating of Paper and Paperboard: Equipment and Materials, Third Edition, TAPPI, USA, 1990, 375 p.
- [5] CHEMnetBASE, Polymers: A Property Database, Taylor & Francis Group, 2017. Available: <http://poly.chemnetbase.com/dictionary-search.do;jsessionid=EB68534EAA4A1932F167680632BD8BDE?method=view&id=12135334&si=POLY>
- [6] K. R. Frey, Extrusion Coating of Polyethylene & Polypropylene, Chevron Phillips Chemical Company LP, TAPPI Extrusion Coating Course, USA, 25 p. Available: <http://www.tappi.org/content/events/10extru/papers/1.2.pdf>
- [7] R. W. Halle, D. M. Simpson, A New Enhanced Polyethylene for Extrusion Coating and Laminating, TAPPI Place Conference, USA, 2002, 13 p.
- [8] E. Nijhof, Relationship Rheological Behavior and Molecular Architecture of LDPE's Designed for Extrusion Coating, TAPPI European Place Conference, 2007, 25 p.
- [9] R. Edwards, Fundamentals of Extrusion Coating: Polyolefins, Eastman Chemical Company, TAPPI, Polymers, Laminations & Coatings Conference, 1994, pp. 237-241.
- [10] R. Edwards, Polyolefin Properties in Extrusion Coating, Eastman Chemical Company, TAPPI, Polymers, Laminations & Coatings Conference, 1995, pp. 13-16.
- [11] C. Istvan, LDPE Technology, MOL Group, Hungary, 2010, 29 p. Available: https://mol.hu/images/pdf/A_MOL_rol/tvk-rol/tarsasagunkr%C3%B3l_roviden/egytemi_kapcsolatok/miskolci_egytem/oktatasi_anyagok/LDPE%20eloallitasa.pdf
- [12] M. Biscoglio, Advances in LDPE Resins for Extrusion Coating Applications, The Dow Chemical Company, TAPPI Place, USA, 2016, 22 p.

- [13] M. G. M. Neilen, J. J. J. A. Bosch, Tubular LDPE Has the Extrusion Coating Future, SABIC Europe, TAPPI European Place Conference, 2007, 10 p.
- [14] J. Auger, P. Tas, Blending Novapol Tubular LDPE in Autoclave LDPE for Extrusion Coating Applications, NOVA Chemicals Corporation, TAPPI Place Conference, USA, 2010, 35 p.
- [15] J. G. Smith, Organic Chemistry, Third Edition, McGraw-Hill, USA, 2010, 1178 p.
- [16] M. Asteasuain, A. Brandolin, High-Pressure Polymerization of Ethylene in Tubular Reactors: A Rigorous Dynamic Model Able to Predict the Full Molecular Weight Distribution, Macromolecular Reaction Engineering, WILEY-VCH Verlag GmbH & Co. KGaA, Germany, 2009, pp. 398-411. Available: https://www.researchgate.net/publication/230457827_High-Pressure_Polymerization_of_Ethylene_in_Tubular_Reactors_A_Rigorous_Dynamic_Model_Able_to_Predict_the_Full_Molecular_Weight_Distribution
- [17] J. Kuusipalo (ed), Paper and Paperboard Converting, Second Edition, Finnish Paper Engineers' Association/Paperi ja Puu Oy, Jyväskylä, Finland, 2008, 346 p.
- [18] Paper Converting and Packaging Technology, Pilot Line, Tampere University of Technology, Tampere, Finland, 2014, 6 p. Available <http://www.tut.fi/cs/groups/public/@1102/@web/@p/documents/liit/x136156.pdf>
- [19] I. Jönkkäri, Processing of Plastics: Extrusion, Tampere University Of Technology, Tampere, Finland, 2015.
- [20] W. Michaeli, Plastic Processing: An Introduction, Carl Hanser Verlag, Germany, 1995, 211 p.
- [21] Extrusion Coating & Lamination, Technical Guide, Qenos Pty Ltd., Australia, 2015, 24 p. Available [http://www.qenos.com/internet/home.nsf/\(LUI-mages\)/TG4Exco/\\$File/TG4Exco.pdf](http://www.qenos.com/internet/home.nsf/(LUI-mages)/TG4Exco/$File/TG4Exco.pdf)
- [22] D. V. Rosato, D. V. Rosato, Plastics Processing Data Handbook, Van Nostrand Reinhold, USA, 1990, 392 p.
- [23] H. F. Giles Jr., J. R. Wagner Jr., E. M. Mount, Extrusion (Second Edition): The Definitive Processing Guide and Handbook, Part VI: Coextrusion, Elsevier Inc., 2013, pp. 467-476.
- [24] H. F. Giles Jr., J. R. Wagner Jr., E. M. Mount, Extrusion (Second Edition): The Definitive Processing Guide and Handbook, Part I: Single Screw Extrusion, Elsevier Inc., 2013, pp. 89-99.

- [25] B. A. Morris, Understanding Why Adhesion in Extrusion Coating Decreases with Diminishing Coating Thickness, DuPont Packaging and Industrial Polymers, Journal of Plastic Film & Sheeting, Vol. 24, USA, 2008, 36 p.
- [26] F. Awaja, M. Gilbert, G. Kelly, B. Fox, P. J. Pigram, Adhesion of Polymers, Progress in Polymer Science 34, Elsevier Ltd., Australia, 2009, pp. 948-968. Available <http://www.sciencedirect.com/science/article/pii/S0079670009000501>
- [27] B. Foster, Adhesion in Extrusion Coating & Laminating – the Importance of Machine Variables, Mica Corporation, USA, 2006, 66 p. Available <http://www.tappi.org/content/06asiaplace/pdfs-english/adhesion.pdf>
- [28] W. M. Karszes, Solidification Process in Extrusion Coating, DVG Plastics, Polymers, Laminations & Coatings Conference, USA, 1991, pp. 545-551.
- [29] B. A. Morris, Adhesion in Extrusion Coating: Time in the Air Gap Revisited, DuPont, TAPPI Place, USA, 2016, 39 p.
- [30] J. Lahti, J. Kuusipalo, S. Auvinen, Novel Equipment to Simulate Hot Air Sealability of Packaging Materials, Tampere University of Technology, Tampere, Finland, 2016.
- [31] E. Abdel-Bary, Handbook of Plastic Films, Rapra Technology Limited, United Kingdom, 2003, 406 p.
- [32] K. Hishinuma, Heat Sealing Technology and Engineering for Packaging: Principles and Applications, DEStech Publications Inc., USA, 2009, 251 p.
- [33] C. Mueller, G. Capaccio, A. Hiltner, E. Baer, Heat Sealing of LLDPE: Relationships to Melting and Interdiffusion, Journal of Applied Polymer Science, Vol. 70, John Wiley & Sons Inc., 1998, pp. 2012-2030. Available [http://onlinelibrary.wiley.com/doi/10.1002/\(SICI\)1097-4628\(19981205\)70:10%3C2021::AID-APP18%3E3.0.CO;2-A/epdf](http://onlinelibrary.wiley.com/doi/10.1002/(SICI)1097-4628(19981205)70:10%3C2021::AID-APP18%3E3.0.CO;2-A/epdf)
- [34] R. H. Cramm, The Influence of Processing Conditions on the Hot Tack of Polyethylene Extrusion Coatings, Dow Chemical Co., TAPPI Journal, USA, 1989, pp. 185-189.
- [35] Extrusion Coating and Lamination, Reference Manual, Iggesund Paperboard, Sweden, pp. 38-43. Available https://www.iggesund.com/globalassets/iggesund-documents/rm-pdf/1.-from-forest-to-market/extrusion_coating_and_lamination_en.pdf

- [36] S. Kouda, Prediction of Processability at Extrusion Coating for Low-Density Polyethylene, Society of Plastic Engineers, Japan, 2008, pp. 1094-1102. Available <http://onlinelibrary.wiley.com/doi/10.1002/pen.21056/pdf>
- [37] P. R. N. Childs, Practical Temperature Measurement, Butterworth-Heinemann, United Kingdom, 2001, 372 p.
- [38] T. Weckström, Lämpötilan mittaus, 2. Edition, Mikes metrologia, Helsinki, Finland, 2005, 138 p.
- [39] K-D. Gruner, Principles of Non-Contact Temperature Measurement, Raytek GmbH, Germany, 2003, 32 p.
- [40] G. C. Holst, Common Sense Approach to Thermal Imaging, JCD Publishing, USA, 2000, 377 p.
- [41] W. R. Barron, Principles of Infrared Thermometry, Williamson Corporation, USA, 5 p. Available <http://www.omega.com/temperature/Z/pdf/z059-062.pdf>
- [42] B. M. Foederer, B. A. Morris, Use of IR Technology to Model Temperature Loss in the Air Gap, TAPPI Place Conference, USA, 2014, 39 p.
- [43] Thermalert Messköpfe, Raytek Corporation, USA, 1998, 2 p. Available http://selmatec.de/RH-Serie.html?file=files/Selmatec_IMG/PDF/IR-Sensoren/Thermalert-Serie/rh.pdf
- [44] Thermalert Monitor T3 Plus, Raytek Corporation, USA, 1998, 2 p. Available http://selmatec.de/RH-Serie.html?file=files/Selmatec_IMG/PDF/IR-Sensoren/Thermalert-Serie/t3p.pdf
- [45] Paper Converting and Packaging Technology, Laboratory, Tampere University of Technology, Tampere, Finland, 2015, 13 p. Available <http://www.tut.fi/cs/groups/public/@1102/@web/@p/documents/liit/x146932.pdf>

APPENDIX A: LABORATORY RESULTS OF TRIAL RUNS

DATE:20170125												
TEST POINT AND RPM	1	2	3	4	5	AVERAGE	STDEV	ADHESION	DECKLES	WIDTH	NECK-IN	PINHOLES
LINE SPEED	COATING WEIGHT, g/m ²					AVERAGE	STDEV	VALUE	VALUE	(mm)	(mm)	
REFERENCE	1.921	1.92	1.916	1.938	1.928	192.46	0.86					
20170125-1	1	2	3	4	5	AVERAGE	STDEV	ADHESION	DECKLES	WIDTH	NECK-IN	PINHOLES
low1	2.138	2.122	2.136	2.123	2.142	20.76	0.91	5	550	447	104	106
low2	2.1	2.131	2.086	2.114	2.12	18.56	1.76	5	550	449	101	100
low3	2.086	2.069	2.079	2.077	2.063	15.02	0.90	5	550	448	102	104
low4	2.061	2.051	2.06	2.07	2.049	13.36	0.85	5	550	446	104	106
medium1	2.039	2.062	2.021	2.054	2.05	12.06	1.59	4	550	450	101	100
REFERENCE	1	2	3	4	5	AVERAGE	STDEV					
20170125-2	1	2	3	4	5	COATING WEIGHT, g/m ²	STDEV	ADHESION	DECKLES	WIDTH	NECK-IN	PINHOLES
LINE SPEED	COATING WEIGHT, g/m ²					AVERAGE	STDEV	VALUE	VALUE	(mm)	(mm)	
low1	2.284	2.283	2.28	2.279	2.304	36.14	1.03	5	550	423	125	125
low2	2.192	2.217	2.214	2.206	2.207	28.26	0.97	5	550	428	122	119
low3	2.19	2.161	2.16	2.19	2.141	24.38	2.13	5	550	432	118	117
medium1	2.106	2.11	2.114	2.118	2.095	18.4	0.88	4	550	436	114	113
medium2	2.07	2.097	2.096	2.077	2.083	16	1.18	3	550	437	113	112
medium3	2.095	2.053	2.099	2.058	2.064	14.92	2.16	3	550	439	111	111
REFERENCE	1	2	3	4	5	AVERAGE	STDEV					
20170125-3	1	2	3	4	5	COATING WEIGHT, g/m ²	STDEV	ADHESION	DECKLES	WIDTH	NECK-IN	PINHOLES
LINE SPEED	COATING WEIGHT, g/m ²					AVERAGE	STDEV	VALUE	VALUE	(mm)	(mm)	
low1	2.152	2.12	2.153	2.163	2.125	21.8	1.89	5	550	419	132	128
low2	2.12	2.107	2.126	2.133	2.118	19.62	0.97	5	550	430	120	119
low3	2.071	2.089	2.085	2.086	2.079	15.74	0.71	5	550	434	116	114
medium1	2.071	2.059	2.044	2.059	2.04	13	1.26	5	550	438	112	109
medium2	2.018	2.038	2.056	2.023	2.039	11.02	1.50	5	550	443	107	108
medium3	2.036	2.032	2.033	2.022	2.064	11.28	1.58	4.5	550	453	97	95

	REFERENCE	1	2	3	4	5	AVERAGE	STDEV													
TEST POINT AND RPM 20170125-4	LINE SPEED	1	2	3	4	5	COATING WEIGHT, g/m ² AVERAGE	STDEV	ADHESION	DECKLES VALUE	WIDTH (mm)	NECK-IN (mm)	PINHOLES								
	low1	2.269	2.303	2.291	2.268	2.285	35.86	1.49	5	550	413	413	137	137	137	137	137	137	off		
	low2	2.224	2.203	2.235	2.22	2.208	29.34	1.28	5	550	419	420	131	130	131	131	131	131	131	off	
	low3	2.186	2.188	2.188	2.172	2.178	25.78	0.71	5	550	425	424	125	126	125	125	125	125	125	125	off
	medium1	2.147	2.117	2.154	2.132	2.101	20.56	2.17	5	550	433	433	117	117	117	117	117	117	117	117	off
	medium2	2.088	2.122	2.089	2.107	2.106	17.78	1.42	4.5	550	437	436	113	114	114	114	114	114	114	114	off
	medium3	2.1	2.101	2.087	2.096	2.096	17.24	0.60	4	550	438	438	112	112	111	111	111	111	111	111	off
	high1	2.061	2.066	2.024	2.064	2.07	13.24	1.87	4	550	438	438	112	112	112	112	112	112	112	112	off
	high2	2.049	2.058	2.061	2.051	2.052	12.96	0.51	4	550	441	440	109	110	108	108	108	108	108	108	1
	REFERENCE	1	2	3	4	5	AVERAGE	STDEV													
			1.92	1.9	1.908	1.908	1.903	190.78	0.76												
TEST POINT AND RPM 20170125-5	LINE SPEED	1	2	3	4	5	COATING WEIGHT, g/m ² AVERAGE	STDEV	ADHESION	DECKLES VALUE	WIDTH (mm)	NECK-IN (mm)	PINHOLES								
	low1	2.12	2.148	2.113	2.11	2.145	21.94	1.80	5	550	352	354	188	199	196	196	196	196	196	off	
	low2	2.052	2.065	2.082	2.062	2.067	15.78	1.08	5	550	364	366	186	184	183	183	183	183	183	off	
	low3	2.022	2.074	2.065	2.065	2.062	14.78	2.00	5	550	374	374	175	176	175	175	175	175	175	175	off
	medium1	2.053	2.053	2.017	2.022	2.056	13.24	1.90	5	550	391	391	159	159	158	158	158	158	158	158	off
	medium2	2.004	1.997	2.033	2.016	2.021	10.64	1.42	5	550	400	401	149	149	149	149	149	149	149	149	1
	medium3	2.014	1.998	1.994	1.994	1.991	9.04	0.92	5	550	407	406	143	144	143	143	143	143	143	143	1
	high1	1.992	1.981	1.975	1.975	1.972	7.12	0.80	5	550	411	410	139	140	140	140	140	140	140	140	on
	high2	1.995	1.977	1.964	1.994	1.973	7.28	1.35	5	550	414	413	136	137	136	136	136	136	136	136	on
	high3	1.985	1.965	1.986	1.987	1.964	6.96	1.18	5	550	419	419	131	131	131	131	131	131	131	131	on
	REFERENCE	1	2	3	4	5	AVERAGE	STDEV													
		2.213	2.245	2.25	2.252	2.25	33.42	1.64													
TEST POINT AND RPM 20170125-6	LINE SPEED	1	2	3	4	5	COATING WEIGHT, g/m ² AVERAGE	STDEV	ADHESION	DECKLES VALUE	WIDTH (mm)	NECK-IN (mm)	PINHOLES								
	low1	2.213	2.245	2.25	2.252	2.25	33.42	1.64	5	550	379	380	171	170	171	171	171	171	171	171	off
	low2	2.19	2.164	2.156	2.198	2.152	26.42	2.07	5	550	390	390	160	160	160	160	160	160	160	160	off
	low3	2.15	2.137	2.154	2.139	2.138	23.58	0.78	5	550	398	398	152	152	152	152	152	152	152	152	off
	medium1	2.066	2.09	2.076	2.095	2.11	17.96	1.71	5	550	410	409	140	141	140	140	140	140	140	140	off
	medium2	2.059	2.09	2.056	2.06	2.081	16.14	1.53	5	550	417	417	133	133	133	133	133	133	133	133	off
	medium3	2.062	2.044	2.059	2.043	2.051	14.4	0.86	5	550	422	422	128	128	127	127	127	127	127	127	off
	high1	2.032	2.012	2.016	2.029	2.004	11.08	1.17	5	550	425	425	125	125	124	124	124	124	124	124	off
	high2	1.999	2.012	2.025	2.024	2.019	10.8	1.07	5	550	428	428	122	121	122	122	122	122	122	122	1
	high3	2.01	2.012	1.989	2.03	1.985	9.74	1.84	5	550	432	432	118	118	120	118	118	118	118	118	on

REFERENCE	1	2	3	4	5	AVERAGE	STDEV	DECKLES VALUE	ADHESION	COATING WEIGHT, g/m ² AVERAGE	STDEV	WIDTH (mm)	NECK-IN (mm)	PINHOLES
TEST POINT AND RPM 20170131-B17-4	LINE SPEED	1	2	3	4	5								
	low1	2.281	2.294	2.259	2.261	2.272	1.45	550	5	31.9	1.45	402	148	145
	low2	2.181	2.22	2.228	2.212	2.22	1.83	550	5	25.78	1.83	412	138	138
	low3	2.159	2.164	2.196	2.191	2.169	1.66	550	5	22.14	1.66	417	134	132
	medium1	2.129	2.124	2.127	2.13	2.107	0.94	550	5	16.9	0.94	427	123	123
	medium2	2.097	2.119	2.127	2.106	2.114	1.16	550	5	15.82	1.16	430	120	120
	medium3	2.064	2.1	2.064	2.07	2.087	1.59	550	5	12.26	1.59	433	117	117
	high1	2.052	2.071	2.062	2.048	2.051	0.95	550	5	10.24	0.95	434	116	114
	high2	2.057	2.075	2.052	2.092	2.074	1.60	550	5	11.56	1.60	437	113	112
	high3	2.045	2.011	2.015	2.049	2.023	1.74	550	5	7.42	1.74	437	113	111
REFERENCE	1	2	3	4	5	AVERAGE	STDEV							
	1.949	1.957	1.959	1.936	1.947	194.96	0.92							
TEST POINT AND RPM 20170131-B17-5	LINE SPEED	1	2	3	4	5								
	low1	2.15	2.137	2.115	2.126	2.117	1.46	550	5	17.94	1.46	358	192	192
	low2	2.116	2.133	2.156	2.081	2.134	2.79	550	5	17.44	2.79	374	177	176
	low3	2.074	2.067	2.107	2.045	2.097	2.46	550	5	12.84	2.46	385	165	164
	medium1	2.051	2.041	2.071	2.06	2.058	1.11	550	5	10.66	1.11	397	153	153
	medium2	2.044	2.022	2.033	2.044	2.058	1.35	550	5	9.06	1.35	404	146	144
	medium3	2.044	2.04	2.023	2.067	2.036	1.60	550	5	9.24	1.60	412	138	140
	high1	2.034	2.036	2.057	2.059	2.035	1.26	550	5	9.46	1.26	415	135	135
	high2	2.022	1.999	2.017	2.049	2.026	1.80	550	5	7.3	1.80	420	130	132
	high3	2.007	2.014	2.005	2.048	2.03	1.81	550	5	7.12	1.81	424	126	126
REFERENCE	1	2	3	4	5	AVERAGE	STDEV							
	1.949	1.957	1.959	1.936	1.947	194.96	0.92							
TEST POINT AND RPM 20170131-B17-6	LINE SPEED	1	2	3	4	5								
	low1	2.276	2.276	2.253	2.286	2.279	1.24	550	5	32.44	1.24	378	172	171
	low2	2.199	2.188	2.225	2.196	2.218	1.56	550	5	25.56	1.56	390	160	160
	low3	2.164	2.167	2.176	2.18	2.15	1.17	550	5	21.78	1.17	400	150	150
	medium1	2.143	2.109	2.143	2.119	2.118	1.56	550	5	17.68	1.56	401	149	148
	medium2	2.119	2.113	2.111	2.088	2.104	1.19	550	5	15.74	1.19	408	142	142
	medium3	2.088	2.086	2.103	2.098	2.074	1.13	550	5	14.02	1.13	422	128	127
	high1	2.069	2.046	2.055	2.073	2.082	1.44	550	5	11.54	1.44	428	122	123
	high2	2.037	2.078	2.051	2.056	2.054	1.48	550	5	10.56	1.48	428	122	122
	high3	2.038	2.069	2.062	2.052	2.058	1.67	550	5	11.02	1.67	431	119	118

DATE:20170216														
TEST POINT AND RPM	LINE SPEED	1	2	3	4	5	AVERAGE	STDEV	ADHESION	DECKLES VALUE	WIDTH (mm)	NECK-IN (mm)	PINHOLES	
20170216-B18-1		COATING WEIGHT, g/m ²					AVERAGE	STDEV						
REFERENCE		1.931	1.943	1.952	1.938	1.938	194.04	0.78						
low1		2.139	2.147	2.135	2.125	2.155	19.98	1.15	5	550	440	110	111	
low2		2.106	2.128	2.101	2.111	2.138	17.64	1.56	5	550	443	107	106	
low3		2.067	2.082	2.086	2.095	2.083	14.22	1.01	5	550	445	105	104	
medium1		2.046	2.056	2.062	2.039	2.036	10.74	1.11	3	550	448	102	101	
REFERENCE		1	2	3	4	5 <td>AVERAGE</td> <td>STDEV</td> <td></td> <td></td> <td></td> <td></td> <td></td>	AVERAGE	STDEV						
TEST POINT AND RPM	LINE SPEED	COATING WEIGHT, g/m ²					AVERAGE	STDEV	ADHESION	DECKLES VALUE	WIDTH (mm)	NECK-IN (mm)	PINHOLES	
20170216-B18-2		COATING WEIGHT, g/m ²					AVERAGE	STDEV						
low1		2.248	2.293	2.255	2.269	2.28	32.86	1.83	5	550	421	129	128	
low2		2.233	2.236	2.207	2.222	2.21	28.12	1.31	5	550	428	122	122	
low3		2.175	2.185	2.174	2.17	2.147	22.98	1.41	5	550	432	118	118	
medium1		2.106	2.104	2.117	2.131	2.118	17.48	1.08	5	550	437	113	114	
medium2		2.096	2.132	2.101	2.079	2.098	16.08	1.92	3	550	438	112	112	
medium3		2.081	2.07	2.075	2.063	2.055	12.84	1.02	2	550	438	112	111	
high1		2.063	2.05	2.037	2.066	2.061	10.9	1.28	2	550	440	110	111	
REFERENCE		1	2	3	4	5 <td>AVERAGE</td> <td>STDEV</td> <td></td> <td></td> <td></td> <td></td> <td></td>	AVERAGE	STDEV						
low1		2.137	2.133	2.132	2.168	2.139	19.46	1.06	5	550	404	146	143	
low2		2.126	2.114	2.092	2.089	2.102	15.94	1.55	5	550	414	136	137	
low3		2.094	2.107	2.067	2.1	2.125	15.34	2.11	5	550	423	127	127	
medium1		2.05	2.056	2.048	2.062	2.046	10.52	0.38	5	550	430	120	119	
medium2		2.04	2.036	2.044	2.027	2.032	9.06	0.66	5	550	433	117	117	
medium3		2.034	2.031	2.034	2.049	2.02	8.84	1.04	5	550	438	112	111	
high1		2.018	2.004	2.012	2.015	2.029	7.04	0.91	4.5	550	442	108	111	
high2		2.02	2.002	2.002	2.017	2.007	6.44	0.84	4.5	550	439	111	111	
TEST POINT AND RPM	LINE SPEED	COATING WEIGHT, g/m ²					AVERAGE	STDEV	ADHESION	DECKLES VALUE	WIDTH (mm)	NECK-IN (mm)	PINHOLES	
20170216-B18-3		COATING WEIGHT, g/m ²					AVERAGE	STDEV						
low1		2.137	2.133	2.132	2.168	2.139	19.46	1.06	5	550	404	146	143	
low2		2.126	2.114	2.092	2.089	2.102	15.94	1.55	5	550	414	136	137	
low3		2.094	2.107	2.067	2.1	2.125	15.34	2.11	5	550	423	127	127	
medium1		2.05	2.056	2.048	2.062	2.046	10.52	0.38	5	550	430	120	119	
medium2		2.04	2.036	2.044	2.027	2.032	9.06	0.66	5	550	433	117	117	
medium3		2.034	2.031	2.034	2.049	2.02	8.84	1.04	5	550	438	112	111	
high1		2.018	2.004	2.012	2.015	2.029	7.04	0.91	4.5	550	442	108	111	
high2		2.02	2.002	2.002	2.017	2.007	6.44	0.84	4.5	550	439	111	111	

	REFERENCE	1	2	3	4	5	AVERAGE	STDEV												
TEST POINT AND RPM 20170216-B18-4	LINE SPEED	1	2	3	4	5	COATING WEIGHT, g/m ² AVERAGE	STDEV	ADHESION	DECKLES VALUE	WIDTH (mm)	NECK-IN (mm)	PINHOLES							
	low1	2.301	2.3	2.284	2.278	2.281	34.36	1.09	5	550	404	146	146	off						
	low2	2.234	2.231	2.242	2.235	2.235	28.42	1.42	5	550	413	137	137	off						
	low3	2.189	2.192	2.166	2.183	2.186	24	1.11	5	550	420	130	129	off						
	medium1	2.134	2.125	2.124	2.114	2.134	18.1	0.83	5	550	426	124	124	off						
	medium2	2.083	2.087	2.09	2.09	2.094	14.36	0.41	5	550	432	118	118	off						
	medium3	2.076	2.057	2.077	2.087	2.054	12.5	1.41	5	550	436	114	114	off						
	high1	2.082	2.047	2.079	2.073	2.055	12.2	1.54	5	550	437	113	113	off						
	high2	2.056	2.037	2.057	2.062	2.043	10.58	1.05	4.5	550	440	110	110	off						
	high3	2.058	2.044	2.064	2.059	2.067	11.32	0.88	3	550	440	110	109	1						
	REFERENCE	1	2	3	4	5	AVERAGE	STDEV												
		1.911	1.953	1.938	1.941	1.928	193.42	1.57												
	TEST POINT AND RPM 20170216-B18-5	LINE SPEED	1	2	3	4	5	COATING WEIGHT, g/m ² AVERAGE	STDEV	ADHESION	DECKLES VALUE	WIDTH (mm)	NECK-IN (mm)	PINHOLES						
low1		2.159	2.134	2.139	2.139	2.132	20.64	1.07	5	550	360	190	190	off						
low2		2.073	2.074	2.08	2.104	2.087	14.94	1.27	5	550	372	177	178	off						
low3		2.065	2.076	2.071	2.082	2.095	14.36	1.15	5	550	382	168	168	off						
medium1		2.041	2.018	2.057	2.037	2.043	10.5	1.40	5	550	398	152	152	off						
medium2		2.049	2.044	2.01	2.043	2.02	9.9	1.71	5	550	407	143	142	off						
medium3		2.05	2.011	2.04	2.029	2.011	9.4	1.74	5	550	412	138	138	1						
high1		2.014	2.012	1.987	2.015	2.016	7.46	1.23	5	550	417	133	133	on						
high2		1.994	1.986	1.991	2.031	2.01	6.82	1.83	5	550	421	129	130	on						
high3		2.008	1.991	2.003	2.004	2.004	6.78	0.64	5	550	424	126	127	on						
REFERENCE		1	2	3	4	5	AVERAGE	STDEV												
		2.263	2.271	2.252	2.249	2.245	32.18	1.07	5	550	379	171	169	off						
TEST POINT AND RPM 20170216-B18-6		LINE SPEED	1	2	3	4	5	COATING WEIGHT, g/m ² AVERAGE	STDEV	ADHESION	DECKLES VALUE	WIDTH (mm)	NECK-IN (mm)	PINHOLES						
	low1	2.263	2.271	2.252	2.249	2.245	32.18	1.07	5	550	379	171	169	off						
	low2	2.206	2.198	2.166	2.195	2.18	25.48	1.59	5	550	392	158	159	off						
	low3	2.132	2.145	2.143	2.156	2.143	20.96	0.85	5	550	402	148	149	off						
	medium1	2.161	2.131	2.145	2.116	2.137	20.38	1.67	5	550	413	137	137	off						
	medium2	2.086	2.125	2.088	2.081	2.078	15.74	1.91	5	550	421	129	129	off						
	medium3	2.074	2.077	2.091	2.081	2.071	14.46	0.78	5	550	428	122	123	1						
	high1	2.047	2.067	2.014	2.065	2.052	11.48	2.13	5	550	428	122	122	off						
	high2	2.015	2.032	2.055	2.069	2.018	10.36	2.35	5	550	432	118	118	off						
	high3	2.026	2.013	2.03	2.019	2.032	8.98	0.79	5	550	431	119	118	on						

	1	2	3	4	5	AVERAGE	STDEV													
REFERENCE	1.948	1.942	1.961	1.967	1.944	195.24														
TEST POINT AND RPM 20170223-B19-4																				
LINE SPEED	1	2	3	4	5	COATING WEIGHT, g/m ² AVERAGE	STDEV	ADHESION	DECKLES VALUE	WIDTH (mm)	NECK-IN (mm)	PINHOLES								
low1	2.314	2.31	2.318	2.272	2.316	35.36	1.92	5	550	393	157	156	off							
low2	2.27	2.247	2.232	2.231	2.231	29.42	1.62	5	550	402	148	149	off							
low3	2.21	2.19	2.183	2.204	2.203	24.56	1.11	5	550	408	142	143	off							
medium1	2.177	2.17	2.144	2.175	2.169	21.46	1.33	5	550	416	134	136	off							
medium2	2.126	2.119	2.136	2.115	2.102	16.72	1.27	5	550	420	130	132	off							
medium3	2.096	2.13	2.088	2.097	2.104	15.06	1.61	5	550	422	128	127	off							
high1	2.094	2.077	2.066	2.061	2.077	12.26	1.27	5	550	424	126	127	off							
high2	2.082	2.062	2.067	2.067	2.067	11.66	0.76	4.5	550	425	125	125	on							
high3	2.047	2.072	2.063	2.064	2.082	11.72	1.48	4	550	426	124	123	on							
REFERENCE	1	2	3	4	5	AVERAGE	STDEV													
TEST POINT AND RPM 20170223-B19-5																				
LINE SPEED	1	2	3	4	5	COATING WEIGHT, g/m ² AVERAGE	STDEV	ADHESION	DECKLES VALUE	WIDTH (mm)	NECK-IN (mm)	PINHOLES								
low1	2.13	2.132	2.143	2.12	2.165	18.56	1.72	5	550	360	190	190	off							
low2	2.114	2.105	2.093	2.121	2.108	15.58	1.05	5	550	373	177	177	off							
low3	2.087	2.08	2.101	2.087	2.058	13.02	1.57	5	550	381	169	169	off							
medium1	2.073	2.052	2.042	2.051	2.039	9.9	1.33	5	550	391	158	159	off							
medium2	2.063	2.019	2.023	2.063	2.027	8.66	2.21	5	550	402	148	149	off							
medium3	2.017	2.016	2.031	2.025	2.011	6.76	0.79	5	550	402	148	148	on							
high1	2.02	2	2.033	2.021	2.025	6.74	1.22	5	550	408	142	143	on							
high2	2.022	2.012	2.025	2.01	2.027	6.68	0.77	5	550	408	142	142	on							
high3	2	2.01	2.008	2.007	2.025	5.76	0.92	4.5	550	412	138	138	on							
REFERENCE	1	2	3	4	5	AVERAGE	STDEV													
TEST POINT AND RPM 20170223-B19-6																				
LINE SPEED	1	2	3	4	5	COATING WEIGHT, g/m ² AVERAGE	STDEV	ADHESION	DECKLES VALUE	WIDTH (mm)	NECK-IN (mm)	PINHOLES								
low1	2.286	2.268	2.285	2.285	2.285	32.94	0.77	5	550	370	180	179	off							
low2	2.2	2.235	2.227	2.2	2.205	26.1	1.64	5	550	381	169	169	off							
low3	2.208	2.173	2.184	2.192	2.158	23.06	1.89	5	550	388	162	162	off							
medium1	2.128	2.15	2.139	2.139	2.122	18.32	1.09	5	550	399	151	151	off							
medium2	2.12	2.105	2.129	2.149	2.116	17.14	1.65	5	550	406	144	144	off							
medium3	2.084	2.093	2.079	2.072	2.07	12.72	0.93	5	550	409	141	140	off							
high1	2.074	2.077	2.099	2.04	2.07	10.76	1.89	5	550	413	137	136	off							
high2	2.039	2.053	2.059	2.03	2.037	8.72	0.84	5	550	417	133	133	on							
high3	2.03	2.044	2.048	2.03	2.034	8.48	0.83	5	550	418	132	132	on							

DATE:20170302														
TEST POINT AND RPM	LINE SPEED	1	2	3	4	5	AVERAGE	STDEV	ADHESION	DECKLES VALUE	WIDTH (mm)	NECK-IN (mm)	PINHOLES	
20170302-1		COATING WEIGHT, g/m ²					AVERAGE	STDEV						
REFERENCE		1.967	1.997	1.973	1.959	1.943	196.78	1.98						
low1		2.187	2.142	2.167	2.163	2.144	19.08	1.87	5	550	471	79	78	
low2		2.145	2.118	2.142	2.11	2.119	15.9	1.57	5	550	472	78	74	
low3		2.095	2.098	2.102	2.089	2.096	12.82	0.47	5	550	481	69	69	
medium1		2.068	2.076	2.108	2.094	2.056	11.26	2.07	5	550	482	68	67	
medium2		2.026	2.029	2.064	2.029	2.045	7.08	1.60	5	550	486	64	66	
medium3		2.062	2.049	2.037	2.038	2.044	7.82	1.02	5	550	487	65	63	
REFERENCE		1	2	3	4	5	AVERAGE	STDEV						
TEST POINT AND RPM	LINE SPEED	COATING WEIGHT, g/m ²					AVERAGE	STDEV	ADHESION	DECKLES VALUE	WIDTH (mm)	NECK-IN (mm)	PINHOLES	
20170302-2		COATING WEIGHT, g/m ²					AVERAGE	STDEV						
low1		2.154	2.157	2.147	2.134	2.156	18.18	0.96	5	550	409	141	141	
low2		2.091	2.075	2.118	2.082	2.105	12.64	1.74	5	550	416	134	136	
low3		2.098	2.061	2.079	2.117	2.107	12.46	2.24	5	550	426	124	127	
medium1		2.09	2.044	2.055	2.076	2.06	9.72	1.81	5	550	433	117	117	
medium2		2.041	2.052	2.054	2.034	2.07	8.24	1.38	5	550	439	111	110	
medium3		2.05	2.04	2.051	2.058	2.05	8.2	0.64	5	550	446	104	105	
high1		2.03	2.045	2.058	2.011	2.046	7.02	1.81	5	551	446	104	107	
high2		2.028	2.006	2.017	2.005	1.988	4.1	1.49	5	552	446	106	108	
REFERENCE		1	2	3	4	5	AVERAGE	STDEV						
TEST POINT AND RPM	LINE SPEED	COATING WEIGHT, g/m ²					AVERAGE	STDEV	ADHESION	DECKLES VALUE	WIDTH (mm)	NECK-IN (mm)	PINHOLES	
20170302-3		COATING WEIGHT, g/m ²					AVERAGE	STDEV						
low1		2.262	2.252	2.242	2.23	2.243	27.8	1.20	5	550	224	326	327	
low2		2.176	2.184	2.17	2.17	2.21	21.42	1.67	5	550	237	313	314	
low3		2.128	2.147	2.138	2.146	2.145	17.3	0.80	5	550	256	294	294	
medium1		2.072	2.069	2.08	2.071	2.081	10.68	0.55	5	550	280	270	270	
medium2		2.053	2.054	2.044	2.05	2.052	8.28	0.40	5	550	294	256	256	
medium3		2.038	2.037	2.027	2.019	2.019	6.02	0.93	5	550	302	248	249	
high1		2.01	2.008	2.013	2.018	2.018	4.56	0.46	5	551	311	241	241	
high2		1.999	1.997	1.989	2.026	2.016	3.76	1.51	5	552	323	229	231	
high3		2.002	2.002	2.007	2.008	1.995	3.5	0.52	5	553	328	225	225	

	REFERENCE	1	2	3	4	5	AVERAGE	STDEV											
TEST POINT AND RPM 20170302-4	LINE SPEED	1	2	3	4	5	COATING WEIGHT, g/m ² AVERAGE	STDEV	ADHESION	DECKLES VALUE	WIDTH (mm)	NECK-IN (mm)	PINHOLES						
	low1	2.28	2.271	2.295	2.284	2.276	30.94	1.16	5	550	470	80	80	off					
	low2	2.226	2.22	2.205	2.218	2.218	24.6	1.09	5	550	477	73	73	off					
	low3	2.183	2.176	2.191	2.189	2.189	21.38	0.92	5	550	478	72	72	off					
	medium1	2.123	2.114	2.117	2.133	2.116	15.28	0.77	5	550	483	67	67	off					
	medium2	2.119	2.104	2.089	2.118	2.09	13.62	1.45	4.5	550	485	65	66	off					
	medium3	2.074	2.079	2.069	2.08	2.071	10.68	0.48	4	550	486	64	64	2					
	high1	2.052	2.049	2.065	2.044	2.054	8.5	0.78	3	550	486	64	63	on					
	REFERENCE	1	2	3	4	5	AVERAGE	STDEV											
		1.938	1.966	1.937	1.967	1.945	195.06	1.48											
TEST POINT AND RPM 20170302-5	LINE SPEED	1	2	3	4	5	COATING WEIGHT, g/m ² AVERAGE	STDEV	ADHESION	DECKLES VALUE	WIDTH (mm)	NECK-IN (mm)	PINHOLES						
	low1	2.299	2.264	2.269	2.304	2.258	32.82	2.12	5	550	403	147	147	off					
	low2	2.228	2.223	2.211	2.253	2.237	27.98	1.57	5	550	415	135	136	off					
	low3	2.186	2.19	2.163	2.173	2.198	23.14	1.39	5	550	421	129	127	off					
	medium1	2.151	2.122	2.163	2.152	2.108	18.86	2.31	5	550	429	120	120	off					
	medium2	2.122	2.1	2.074	2.092	2.093	14.56	1.73	5	550	435	115	115	off					
	medium3	2.099	2.071	2.086	2.092	2.095	13.8	1.09	5	550	441	109	110	off					
	high1	2.07	2.061	2.076	2.08	2.071	12.1	0.72	4.5	550	442	108	107	off					
	high2	2.067	2.056	2.037	2.061	2.075	10.86	1.43	4	550	444	106	104	on					
	REFERENCE	1	2	3	4	5	AVERAGE	STDEV											
	2.052	2.049	2.065	2.044	2.054	8.5	0.78												
TEST POINT AND RPM 20170302-6	LINE SPEED	1	2	3	4	5	COATING WEIGHT, g/m ² AVERAGE	STDEV	ADHESION	DECKLES VALUE	WIDTH (mm)	NECK-IN (mm)	PINHOLES						
	low1	2.459	2.436	2.424	2.464	2.477	50.14	2.16	5	550	247	303	303	off					
	low2	2.329	2.341	2.341	2.344	2.279	37.62	2.73	5	550	269	291	289	off					
	low3	2.216	2.219	2.219	2.233	2.235	27.38	0.89	5	550	277	276	274	off					
	medium1	2.111	2.15	2.116	2.119	2.165	18.16	2.39	5	550	293	295	255	off					
	medium2	2.11	2.085	2.081	2.1	2.09	14.26	1.18	5	550	308	308	242	off					
	medium3	2.071	2.066	2.057	2.066	2.037	10.88	1.35	5	550	318	318	232	off					
	high1	2.015	2.059	2.049	2.024	2.041	8.7	1.80	5	550	324	324	226	off					
	high2	2.026	2.026	1.991	2.011	2.026	6.54	1.54	5	550	332	332	218	off					
	high3	2.012	2.015	2.019	2.017	2.019	6.58	0.30	5	550	335	334	215	off					

DATE:20170308													
TEST POINT AND RPM	LINE SPEED	1	2	3	4	5	AVERAGE	STDEV	ADHESION	DECKLES VALUE	WIDTH (mm)	NECK-IN (mm)	PINHOLES
20170308-1		1	2	3	4	5	COATING WEIGHT, g/m ²	STDEV					
REFERENCE		1.935	1.928	1.943	1.926	1.95	193.64	1.01					
low1		2.111	2.143	2.169	2.116	2.136	19.86	2.32	5	550	426	124	123
low2		2.102	2.104	2.1	2.093	2.092	16.18	0.54	5	550	435	436	115
low3		2.055	2.061	2.078	2.086	2.044	12.84	1.71	5	550	443	443	107
medium1		2.049	2.046	2.039	2.029	2.023	10.08	1.11	5	550	451	453	97
medium2		2.021	2.031	2.005	2.034	2.032	8.82	1.21	5	550	458	460	90
medium3		2.012	2.004	2.011	2.008	2.013	7.32	0.36	5	550	465	464	85
high1		2.026	2.008	1.982	2.021	2.004	7.18	1.72	5	551	467	468	84
high2		1.974	1.983	1.993	1.975	1.994	4.74	0.95	5	552	469	469	83
high3		1.998	1.978	1.948	1.972	2	4.28	2.13	5	553	471	472	81
REFERENCE		1	2	3	4	5	AVERAGE	STDEV					
TEST POINT AND RPM	LINE SPEED	1	2	3	4	5	COATING WEIGHT, g/m ²	STDEV	ADHESION	DECKLES VALUE	WIDTH (mm)	NECK-IN (mm)	PINHOLES
20170308-2		1	2	3	4	5	AVERAGE	STDEV					
low1		2.108	2.09	2.104	2.097	2.092	16.18	0.77	5	550	324	324	226
low2		2.099	2.071	2.106	2.095	2.064	15.06	1.84	5	550	347	346	203
low3		2.058	2.055	2.079	2.049	2.048	12.14	1.26	5	550	361	360	189
medium1		2.035	2.039	2.04	2.021	2.049	10.04	1.02	5	550	380	381	169
medium2		2.021	2.044	2.029	2.012	2.036	9.2	1.25	5	550	393	394	157
medium3		2.023	2.014	2.034	2.019	2.02	8.56	0.74	5	550	398	400	152
high1		2.011	2.042	2.01	1.999	2.016	7.92	1.60	5	550	406	406	144
high2		2.002	1.988	2.02	1.982	1.988	6.16	1.36	5	550	409	410	141
high3		1.999	1.994	1.993	2.005	1.99	5.98	0.59	5	550	412	412	138
REFERENCE		1	2	3	4	5	AVERAGE	STDEV					
TEST POINT AND RPM	LINE SPEED	1	2	3	4	5	COATING WEIGHT, g/m ²	STDEV	ADHESION	DECKLES VALUE	WIDTH (mm)	NECK-IN (mm)	PINHOLES
20170308-3		1	2	3	4	5	AVERAGE	STDEV					
low1		2.398	2.413	2.403	2.401	2.413	46.92	0.70	5	550	159	158	391
low2		2.322	2.325	2.327	2.301	2.344	38.74	1.54	5	550	154	153	396
low3		2.259	2.263	2.209	2.256	2.271	31.52	2.45	5	550	154	154	396
medium1		2.168	2.138	2.139	2.156	2.123	20.84	1.75	5	550	164	164	386
medium2		2.053	2.071	2.066	2.058	2.074	12.8	0.88	5	550	182	183	368
medium3		2.024	2.027	2.027	2.016	2.019	8.62	0.49	5	550	199	198	351
high1		2.004	2.012	2.007	1.996	2.012	6.98	0.66	5	550	213	210	337
high2		1.971	1.987	1.989	1.98	1.99	4.7	0.80	5	550	226	224	324
high3		1.993	1.963	1.969	1.985	1.986	4.48	1.44	5	550	238	238	312

TEST POINT AND RPM 20170308-4	REFERENCE					AVERAGE		STDEV		ADHESION	DECKLES VALUE	WIDTH (mm)	NECK-IN (mm)	PINHOLES
	1	2	3	4	5	COATING WEIGHT, g/m ² AVERAGE	STDEV	ADHESION	DECKLES VALUE					
LINE SPEED	1.954	1.958	1.977	1.945	1.969	196.06	1.26							
low1	2.241	2.27	2.281	2.291	2.268	30.96	1.88	5	550	444	106	105	off	
low2	2.24	2.22	2.233	2.224	2.226	26.8	0.79	5	550	453	97	96	off	
low3	2.171	2.18	2.171	2.175	2.182	21.52	0.51	5	550	458	92	92	off	
medium1	2.147	2.104	2.148	2.134	2.142	17.44	1.82	5	550	464	86	84	off	
medium2	2.113	2.107	2.115	2.124	2.115	15.42	0.61	5	550	472	78	78	off	
medium3	2.095	2.088	2.086	2.11	2.106	13.64	1.07	5	550	477	73	74	off	
high1	2.067	2.056	2.071	2.06	2.067	10.36	0.61	5	550	477	73	73	off	
high2	2.072	2.07	2.029	2.06	2.064	9.84	1.74	5	550	478	72	72	on	
high3	2.05	2.059	2.051	2.057	2.066	9.6	0.65	5	550	478	72	72	on	
REFERENCE	1	2	3	4	5	AVERAGE	STDEV							
TEST POINT AND RPM 20170308-5	REFERENCE					AVERAGE		STDEV		ADHESION	DECKLES VALUE	WIDTH (mm)	NECK-IN (mm)	PINHOLES
LINE SPEED	1	2	3	4	5	COATING WEIGHT, g/m ² AVERAGE	STDEV	ADHESION	DECKLES VALUE					
low1	2.308	2.274	2.269	2.308	2.272	32.56	2.00	5	550	367	368	183	181	off
low2	2.247	2.249	2.216	2.254	2.231	27.88	1.57	5	550	383	383	167	167	off
low3	2.198	2.192	2.211	2.187	2.214	23.98	1.18	5	550	392	391	158	159	off
medium1	2.132	2.147	2.166	2.137	2.162	18.82	1.50	5	550	403	403	147	147	off
medium2	2.113	2.113	2.13	2.133	2.128	16.28	0.97	5	550	412	412	138	138	off
medium3	2.109	2.089	2.111	2.113	2.116	14.7	1.07	5	550	418	418	132	132	off
high1	2.091	2.072	2.106	2.068	2.075	11.98	1.85	5	550	422	422	128	128	off
high2	2.088	2.061	2.073	2.07	2.088	11.54	1.18	5	550	424	424	126	126	off
high3	2.042	2.056	2.045	2.027	2.073	8.8	1.71	5	550	427	427	123	124	1
REFERENCE	1	2	3	4	5	AVERAGE	STDEV							
TEST POINT AND RPM 20170308-6	REFERENCE					AVERAGE		STDEV		ADHESION	DECKLES VALUE	WIDTH (mm)	NECK-IN (mm)	PINHOLES
LINE SPEED	1	2	3	4	5	COATING WEIGHT, g/m ² AVERAGE	STDEV	ADHESION	DECKLES VALUE					
low1	2.6	2.588	2.595	2.588	2.587	63.1	0.57	5	550	208	209	342	341	off
low2	2.439	2.469	2.451	2.448	2.457	49.22	1.11	5	550	211	210	339	340	off
low3	2.326	2.311	2.344	2.328	2.317	36.46	1.26	5	550	217	218	333	333	off
medium1	2.221	2.194	2.198	2.199	2.188	23.94	1.25	5	550	237	236	313	314	off
medium2	2.112	2.119	2.104	2.13	2.103	15.3	1.12	5	550	257	257	293	293	off
medium3	2.085	2.113	2.113	2.076	2.118	14.04	1.91	5	550	273	273	277	277	off
high1	2.132	2.1	2.084	2.091	2.085	13.78	1.98	5	550	284	284	266	266	off
high2	2.074	2.089	2.084	2.068	2.083	11.7	1.22	5	550	293	292	257	259	off
high3	2.079	2.042	2.048	2.059	2.063	9.76	1.43	5	550	298	299	252	251	off

DATE:20170309-B20												
REFERENCE	1	2	3	4	5	AVERAGE	STDEV	ADHESION	DECKLES VALUE	WIDTH (mm)	NECK-IN (mm)	PINHOLES
TEST POINT AND RPM 20170309-1	1.951	1.953	1.937	1.973	1.946	195.2	1.33					
LINE SPEED	1	2	3	4	5	COATING WEIGHT, g/m ² AVERAGE	STDEV	ADHESION	DECKLES VALUE	WIDTH (mm)	NECK-IN (mm)	PINHOLES
low1	2.148	2.117	2.148	2.155	2.125	18.66	1.68	5	550	468	82	83
low2	2.133	2.118	2.116	2.118	2.098	16.46	1.24	5	550	473	77	78
low3	2.089	2.1	2.112	2.104	2.095	14.8	0.87	5	550	477	73	72
medium1	2.036	2.058	2.053	2.051	2.084	10.44	1.75	5	550	480	70	70
medium2	2.054	2.023	2.064	2.046	2.023	9.00	1.85	5	550	480	70	74
medium3	2.045	2.025	2.032	2.028	2.042	8.24	0.87	4.5	550	485	65	71
REFERENCE	1	2	3	4	5	AVERAGE	STDEV					
TEST POINT AND RPM 20170309-2	2.115	2.073	2.085	2.081	2.103	16.18	1.24	5	550	398	152	150
LINE SPEED	1	2	3	4	5	COATING WEIGHT, g/m ² AVERAGE	STDEV	ADHESION	DECKLES VALUE	WIDTH (mm)	NECK-IN (mm)	PINHOLES
low1	2.115	2.073	2.085	2.081	2.103	16.18	1.24	5	550	411	139	140
low2	2.088	2.088	2.083	2.049	2.095	12.86	1.63	5	550	417	133	134
low3	2.022	2.047	2.068	2.04	2.034	9.02	1.71	5	550	426	124	125
medium1	2.036	2.05	2.039	2.033	2.044	8.84	0.67	5	550	428	122	120
medium2	2.029	2.021	2.022	2.028	2.022	7.24	0.38	5	550	434	116	116
medium3	2.043	2.007	2.011	2.066	2.018	7.1	1.58	5	550	433	117	112
high1												
REFERENCE	1	2	3	4	5	AVERAGE	STDEV					
TEST POINT AND RPM 20170309-3	2.243	2.237	2.252	2.24	2.239	29.02	0.99	5	550	233	317	317
LINE SPEED	1	2	3	4	5	COATING WEIGHT, g/m ² AVERAGE	STDEV	ADHESION	DECKLES VALUE	WIDTH (mm)	NECK-IN (mm)	PINHOLES
low1	2.243	2.237	2.252	2.24	2.239	29.02	0.99	5	550	247	303	302
low2	2.14	2.147	2.155	2.143	2.152	19.54	0.62	5	550	263	287	288
low3	2.133	2.104	2.112	2.117	2.092	15.96	1.52	5	550	283	268	267
medium1	2.078	2.068	2.058	2.09	2.057	11.82	1.40	5	550	293	257	257
medium2	2.065	2.076	2.068	2.066	2.033	10.76	1.65	5	550	301	249	249
medium3	2.037	2.026	2.041	2.034	2.022	8	0.78	5	550	307	243	243
high1	2.018	2.032	2	2.022	2.012	6.48	1.19	5	550	311	239	239
high2	2.001	1.985	1.994	1.984	1.987	3.82	0.72	5	550	317	233	232
high3	1.995	1.987	1.99	1.981	1.999	3.84	0.70	5	550	317	233	232

	REFERENCE	1	2	3	4	5	AVERAGE	STDEV												
TEST POINT AND RPM 20170309-4	LINE SPEED	1	2	3	4	5	COATING WEIGHT, g/m ² AVERAGE	STDEV	ADHESION	DECKLES VALUE	WIDTH (mm)	NECK-IN (mm)	PINHOLES							
	low1	2.302	2.311	2.324	2.277	2.305	35.18	1.72	5	550	462	88	89	off						
	low2	2.228	2.239	2.217	2.242	2.226	27.84	1.02	5	550	468	82	82	off						
	low3	2.182	2.197	2.193	2.192	2.216	24.4	1.25	5	550	470	80	80	off						
	medium1	2.148	2.112	2.133	2.156	2.135	18.48	1.68	5	550	473	77	76	off						
	medium2	2.1	2.096	2.109	2.091	2.105	14.82	0.71	4.5	550	474	76	75	off						
	medium3	2.069	2.069	2.073	2.078	2.061	11.8	0.62	3	550	477	73	74	off						
	REFERENCE	1	2	3	4	5	AVERAGE	STDEV												
	TEST POINT AND RPM 20170309-5	LINE SPEED	1	2	3	4	5	COATING WEIGHT, g/m ² AVERAGE	STDEV	ADHESION	DECKLES VALUE	WIDTH (mm)	NECK-IN (mm)	PINHOLES						
	low1	2.257	2.258	2.294	2.264	2.282	31.9	1.63	5	550	401	149	150	off						
low2	2.22	2.242	2.218	2.219	2.222	27.22	1.01	5	550	407	143	143	off							
low3	2.191	2.184	2.186	2.22	2.169	23.8	1.87	5	550	415	135	134	off							
medium1	2.137	2.138	2.124	2.135	2.138	18.24	0.59	5	550	422	128	128	off							
medium2	2.076	2.093	2.111	2.088	2.092	14.24	1.26	5	550	426	124	124	off							
medium3	2.063	2.054	2.054	2.079	2.097	12.52	1.86	5	550	430	120	120	off							
high1	2.062	2.046	2.06	2.063	2.06	10.42	0.66	4.5	550	430	120	119	off							
high2	2.051	2.046	2.029	2.051	2.05	9.34	0.94	4	550	432	118	118	off							
high3	2.036	2.056	2.041	2.039	2.047	9.18	0.79	2	550	434	116	117	off							
REFERENCE	1	2	3	4	5	AVERAGE	STDEV													
TEST POINT AND RPM 20170309-6	LINE SPEED	1	2	3	4	5	COATING WEIGHT, g/m ² AVERAGE	STDEV	ADHESION	DECKLES VALUE	WIDTH (mm)	NECK-IN (mm)	PINHOLES							
low1	2.432	2.461	2.458	2.477	2.464	49.7	1.64	5	550	248	248	302	302	off						
low2	2.306	2.311	2.306	2.312	2.33	35.16	0.99	5	550	259	257	291	293	off						
low3	2.188	2.216	2.233	2.211	2.217	25.16	1.62	5	550	274	273	276	277	off						
medium1	2.14	2.143	2.154	2.143	2.161	18.68	0.89	5	550	290	291	260	259	off						
medium2	2.119	2.121	2.096	2.105	2.134	15.36	1.48	5	550	302	302	248	248	off						
medium3	2.071	2.083	2.093	2.051	2.09	11.62	1.71	5	550	310	309	240	241	off						
high1	2.067	2.056	2.058	2.039	2.071	9.68	1.24	5	550	316	316	234	234	off						
high2	2.052	2.056	2.063	2.05	2.049	9.26	0.57	5	550	320	319	231	231	off						
high3	2.038	2.06	2.034	2.063	2.034	8.44	1.45	5	550	322	322	228	227	off						

	REFERENCE	1	2	3	4	5	AVERAGE	STDEV															
TEST POINT AND RPM 20170404-4	LINE SPEED	1.926	1.949	1.926	1.934	1.908	192.86	1.49															
		1	2	3	4	5	COATING WEIGHT, g/m ²	STDEV															
	low1	2.303	2.279	2.284	2.304	2.281	36.16	1.23	5	550	460	459	458	90	91	91						off	
	low2	2.212	2.234	2.211	2.217	2.245	29.52	1.50	5	550	461	462	463	89	88	87							off
	low3	2.169	2.196	2.184	2.184	2.155	24.9	1.59	5	550	465	465	465	85	85	85							off
	medium1	2.122	2.149	2.128	2.134	2.15	20.8	1.25	5	550	467	468	468	83	82	82							off
	medium2	2.113	2.105	2.108	2.102	2.097	17.64	0.60	2-3	550	467	467	467	83	83	83							off
	REFERENCE	1	2	3	4	5	AVERAGE	STDEV															
TEST POINT AND RPM 20170404-5	LINE SPEED	1.926	1.949	1.926	1.934	1.908	192.86	1.49															
		1	2	3	4	5	COATING WEIGHT, g/m ²	STDEV															
	low1	2.288	2.303	2.293	2.306	2.316	37.26	1.10	5	550	396	395	395	154	155	155						off	
	low2	2.226	2.219	2.245	2.227	2.228	30.04	0.96	5	550	403	404	403	147	146	147							off
	low3	2.199	2.181	2.171	2.19	2.19	25.76	1.06	5	550	409	408	409	141	142	141							off
	medium1	2.115	2.138	2.141	2.13	2.112	19.86	1.32	5	550	414	414	414	136	136	136							off
	medium2	2.106	2.065	2.106	2.102	2.11	17.32	0.98	5	550	417	418	419	133	132	131							off
medium3	2.099	2.08	2.105	2.092	2.103	16.72	1.01	5	550	421	421	421	129	129	129							off	
	REFERENCE	1	2	3	4	5	AVERAGE	STDEV															
TEST POINT AND RPM 20170404-6	LINE SPEED	1.926	1.949	1.926	1.934	1.908	192.86	1.49															
		1	2	3	4	5	COATING WEIGHT, g/m ²	STDEV															
	low1	2.478	2.51	2.506	2.475	2.489	56.3	1.59	5	550	235	235	235	315	315	315							off
	low2	2.319	2.362	2.361	2.326	2.334	41.18	2.00	5	550	243	242	242	307	308	308							off
	low3	2.243	2.267	2.253	2.27	2.257	32.94	1.09	5	550	254	255	255	296	295	295							off
	medium1	2.18	2.187	2.181	2.17	2.177	25.04	0.62	5	550	268	268	268	282	282	282							off
	medium2	2.096	2.141	2.074	2.095	2.133	17.92	2.82	5	550	282	281	280	268	269	270							off
medium3	2.105	2.066	2.097	2.113	2.072	16.2	2.06	5	550	290	290	290	260	260	260							off	
high1	2.078	2.071	2.056	2.059	2.065	13.72	0.89	5	550	296	296	296	254	254	254							off	
high2	2.055	2.073	2.06	2.07	2.063	13.56	0.73	5	550	302	302	302	248	248	248							off	
high3	2.049	2.018	2.046	2.043	2.022	10.7	1.45	5	550	305	305	305	245	245	245							off	

DATE:20170406-B22												
TEST POINT AND RPM	1	2	3	4	5	AVERAGE	STDEV	ADHESION	DECKLES	WIDTH	NECK-IN	PINHOLES
20170406-1	1	2	3	4	5	COATING WEIGHT, g/m ²	STDEV	VALUE	VALUE	(mm)	(mm)	
REFERENCE	1.938	1.934	1.921	1.915	1.928	192.72	0.94					
LINE SPEED	1	2	3	4	5	AVERAGE	STDEV	ADHESION	DECKLES	WIDTH	NECK-IN	PINHOLES
low1	2.144	2.13	2.159	2.168	2.104	21.18	2.29	5	550	451	98	99
low2	2.065	2.103	2.09	2.085	2.086	15.46	1.66	5	550	461	89	89
low3	2.08	2.044	2.069	2.085	2.066	14.16	1.59	5	550	466	83	84
medium1	2.063	2.048	2.02	2.032	2.025	11.04	1.77	5	550	475	75	76
medium2	2.025	2.035	2.023	2.031	2.038	10.32	0.64	5	550	479	71	71
medium3	2.02	2.022	2.034	2.033	2.024	9.94	0.65	5	550	483	67	68
high1	2.034	2.013	1.995	2.015	2	8.42	1.52	5	550	485	66	66
high2	1.986	2.013	2.005	1.976	2.017	7.22	1.77	5	550	487	63	64
high3	1.989	1.999	1.972	1.992	1.976	5.84	1.13	4.5	550	486	64	62
REFERENCE	1	2	3	4	5	AVERAGE	STDEV					
TEST POINT AND RPM <th>1</th> <th>2</th> <th>3</th> <th>4</th> <th>5</th> <th>COATING WEIGHT, g/m²</th> <th>STDEV</th> <th>ADHESION</th> <th>DECKLES</th> <th>WIDTH</th> <th>NECK-IN</th> <th>PINHOLES</th>	1	2	3	4	5	COATING WEIGHT, g/m ²	STDEV	ADHESION	DECKLES	WIDTH	NECK-IN	PINHOLES
20170406-2	1	2	3	4	5	AVERAGE	STDEV	VALUE <td>VALUE <td>(mm) <td>(mm) <td></td> </td></td></td>	VALUE <td>(mm) <td>(mm) <td></td> </td></td>	(mm) <td>(mm) <td></td> </td>	(mm) <td></td>	
low1	2.12	2.119	2.12	2.123	2.117	19.26	0.22	5	550	364	188	186
low2	2.075	2.076	2.057	2.089	2.091	15.04	1.36	5	550	380	170	170
low3	2.038	2.071	2.043	2.066	2.077	13.18	1.74	5	550	391	159	157
medium1	2.034	2.057	2.039	2.018	2.057	11.38	1.65	5	550	406	144	143
medium2	2.024	2.001	2.033	2.024	2.012	9.16	1.24	5	550	415	135	134
medium3	2.01	2.007	2.031	2.029	1.999	8.8	1.41	5	550	421	129	130
high1	2.007	2.013	2.027	1.983	2.037	8.82	1.72	5	550	423	126	125
high2	2.006	1.988	2.01	2.018	1.989	7.5	1.32	5	550	429	122	122
high3	1.994	2.007	1.995	1.991	2.005	7.12	0.71	5	550	430	120	119
REFERENCE	1	2	3	4	5	AVERAGE	STDEV					
TEST POINT AND RPM <th>1</th> <th>2</th> <th>3</th> <th>4</th> <th>5</th> <th>COATING WEIGHT, g/m²</th> <th>STDEV</th> <th>ADHESION</th> <th>DECKLES</th> <th>WIDTH</th> <th>NECK-IN</th> <th>PINHOLES</th>	1	2	3	4	5	COATING WEIGHT, g/m ²	STDEV	ADHESION	DECKLES	WIDTH	NECK-IN	PINHOLES
20170406-3	1	2	3	4	5	AVERAGE	STDEV	VALUE <td>VALUE <td>(mm) <td>(mm) <td></td> </td></td></td>	VALUE <td>(mm) <td>(mm) <td></td> </td></td>	(mm) <td>(mm) <td></td> </td>	(mm) <td></td>	
low1	2.393	2.355	2.378	2.367	2.364	44.42	1.46	5	550	172	378	376
low2	2.256	2.277	2.272	2.266	2.266	33.62	1.03	5	550	171	379	379
low3	2.188	2.215	2.196	2.167	2.222	27.04	2.20	5	550	176	372	374
medium1	2.103	2.129	2.101	2.111	2.1	18.16	1.21	5	550	192	358	358
medium2	2.061	2.089	2.102	2.079	2.086	15.62	1.50	5	550	206	342	344
medium3	2.042	2.026	2.019	2.037	2.023	10.22	0.97	5	550	225	325	325
high1	2.016	2.043	2.011	2.01	2	8.88	1.62	5	550	239	311	310
high2	2.002	2.027	2.004	2.02	2.003	8.4	1.15	5	550	251	299	300
high3	1.979	1.996	1.988	1.984	1.984	6.1	0.70	5	550	257	293	292

	1	2	3	4	5	AVERAGE	STDEV														
REFERENCE	1.942	1.936	1.949	1.953	1.932	194.24	0.87														
TEST POINT AND RPM 20170406-4																					
LINE SPEED	1	2	3	4	5	COATING WEIGHT, g/m ² AVERAGE	STDEV	ADHESION	DECKLES VALUE	WIDTH (mm)	NECK-IN (mm)	PINHOLES									
low1	2.267	2.284	2.25	2.273	2.257	32.38	1.33	5	550	465	85	86									
low2	2.218	2.217	2.194	2.193	2.2	26.2	1.23	5	550	471	79	78									
low3	2.168	2.149	2.145	2.148	2.169	21.34	1.17	5	550	478	72	72									
medium1	2.116	2.079	2.103	2.096	2.09	15.44	1.39	5	550	485	65	65									
medium2	2.083	2.079	2.098	2.065	2.069	13.64	1.30	5	550	488	62	61									
medium3	2.055	2.047	2.044	2.067	2.046	10.94	0.95	5	550	491	59	59									
high1	2.026	2.054	2.064	2.059	2.027	10.36	1.82	5	550	492	58	58									
high2	2.038	2.038	2.023	2.064	2.051	10.04	1.54	5	550	492	58	59									
high3	2.032	2.041	2.02	2.022	2.046	8.98	1.14	4.5	550	492	58	58									
REFERENCE	1.942	1.936	1.949	1.953	1.932	194.24	0.87														
TEST POINT AND RPM 20170406-5																					
LINE SPEED	1	2	3	4	5	COATING WEIGHT, g/m ² AVERAGE	STDEV	ADHESION	DECKLES VALUE	WIDTH (mm)	NECK-IN (mm)	PINHOLES									
low1	2.27	2.243	2.252	2.264	2.233	31	1.51	5	550	390	160	160									
low2	2.192	2.207	2.193	2.199	2.184	25.26	0.86	5	550	405	145	147									
low3	2.152	2.135	2.178	2.163	2.161	21.54	1.58	5	550	410	140	138									
medium1	2.123	2.097	2.141	2.102	2.113	17.28	1.76	5	550	423	127	127									
medium2	2.088	2.099	2.097	2.093	2.094	15.18	0.42	5	550	431	119	120									
medium3	2.086	2.074	2.084	2.055	2.106	13.86	1.86	5	550	437	113	112									
high1	2.046	2.039	2.048	2.046	2.037	10.08	0.49	5	550	442	108	109									
high2	2.043	2.02	2.027	2.04	2.032	9	0.94	5	550	444	106	107									
high3	2.037	2.022	2.011	2.055	2.009	8.44	1.93	5	550	445	105	106									
REFERENCE	1.942	1.936	1.949	1.953	1.932	194.24	0.87														
TEST POINT AND RPM 20170406-6																					
LINE SPEED	1	2	3	4	5	COATING WEIGHT, g/m ² AVERAGE	STDEV	ADHESION	DECKLES VALUE	WIDTH (mm)	NECK-IN (mm)	PINHOLES									
low1	2.536	2.518	2.517	2.55	2.523	58.64	1.41	5	550	222	328	327									
low2	2.39	2.406	2.4	2.396	2.298	43.56	4.51	5	550	228	322	322									
low3	2.298	2.279	2.264	2.307	2.296	34.64	1.72	5	550	233	317	317									
medium1	2.16	2.15	2.18	2.165	2.183	22.52	1.38	5	550	253	297	297									
medium2	2.094	2.116	2.108	2.108	2.094	16.16	0.97	5	550	275	275	276									
medium3	2.072	2.06	2.076	2.089	2.082	13.34	1.09	5	550	285	265	266									
high1	2.056	2.057	2.062	2.054	2.062	11.58	0.36	5	550	295	255	256									
high2	2.067	2.075	2.045	2.062	2.034	11.22	1.65	5	550	305	245	246									
high3	2.058	2.043	2.038	2.046	2.032	10.08	0.97	5	550	308	241	242									

DATE:20170411-B23												
TEST POINT AND RPM	1	2	3	4	5	AVERAGE	STDEV	ADHESION	DECKLES	WIDTH	NECK-IN	PINHOLES
201700411-1	1	2	3	4	5	COATING WEIGHT, g/m ²	STDEV	ADHESION	VALUE	(mm)	(mm)	
REFERENCE	1.945	1.946	1.951	1.968	1.958	195.36	0.96					
LINE SPEED	1	2	3	4	5	AVERAGE	STDEV					
low1	2.141	2.117	2.117	2.168	2.133	17.96	1.73	5	550	429	430	120
low2	2.105	2.106	2.122	2.102	2.117	15.68	0.86	5	550	439	440	111
low3	2.104	2.102	2.113	2.082	2.109	15.04	0.80	5	550	443	444	106
medium1	2.072	2.076	2.068	2.043	2.075	11.32	1.37	5	550	448	449	101
medium2	2.047	2.047	2.06	2.034	2.056	9.52	1.00	5	550	454	455	96
medium3	2.05	2.046	2.034	2.026	2.032	8.40	1.00	5	550	458	457	93
high1	2.041	2.024	2.025	2.023	2.04	7.70	0.91	5	550	460	461	90
high2	2.009	2.026	2.025	2.008	2.013	6.26	0.87	5	550	462	461	89
high3	2.006	2.014	2.004	2.02	2.02	5.92	0.76	4.5	550	462	463	87
REFERENCE	1	2	3	4	5	AVERAGE	STDEV					
20170411-2	1.941	1.957	1.925	1.939	1.939	194.02	1.14					
LINE SPEED	1	2	3	4	5	COATING WEIGHT, g/m ²	STDEV					
low1	2.131	2.122	2.087	2.142	2.124	18.1	2.07	5	550	343	344	206
low2	2.102	2.112	2.082	2.093	2.112	16.2	0.98	5	550	360	359	190
low3	2.103	2.095	2.079	2.079	2.106	15.22	1.29	5	550	368	367	183
medium1	2.076	2.049	2.037	2.042	2.047	11	1.52	5	550	381	381	169
medium2	2.036	2.024	2.045	2.028	2.026	9.16	0.87	5	550	391	390	160
medium3	2.037	2.031	2.025	2.027	2.032	9.02	0.47	5	550	394	392	156
high1	2.019	2.03	2.014	1.987	2.025	7.48	1.68	5	550	400	399	151
high2	2.014	2.029	1.998	2.006	2.007	7.06	1.16	5	550	404	405	145
high3	2.012	1.991	2.002	2.007	1.992	6.06	0.92	5	550	405	407	143
REFERENCE	1	2	3	4	5	AVERAGE	STDEV					
20170411-3	1.945	1.946	1.951	1.968	1.958	195.36	0.96					
LINE SPEED	1	2	3	4	5	COATING WEIGHT, g/m ²	STDEV					
low1	2.386	2.37	2.393	2.362	2.365	42.16	1.36	5	550	165	165	385
low2	2.263	2.315	2.276	2.267	2.304	33.14	2.32	5	550	163	164	387
low3	2.206	2.226	2.22	2.23	2.222	26.72	0.91	5	550	164	165	385
medium1	2.148	2.158	2.137	2.113	2.125	18.26	1.79	5	550	180	179	370
medium2	2.086	2.051	2.071	2.088	2.065	11.86	1.54	5	550	194	195	356
medium3	2.05	2.054	2.038	2.03	2.048	9.04	0.98	5	550	209	210	341
high1	2.026	2.035	2.035	2.038	2.02	7.72	0.75	5	550	219	219	331
high2	2.047	2.023	2.012	2.04	2.005	7.18	1.79	5	550	230	230	320
high3	2.029	2.014	2.005	2.031	2.029	6.8	1.15	5	550	242	240	312

	1	2	3	4	5	AVERAGE	STDEV														
REFERENCE	1.945	1.946	1.951	1.968	1.958	195.36	0.96														
TEST POINT AND RPM 201700411-4																					
LINE SPEED	1	2	3	4	5	COATING WEIGHT, g/m ² AVERAGE	STDEV	ADHESION	DECKLES VALUE	WIDTH (mm)	NECK-IN (mm)	PINHOLES									
low1	2.305	2.261	2.295	2.282	2.261	32.72	1.98	5	550	443	107	107									
low2	2.244	2.212	2.227	2.221	2.213	26.98	1.30	5	550	448	102	102									
low3	2.155	2.19	2.191	2.172	2.203	22.86	1.88	5	550	452	98	97									
medium1	2.127	2.136	2.157	2.137	2.138	18.54	1.10	5	550	459	92	91									
medium2	2.105	2.106	2.091	2.1	2.103	14.74	0.60	5	550	462	88	88									
medium3	2.097	2.08	2.069	2.083	2.076	12.74	1.04	5	550	466	84	85									
high1	2.071	2.066	2.049	2.064	2.075	10.94	1.11	5	550	466	84	84									
high2	2.049	2.034	2.036	2.046	2.043	8.8	0.64	5	550	467	83	83									
high3	2.033	2.046	2.032	2.015	2.042	8	1.20	4.5	550	467	83	83									
REFERENCE	1.945	1.946	1.951	1.968	1.958	195.36	0.96														
TEST POINT AND RPM 20170411-5																					
LINE SPEED	1	2	3	4	5	COATING WEIGHT, g/m ² AVERAGE	STDEV	ADHESION	DECKLES VALUE	WIDTH (mm)	NECK-IN (mm)	PINHOLES									
low1	2.29	2.297	2.262	2.311	2.294	33.72	1.79	5	550	363	187	185									
low2	2.211	2.208	2.207	2.212	2.184	25.08	1.16	5	550	377	173	172									
low3	2.18	2.182	2.149	2.184	2.193	22.4	1.67	5	550	387	163	164									
medium1	2.129	2.148	2.14	2.142	2.134	18.5	0.73	5	550	397	153	153									
medium2	2.09	2.105	2.069	2.084	2.108	14.36	1.01	5	550	405	145	147									
medium3	2.087	2.065	2.074	2.077	2.076	12.22	0.79	5	550	408	142	141									
high1	2.045	2.042	2.05	2.057	2.062	9.76	0.83	5	550	411	139	139									
high2	2.06	2.045	2.055	2.039	2.043	9.48	0.88	5	550	413	137	137									
high3	2.051	2.035	2.045	2.047	2.05	9.2	0.64	5	550	416	134	135									
REFERENCE	1.92	1.917	1.905	1.906	1.917	191.3	0.70														
TEST POINT AND RPM 20170411-6																					
LINE SPEED	1	2	3	4	5	COATING WEIGHT, g/m ² AVERAGE	STDEV	ADHESION	DECKLES VALUE	WIDTH (mm)	NECK-IN (mm)	PINHOLES									
low1	2.597	2.559	2.561	2.588	2.609	66.98	2.21	5	550	200	350	350									
low2	2.399	2.433	2.411	2.395	2.425	49.96	1.63	5	550	201	349	348									
low3	2.309	2.328	2.31	2.317	2.337	40.72	1.21	5	550	208	342	343									
medium1	2.203	2.196	2.203	2.193	2.209	28.78	0.63	5	550	225	325	325									
medium2	2.108	2.113	2.12	2.109	2.114	19.98	0.48	5	550	239	311	310									
medium3	2.094	2.082	2.069	2.083	2.111	17.88	1.18	5	550	253	297	297									
high1	2.028	2.059	2.043	2.056	2.061	13.64	1.39	5	550	266	284	284									
high2	2.015	2.058	2.046	2.035	2.038	12.54	1.58	5	550	269	271	279									
high3	2.039	2.034	2.042	2.016	2.034	12	1.01	5	550	276	274	273									

APPENDIX B: HOT AIR SEALING RESULTS

Table 1. Hot air sealing results of trial runs 20170125.

20170125-1 (T1/low)			20170125-2 (T1/high)			20170125-3 (T2/low)		
Line speed	Coating weight (g/m ²)	Sealing temp. (°C)	Line speed	Coating weight (g/m ²)	Sealing temp. (°C)	Line speed	Coating weight (g/m ²)	Sealing temp. (°C)
low2	18.6	310				low2	19.6	260
low3	15.0	340				low3	15.7	270
low4	13.4	380						
medium1	12.1	430	medium1	18.4	390	medium1	13.0	300
			medium2	16.0	410	medium2	11.0	390
			medium3	14.9	450	medium3	11.3	400
20170125-4 (T2/high)			20170125-5 (T3/low)			20170125-6 (T3/high)		
Line speed	Coating weight (g/m ²)	Sealing temp. (°C)	Line speed	Coating weight (g/m ²)	Sealing temp. (°C)	Line speed	Coating weight (g/m ²)	Sealing temp. (°C)
			low1	21.9	230			
			low2	15.8	240			
			low3	14.8	250	low3	23.6	240
medium1	20.6	310	medium1	13.2	280	medium1	18.0	260
medium2	17.8	350	medium2	10.6	310	medium2	16.1	270
medium3	17.2	380	medium3	9.0	350	medium3	14.4	270
high1	13.2	440	high1	7.1	360	high1	11.1	300
high2	13.0	480	high2	7.3	400	high2	10.8	340
			high3	7.0	420	high3	9.7	390

Table 2. Hot air sealing results of trial runs 20170131-B17.

20170131-B17-1 (T1/low)			20170131-B17-2 (T1/high)			20170131-B17-3 (T2/low)		
Line speed	Coating weight (g/m ²)	Sealing temp. (°C)	Line speed	Coating weight (g/m ²)	Sealing temp. (°C)	Line speed	Coating weight (g/m ²)	Sealing temp. (°C)
low1	20.9	280				low1	21.0	240
low2	18.4	290				low2	16.2	240
low3	17.3	320	low3	22.5	330	low3	13.3	260
low4	15.2	370	low4	17.2	350			
			medium1	15.0	350	medium1	10.9	280
			medium2	14.8	420	medium2	10.0	310
						medium3	7.0	360
						high1	7.0	420
						high2	8.1	440
						high3	5.7	460
20170131-B17-4 (T2/high)			20170131-B17-5 (T3/low)			20170131-B17-6 (T3/high)		
Line speed	Coating weight (g/m ²)	Sealing temp. (°C)	Line speed	Coating weight (g/m ²)	Sealing temp. (°C)	Line speed	Coating weight (g/m ²)	Sealing temp. (°C)
			low1	17.9	250			
			low2	17.4	260			
low3	22.1	270	low3	12.8	270	low3	21.8	260
medium1	16.9	270	medium1	10.7	280	medium1	17.7	270
medium2	15.8	290	medium2	9.1	300	medium2	15.7	280
medium3	12.3	330	medium3	9.2	300	medium3	14.0	300
high1	10.2	400	high1	9.5	370	high1	11.5	330
high2	11.6	450	high2	7.3	370	high2	10.6	350
high3	7.4	450	high3	7.1	390	high3	11.0	370

Table 3. Hot air sealing results of trial runs 20170216-B18.

20170216-B18-1 (T1/low)			20170216-B18-2 (T1/high)			20170216-B18-3 (T2/low)		
Line speed	Coating weight (g/m ²)	Sealing temp. (°C)	Line speed	Coating weight (g/m ²)	Sealing temp. (°C)	Line speed	Coating weight (g/m ²)	Sealing temp. (°C)
low1	20.0	310				low1	19.5	250
low2	17.6	350				low2	15.9	270
low3	14.2	370	low3	23.0	380	low3	15.3	270
medium1	10.7	440	medium1	17.5	420	medium1	10.5	340
			medium2	16.1	450	medium2	9.1	360
			medium3	12.8	490	medium3	8.8	400
			high1	10.9	490	high1	7.0	450
						high2	6.4	490
20170216-B18-4 (T2/high)			20170216-B18-5 (T3/low)			20170216-B18-6 (T3/high)		
Line speed	Coating weight (g/m ²)	Sealing temp. (°C)	Line speed	Coating weight (g/m ²)	Sealing temp. (°C)	Line speed	Coating weight (g/m ²)	Sealing temp. (°C)
			low1	20.6	260			
			low2	14.9	270			
low3	24.0	290	low3	14.4	270	low3	21.0	260
medium1	18.1	330	medium1	10.5	310	medium1	20.4	270
medium2	14.4	380	medium2	9.9	350	medium2	15.7	290
medium3	12.5	380	medium3	9.4	350	medium3	14.5	310
high1	12.2	450	high1	7.5	390	high1	11.5	330
high2	10.6	480	high2	6.8	430	high2	10.4	390
high3	11.3	490	high3	6.8	440	high3	9.0	420

Table 4. Hot air sealing results of trial runs 20170223-B19.

20170223-B19-1 (T1/low)			20170223-B19-2 (T1/high)			20170223-B19-3 (T2/low)		
Line speed	Coating weight (g/m ²)	Sealing temp. (°C)	Line speed	Coating weight (g/m ²)	Sealing temp. (°C)	Line speed	Coating weight (g/m ²)	Sealing temp. (°C)
low1	19.6	340				low1	18.2	290
low2	16.6	370				low2	13.9	290
low3	14.1	410	low3	22.2	400	low3	10	320
medium1	10.6	440	medium1	18.4	430	medium1	9.4	340
						medium2	7.2	390
						medium3	6.4	400
20170223-B19-4 (T2/high)			20170223-B19-5 (T3/low)			20170223-B19-6 (T3/high)		
Line speed	Coating weight (g/m ²)	Sealing temp. (°C)	Line speed	Coating weight (g/m ²)	Sealing temp. (°C)	Line speed	Coating weight (g/m ²)	Sealing temp. (°C)
			low1	18.6	270			
			low2	15.6	280			
			low3	13	290	low3	23.1	290
medium1	21.5	330	medium1	9.9	340	medium1	18.3	300
medium2	16.7	360	medium2	8.7	350	medium2	17.1	320
medium3	15.1	370	medium3	6.8	380	medium3	12.7	320
high1	12.3	430	high1	6.7	390	high1	10.8	340
high2	11.7	450	high2	6.7	410	high2	8.7	350
high3	11.7	490	high3	5.8	410	high3	8.5	450

Table 5. Hot air sealing results of trial runs 20170302.

20170302-1 (T2/low/AG1)			20170302-2 (T2/low/AG2)			20170302-3 (T2/low/AG3)		
Line speed	Coating weight (g/m ²)	Sealing temp. (°C)	Line speed	Coating weight (g/m ²)	Sealing temp. (°C)	Line speed	Coating weight (g/m ²)	Sealing temp. (°C)
low1	19.1	250	low1	18.2	250			
low2	15.9	270	low2	12.6	270	low2	21.4	240
low3	12.8	300	low3	12.5	270	low3	17.3	250
medium1	11.3	390	medium1	9.7	290	medium1	10.7	270
medium2	7.1	440	medium2	8.2	350	medium2	8.3	300
medium3	7.8	490	medium3	8.2	460	medium3	6.0	340
			high1	7.0	490	high1	4.6	440
			high2	4.1	490	high2	3.8	470
						high3	3.5	480
20170302-4 (T2/high/AG1)			20170302-5 (T2/high/AG2)			20170302-6 (T2/high/AG3)		
Line speed	Coating weight (g/m ²)	Sealing temp. (°C)	Line speed	Coating weight (g/m ²)	Sealing temp. (°C)	Line speed	Coating weight (g/m ²)	Sealing temp. (°C)
low3	21.4	380	low3	23.1	280	low3	27.4	250
medium1	15.3	400	medium1	18.9	330	medium1	18.2	260
medium2	13.6	450	medium2	14.6	410	medium2	14.3	290
medium3	10.7	470	medium3	13.8	450	medium3	10.9	340
high1	8.5	480	high1	12.1	450	high1	8.7	390
			high2	10.9	480	high2	6.5	420
						high3	6.6	430

Table 6. Hot air sealing results of trial runs 20170308.

20170308-1 (T3/low/AG1)			20170308-2 (T3/low/AG2)			20170308-3 (T3/low/AG3)		
Line speed	Coating weight (g/m ²)	Sealing temp. (°C)	Line speed	Coating weight (g/m ²)	Sealing temp. (°C)	Line speed	Coating weight (g/m ²)	Sealing temp. (°C)
low1	19.9	240	low1	16.2	250			
low2	16.2	250	low2	15.1	250			
low3	12.8	260	low3	12.1	280			
medium1	10.1	280	medium1	10.0	290	medium1	20.8	250
medium2	8.8	330	medium2	9.2	300	medium2	12.8	270
medium3	7.3	350	medium3	8.6	320	medium3	8.6	280
high1	7.2	460	high1	7.9	350	high1	7.0	350
high2	4.7	480	high2	6.2	410	high2	4.7	410
high3	4.3	500	high3	6.0	480	high3	4.5	460
20170308-4 (T3/high/AG1)			20170308-5 (T3/high/AG2)			20170308-6 (T3/high/AG3)		
Line speed	Coating weight (g/m ²)	Sealing temp. (°C)	Line speed	Coating weight (g/m ²)	Sealing temp. (°C)	Line speed	Coating weight (g/m ²)	Sealing temp. (°C)
low3	21.5	260	low3	24.0	250			
medium1	17.4	280	medium1	18.8	260	medium1	23.9	250
medium2	15.4	360	medium2	16.3	280	medium2	15.3	260
medium3	13.6	390	medium3	14.7	330	medium3	14.0	270
high1	10.4	450	high1	12.0	350	high1	13.8	280
high2	9.8	480	high2	11.5	390	high2	11.7	320
high3	9.6	500	high3	8.8	410	high3	9.8	330

Table 7. Hot air sealing results of trial runs 20170309-B20.

20170309-B20-1 (T2/low/AG1)			20170309-B20-2 (T2/low/AG2)			20170309-B20-3 (T2/low/AG3)		
Line speed	Coating weight (g/m ²)	Sealing temp. (°C)	Line speed	Coating weight (g/m ²)	Sealing temp. (°C)	Line speed	Coating weight (g/m ²)	Sealing temp. (°C)
low1	18.7	250	low1	16.2	230			
low2	16.5	270	low2	13.5	240	low2	19.5	240
low3	14.8	290	low3	12.9	250	low3	16.0	250
medium1	10.4	360	medium1	9.0	300	medium1	11.8	260
medium2	9.0	410	medium2	8.8	370	medium2	10.8	340
medium3	8.2	450	medium3	7.2	380	medium3	8.0	380
			high1	7.1	430	high1	6.5	430
						high2	3.8	460
						high3	3.8	470
20170309-B20-4 (T2/high/AG1)			20170309-B20-5 (T2/high/AG2)			20170309-B20-6 (T2/high/AG3)		
Line speed	Coating weight (g/m ²)	Sealing temp. (°C)	Line speed	Coating weight (g/m ²)	Sealing temp. (°C)	Line speed	Coating weight (g/m ²)	Sealing temp. (°C)
low3	24.4	340	low3	23.8	290	low3	25.2	240
medium1	18.5	400	medium1	18.2	320	medium1	18.7	260
medium2	14.8	430	medium2	14.2	370	medium2	15.4	290
medium3	11.8	450	medium3	12.5	410	medium3	11.6	310
			high1	10.4	460	high1	9.7	360
			high2	9.3	460	high2	9.3	400
			high3	9.2	470	high3	8.4	420

Table 8. Hot air sealing results of trial runs 20170404-B21.

20170404-B21-1 (T2/low/AG1)			20170404-B21-2 (T2/low/AG2)			20170404-B21-3 (T2/low/AG3)		
Line speed	Coating weight (g/m ²)	Sealing temp. (°C)	Line speed	Coating weight (g/m ²)	Sealing temp. (°C)	Line speed	Coating weight (g/m ²)	Sealing temp. (°C)
low2	17.8	290	low1	18.0	260	low2	20.2	260
low3	15.7	330	low2	14.7	270	low3	16.8	270
medium1	12.7	380	low3	12.4	290	medium1	11.2	300
medium2	10.4	440	medium1	10.9	340	medium2	8.9	370
			medium2	8.5	380	medium3	8.9	380
			medium3	7.9	430	high1	8.3	420
			high1	6.8	460	high2	8.3	450
			high2	6.7	480	high3	7.6	460
20170404-B21-4 (T2/high/AG1)			20170404-B21-5 (T2/high/AG2)			20170404-B21-6 (T2/high/AG3)		
Line speed	Coating weight (g/m ²)	Sealing temp. (°C)	Line speed	Coating weight (g/m ²)	Sealing temp. (°C)	Line speed	Coating weight (g/m ²)	Sealing temp. (°C)
low3	24.9	370	low3	25.8	290	medium1	25.0	260
medium1	20.8	400	medium1	19.9	340	medium2	17.9	280
medium2	17.6	410	medium2	17.3	380	medium3	16.2	320
			medium3	16.7	420	high1	13.7	350
						high2	13.6	370
						high3	10.7	420

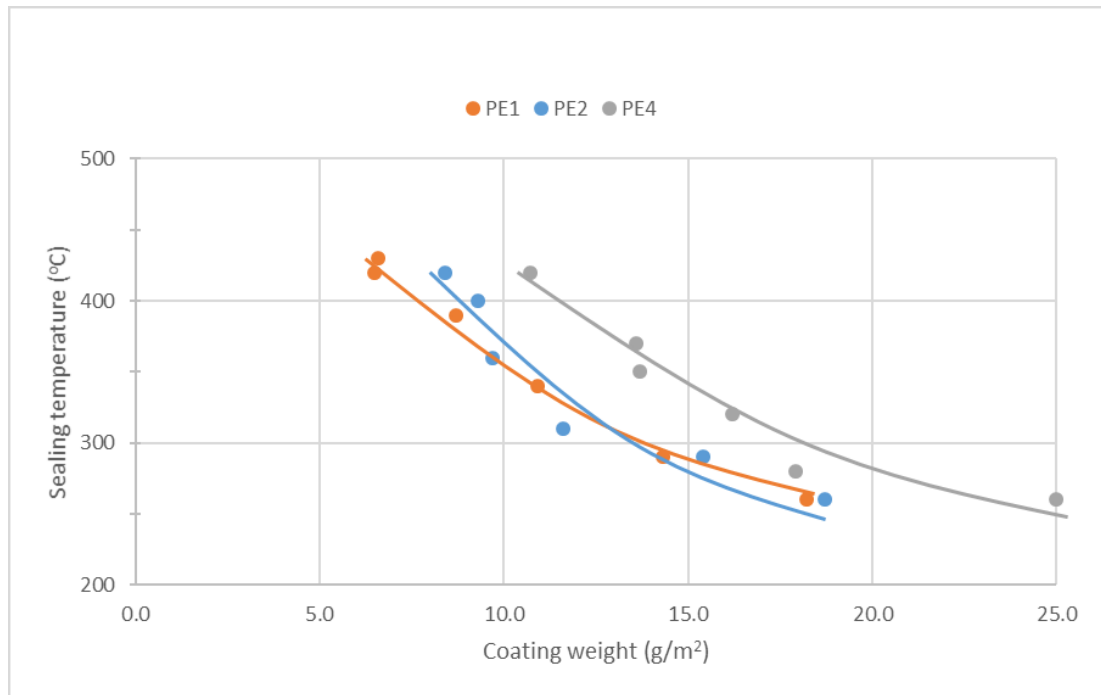
Table 9. Hot air sealing results of trial runs 20170406-B22.

20170406-B22-1 (T3/low/AG1)			20170406-B22-2 (T3/low/AG2)			20170406-B22-3 (T3/low/AG3)		
Line speed	Coating weight (g/m²)	Sealing temp. (°C)	Line speed	Coating weight (g/m²)	Sealing temp. (°C)	Line speed	Coating weight (g/m²)	Sealing temp. (°C)
low1	21.2	240	low1	19.3	240			
low2	15.5	250	low2	15.0	250			
low3	14.2	260	low3	13.2	260	low3	27.0	260
medium1	11.0	310	medium1	11.4	290	medium1	18.2	260
medium2	10.3	360	medium2	9.2	310	medium2	15.6	280
medium3	9.9	380	medium3	8.8	370	medium3	10.2	310
high1	8.4	430	high1	8.8	430	high1	8.9	370
high2	7.2	460	high2	7.5	440	high2	8.4	430
high3	5.8	500	high3	7.1	480	high3	6.1	470
20170406-B22-4 (T3/high/AG1)			20170406-B22-5 (T3/high/AG2)			20170406-B22-6 (T3/high/AG3)		
Line speed	Coating weight (g/m²)	Sealing temp. (°C)	Line speed	Coating weight (g/m²)	Sealing temp. (°C)	Line speed	Coating weight (g/m²)	Sealing temp. (°C)
low3	21.3	270	low3	21.5	240			
medium1	15.4	280	medium1	17.3	250	medium1	22.5	250
medium2	13.6	330	medium2	15.2	290	medium2	16.2	260
medium3	10.9	390	medium3	13.9	310	medium3	13.3	260
high1	10.4	430	high1	10.1	340	high1	12.6	300
high2	10.0	450	high2	9.0	400	high2	11.6	360
high3	9.0	480	high3	8.4	430	high3	10.1	370

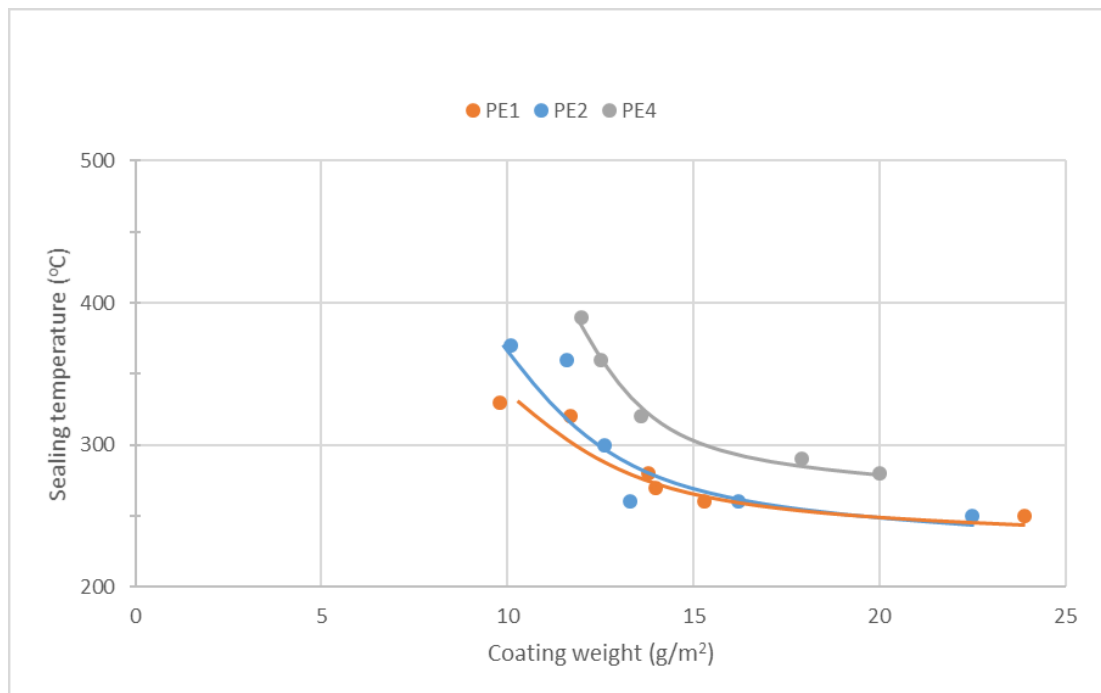
Table 10. Hot air sealing results of trial runs 20170411-B23.

20170411-B23-1 (T3/low/AG1)			20170411-B23-2 (T3/low/AG2)			20170411-B23-3 (T3/low/AG3)		
Line speed	Coating weight (g/m²)	Sealing temp. (°C)	Line speed	Coating weight (g/m²)	Sealing temp. (°C)	Line speed	Coating weight (g/m²)	Sealing temp. (°C)
low1	18.0	250	low1	18.1	240			
low2	15.7	260	low2	16.2	250			
low3	15.0	270	low3	15.2	290	low3	26.7	250
medium1	11.3	310	medium1	11.0	330	medium1	18.3	250
medium2	9.5	340	medium2	9.2	340	medium2	11.9	270
medium3	8.4	380	medium3	9.0	390	medium3	9.0	320
high1	7.7	390	high1	7.5	410	high1	7.7	380
high2	6.3	480	high2	7.1	450	high2	7.2	440
high3	5.9	500	high3	6.1	480	high3	6.8	480
20170411-B23-4 (T3/high/AG1)			20170411-B23-5 (T3/high/AG2)			20170411-B23-6 (T3/high/AG3)		
Line speed	Coating weight (g/m²)	Sealing temp. (°C)	Line speed	Coating weight (g/m²)	Sealing temp. (°C)	Line speed	Coating weight (g/m²)	Sealing temp. (°C)
low2	27.0	250	low2	25.1	250			
low3	22.9	260	low3	22.4	260			
medium1	18.5	320	medium1	18.5	270	medium1	28.8	260
medium2	14.7	340	medium2	14.4	300	medium2	20.0	280
medium3	12.7	360	medium3	12.2	320	medium3	17.9	290
high1	10.9	400	high1	9.8	370	high1	13.6	320
high2	8.8	460	high2	9.5	400	high2	12.5	360
high3	8.0	460	high3	9.2	440	high3	12.0	390

APPENDIX C: HOT AIR SEALING GRAPHS

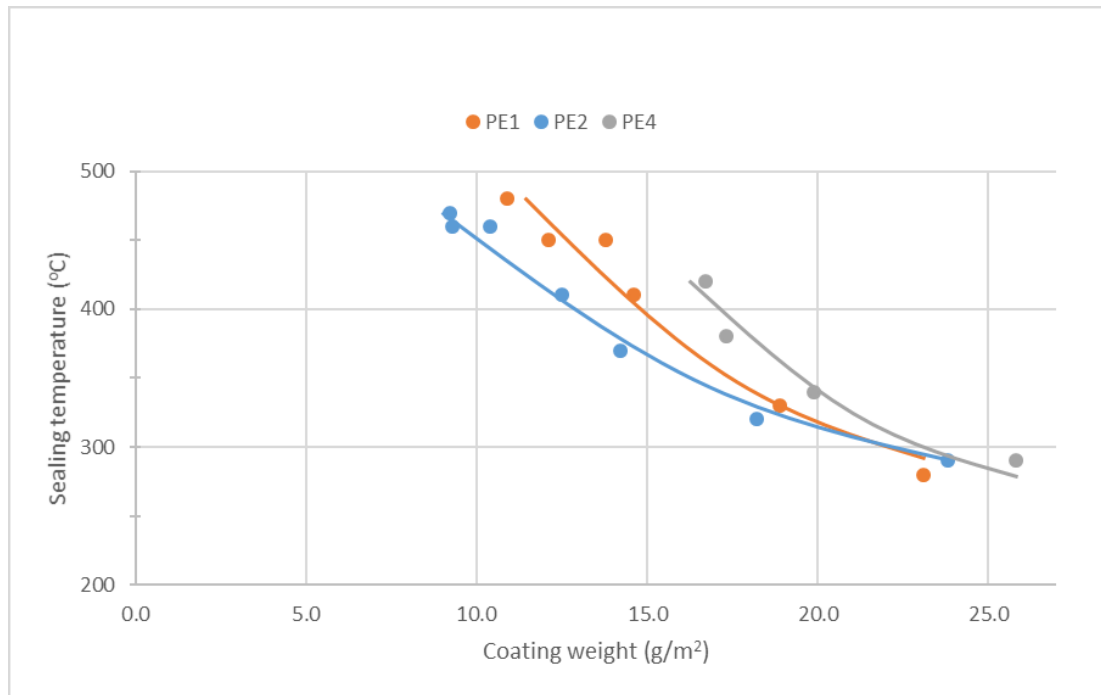


a) T2/high/AG3 setting.

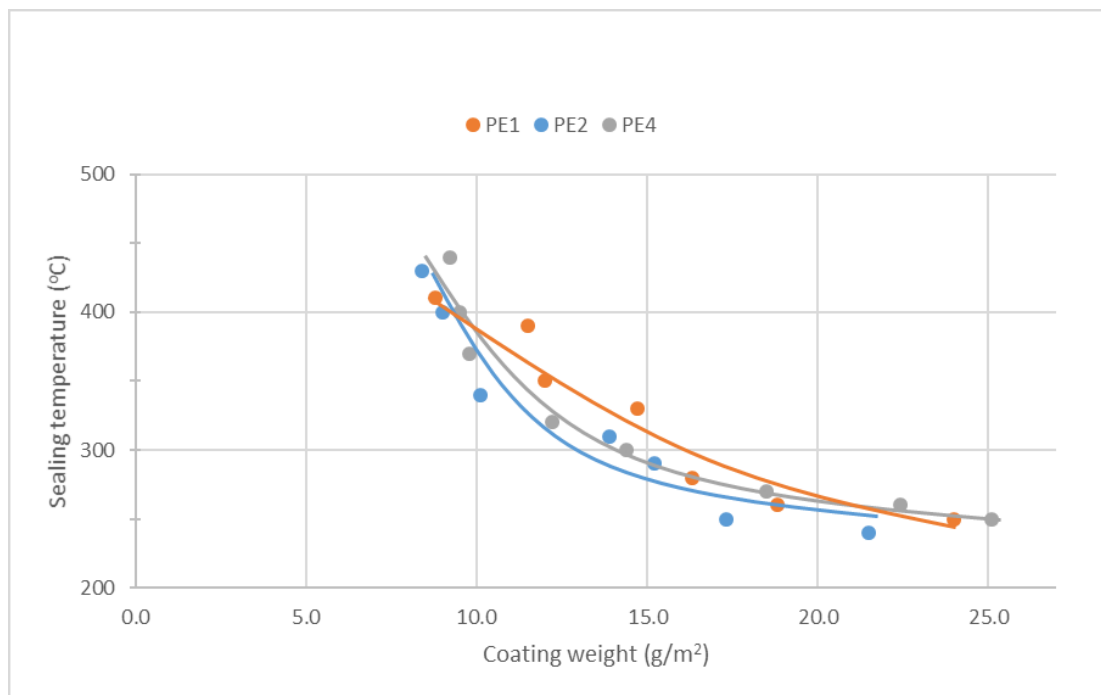


b) T3/high/AG3 setting.

Figure 1. Hot air sealing temperature as a function of coating weight for used PE materials.



a) T2/high/AG2 setting.



b) T3/high/AG2 setting.

Figure 2. Hot air sealing temperature as a function of coating weight for used PE materials.